Agent-based Modelling & Simulation of Airport Terminal Operations under COVID-19-related Restrictions

Master of Science Thesis

Grégory Sanders

TUDelft

Agent-based Modelling & Simulation of Airport Terminal Operations under COVID-19-related Restrictions

Master of Science Thesis

by

Grégory Sanders

to obtain the degree of Master of Science
at the Delft University of Technology,
to be defended publicly on April 12th, 2021

Student number:	4559738	
Project duration:	August 24th 2020 – April 12th 2021	
Thesis committee:	Dr. ir. M.D. Pavel	TU Delft, Chairwoman
	Dr. ir. O.A. Sharpans'kykh	TU Delft, Supervisor
	Dr. ir. A. Bombelli	TU Delft, External Examiner

An electronic version of this thesis is available at http://repository.tudelft.nl/.

Acknowledgements

Dear reader,

This thesis reports on my research for obtaining a Master of Science in Aerospace Engineering at Delft University of Technology. This work focuses on agent-based modelling and simulation and its application to analyse the impact of COVID-19 on airport operations.

This research study has been a very enriching experience. It not only helped me growing educationally but also personally. I would like to express my gratitude to my supervisor Dr. Alexei Sharpanskykh for his guidance, intellectual expertise and support. A big thank you to Adin and Sahand for all the valuable feedback and tips during our weekly meetings. And also a big thank you to Benyamin, Klemens and Didier for the pleasant collaboration.

Lastly, I would like to thank my family, Tanti and Nonke who have always supported me in my journey at the TU Delft.

With this master thesis, I will conclude my journey at Delft University of Technology. It has been 5 years of hard work and a lot of fun.

Grégory Sanders
Delft, April 2021

Contents

List of Figures

List of Tables

List of Abbreviations

General Abbreviations

AATOM	Agent-based Airport Terminal and Operations Model
ACI	Airports Council International
EASA	European Union Aviation Safety Agency
EMA	European Medicine Agency
IATA	International Air Transport Association
KPI	Key Performance Indicator
RTHA	Rotterdam The Hague Airport

Abbreviations for the inputs of the model

GS	Boarding group size
n_c	Number of luggage collect positions
n_d	Number of luggage divest positions
PD	Physical distancing
QT	Queue type
t_c	Time to collect luggage
t_d	Time to divest luggage
t_{bc}	Time to check boarding pass
t_{ci}	Time to check-in

Abbreviations for the outputs of the model

C_{pax}	Average contact time per passenger [min:sec]
$C_{pax_{CD}}$	Average contact time per passenger at check-in desk [min:sec]
$C_{pax_{CQ}}$	Average contact time per passenger in the check-in queue [min:sec]
$C_{pax_{SL}}$	Average contact time per passenger at the security lane [min:sec]
$C_{pax_{SQ}}$	Average contact time per passenger in the security queue [min:sec]
T_B	Time to board 50 passengers [min:sec]
T_C	Check-in throughput [pax/hour]
T_S	Security throughput [pax/hour]

I

Scientific Paper

Agent-based Modelling and Simulation of Airport Terminal Operations under COVID-19-related Restrictions

Grégory Sanders*,

Delft University of Technology, Delft, The Netherlands

Abstract

The worldwide COVID-19 pandemic has had a tremendous impact on the aviation industry, with a reduction in passenger demand never seen before. To minimise the spread of the virus and to gain trust from the public in the airport operations' safety, airports implemented measures, e.g., physical distancing, entry/exit temperature screening and more. However, airports do not know what the impact of these measures will be on the operations' performance and the passengers' safety when passenger demand increases back. The goal of this research is twofold. Firstly, to analyse the impact of current (COVID-19) and future pandemic-related measures on airport terminal operations. Secondly, to identify plans that airport management agents can take to control passengers' flow in a safe, efficient, secure and resilient way. To model and simulate airport operations, an agent-based model was developed. The proposed model covers the main airport's handling processes and simulates local interactions, such as physical distancing between passengers. The obtained results show that COVID-19 measures can significantly affect the passenger throughput of the handling processes and the average time passengers are in contact with each other. For instance, a 20% increase in check-in time (due to additional COVID-19 related paperwork at the check-in desk) can decrease passenger throughput by 16% and increase the time that passengers are in contact by 23%.

Index Terms - Multi-agent system, Airport operations, COVID-19, Physical distancing, Walking behaviour

1 Introduction

The outbreak of the COVID-19 pandemic has led to a worldwide crisis and presents us today unprecedented challenges in our life. The aviation industry has been impacted like no other industrial sector. When in March 2020 large clusters of COVID-19 cases were identified in Europe, many countries started to impose travel restrictions. As a result, the travel demand dropped and global air traffic decreased by 80% compared to the preceding year [ICAO, 2020]. The aviation industry has never faced a challenge this large.

To minimise the spread of the COVID-19 virus and regain the public's trust in the aviation industry's safety, airports needed to be made safe. Since at airports passengers are often exposed to many interactions with other people, airport operators implemented measures. Some examples of measures are physical distancing, entry/exit temperature screening, prevention of queuing, use of personal protective equipment. To help airports implement measures, the European Aviation Safety Agency released in June 2020 their "COVID-19 Aviation Health Safety Protocol" [EASA, 2020]. This report lists measures that airport operators can take for safe operations to guarantee the passengers' safety. These measures, for instance social distancing, are widely considered as a new part of our life. Even though many countries have started vaccination campaigns, it is believed that these measures, especially wearing a mask and social distancing are habits we will have to adapt for some time.

These recommended measures from EASA already helped many airports in providing safe operations. However, many airports still do not know the impact of these measures on their operations when passenger demand will increase. For example, Charleroi Aiport faced a sudden increase in passenger demand during the Christmas Holiday of 2020. As a result, the airport was too crowded and passengers could not perform physical distancing [De Herdt, 2020]. Also, airports are very complex because they involve many processes (e.g, check-in, security, boarding) and many stakeholders (airlines, airport operators), resulting in conflicting objectives. On the one hand, airports operators have the financial intent to increase revenue and decrease costs. On the other hand, they also need to make sure that operations are safe for the passengers. While airports are now under financial pressure, it is hard for them to make decisions primarily since they do not understand the impact of these measures.

Thus, research is needed regarding the impact of the COVID-19 measures on airport operations and the associated safety for passengers.

*Msc Student, Air Transport and Operations, Faculty of Aerospace Engineering, Delft University of Technology

To address this problem agent-based modelling and simulation was used in this research. In agent-based modelling, humans can be modelled as intelligent entities, called agents. These agents can be given certain traits and behaviour that organise their interaction with the environment. This bottom-up approach allows for modelling complex sociotechnical systems, such as an airport terminal, in great detail. It also allows for simulating local interactions in the system, for instance, physical distancing between passengers and analysing the emergent properties of the global system. These emergent properties can be translated into system-wide key performance indicators (KPIs), for example passenger throughput, and can be used to asses, e.g, the system's performance and safety. Altogether, agent-based modelling is a suitable paradigm to model airport terminal operations.

The objective of this research is twofold. Firstly, to analyse the impact of current (COVID-19) and future pandemic-related measures on airport terminal operations. Secondly, to identify plans that airport management agents can take to control passengers' flow in a safe, efficient, secure and resilient way.

The Agent-Based Airport Terminal Operations Model (AATOM) was used for this research study [Janssen et al., 2018]. AATOM is an open-source simulator that can be used for modelling and simulating airport terminal operations. Since the AATOM model was developed before COVID-19, AATOM was extended to include COVID-19 related measures.

For this research, first the COVID-19 measures, as EASA proposed in [EASA, 2020], were implemented in AATOM. Then, to assess the impact of these newly implemented measures new outputs or KPIs were designed and implemented in AATOM. Hereafter, three different case studies were created to explore the impact of various measures. Each case study focuses on a different part of the airport, namely the check-in, the security and the boarding process. These case studies are used to analyse the impact of the COVID-19 measures on the operations' performance and the associated health risk for the passengers. Each case study was translated into a new model-set up of AATOM. Lastly, the results were validated.

This paper is organised as follows. In Section 2 the related work is discussed. The methodology of this research is explained in Section 3. The agent-based model is discussed in Section 4. Verification of the model is explained in Section 5. The different case studies are presented in Section 6 and the results are given and discussed in Section 7 and Section 8. Finally, the conclusions are made in Section 9 together with recommendations for future work.

2 Related work

This section reviews the literature related to this research study. Section 2.1 reviews different pedestrian dynamics models to simulate passenger walking behaviour. Section 2.2 reviews other papers that researched the impact of COVID-19 restrictions on airport operations.

2.1 Pedestrian dynamics models

This section presents the state-of-the-art regarding modelling the dynamics of walking pedestrians. In general pedestrian dynamics models can be categorised into microscopic models and macroscopic models [Teknomo et al., 2016]. In microscopic models, every pedestrian is treated as an individual unit and is given a certain amount of characteristics, for instance direction and speed. The changes in movement of each pedestrian is influenced by other pedestrians and by the environment. These microscopic models can give great insight in the local interactions between the pedestrians. Macroscopic models on the other hand are concerned about the group behaviour of the pedestrians and thus the local interactions are overlooked. It treats pedestrian movement like a continuous fluid or crowd. Because in macroscopic models the pedestrians are not modelled in detail they are computationally efficient. However these models are inapplicable to analyse pedestrians interactions and to analyse if pedestrians are physically distancing. Therefore for this research only microscopic models were analysed. The following models are all microscopic models.

Gips et al. proposed the benefit-cost cellular model for modelling pedestrian flows [Gipps and Marksjö, 1985]. Blue et al. proposed cellular automata microsimulation for modeling bi-directional pedestrian walkways [Blue and Adler, 2001]. These two models are cellular automata based models which means that the environment of the model is discretized in a grid. The downside of this type of models is that the simulation does not reflect the real behavior of pedestrians because updates in the grid are done heuristically [Ma, 2013, Teknomo et al., 2016].

The queueing network model was introduced by Lovas et al. [Løvås, 1994]. In this model the environment is discretized into links and nodes. Pedestrians move from one node to another node. The movement is stochastic because it uses Monte Carlo simulations. This model has several drawbacks. Firstly, movement is uni-dimensional and therefore it is not so realistic because pedestrians walk bi-dimensional. Secondly, the model cannot not deal with high density environments, like airport terminals. Thirdly, because of the discretized environment, the model lacks the ability to analyse local interactions between the different agents.

Okazaki introduced a magnetic force model for pedestrian movement simulation with evacuation and queueing [Okazaki and Matsushita, 1993]. This model is based on the magnetic field theory to simulate pedestrian movement. Helbing et al. came up with the social force model [Helbing et al., 2000]. The social-force model uses psychological forces that drive pedestrians to move towards their goal as well as keep a proper distance from other pedestrians and objects. During the literature study, these five models were compared with each other and it was concluded that the social force model of Helbing et al. [Helbing et al., 2000] was the most suitable to continue with in the AATOM Model. Key reasons are that the model is continuous and therefore the simulations look more realistic and it is able to simulate local interactions between pedestrians better. The values of the parameters of the social forces have a physical meaning and therefore calibrating these parameters for social distancing is easier.

2.2 Pandemic modelling and analysis

This section presents studies which used (agent-based) models to analyse the impact of COVID-19 on the performance of airport terminal operations and on the associated passenger health safety.

Kierzkowski et al. uses a discrete event simulation model for different security lane configurations to analyse the impact of social distancing on the performance of the security [Kierzkowski and Kisiel, 2020]. However this model lacks the ability to model local interactions between passengers because it is a discrete event simulation model. Also Kierzkowski et al. only evaluates the performance of the security lanes and not the associated health safety of the passengers.

Schultz et al. used a cellular automata model to simulate different aircraft boarding strategies under COVID-19 related restrictions [Schultz and Soolaki, 2020]. He assessed for each boarding strategy the impact on total boarding time, the feasibility of the procedure and the associated risk of virus transmission. Schultz et al. used a transmission model which was based on the work of [Müller et al., 2020]. The cellular automata model is discrete and therefore the realistic passenger movement can not be obtained. Also the used transmission model requires assumptions regarding the amount of infected passengers; Schultz et al. considered for each boarding scenario one passenger with COVID-19. The possible amount of infected passengers is in reality not known and therefore assessing a boarding strategy based on this assumption is considered to be not conclusive. The study of Schultz et al. also lacks to analysis of other processes and activities at the airport such as check-in or security.

Ronchi et al. developed a model-agnostic approach to perform a quantitative assessment of pedestrian exposure using the outputs of existing microscopic crowd models, namely the trajectories of pedestrians over time [Ronchi and Lovreglio, 2020]. The model uses a general formulation instead of relying on a specific disease transmission. For instance the quantification of the pedestrian exposure is based on the distances between pedestrians, the time pedestrians are exposed and reference points (e.g. pedestrian face each other). It is therefore universal and can be tailored to new pandemics when there is no compelling understanding in the transmission of the pandemic. However as this is a model agnostic approach the downside is that the results depend on the accuracy of the pedestrian dynamics model.

3 Methodology

This research was carried out in four main steps, as shown in Figure 1.

Step 1 of this research study was the literature review. During the literature review, the scope of the model was set. Firstly, the COVID-19 restrictions for airport operations were identified from [EASA, 2020] and from interviews with a manager from a regional airport terminal. Secondly, relevant parameters contributing to the transmission of COVID-19 were analysed such that requirements for the model's output metrics could be set.

Step 2 was to translate the identified requirements into a specification of the agent-based model. Firstly, the environment of the model was specified in order to represent airport infrastructure under COVID-19 conditions. Secondly, the passenger agents were specified to include the distinction between passengers adhering to COVID-19 rules and others not adhering to rules. Thirdly, the interactions between the agents and the interactions of the agents with the environment were specified. Specifically, the Helbing social force model, which is part of the movement module, was calibrated to implement physical distancing when passengers are moving. The activity module was also extended for the implementation of physical distancing when passengers are queuing.

Step 3 was to implement the defined agent-based model and to set up case studies. Three case studies were set up to analyse the impact of the COVID-19 measures on the check-in process, security process, and boarding process. Hereafter, the model was verified to check if it satisfies the model requirements.

Step 4 was to run simulations using the calibrated model to obtain results. For each experiment, 450 simulations were performed on the server to obtain statistically significant results, and this was checked using the coefficient of variation plot. The coefficient of variation plots can be consulted in Section 2.2 of Supporting

Work. Also a global sensitivity analysis and Vargha-Delaney A-tests were performed, presented in Section 2.3 and 2.4 of Supporting Work. Lastly, the results were used to draw conclusions.

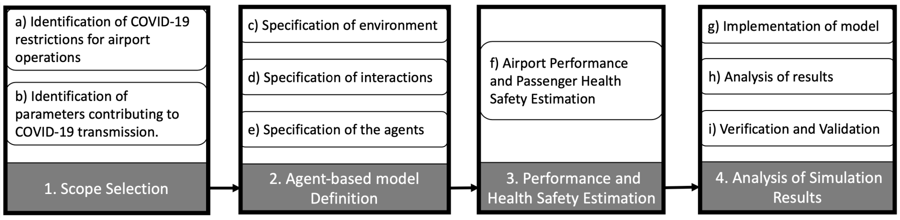

Figure 1: Methodology overview

4 The agent-based model

The model used in this paper is an extension of the baseline "Airport And Terminal Operations Model" (AATOM) with features to simulate passengers adhering to COVID-19 measures and to analyse passengers health safety. In this model, passengers and airport operators are represented as autonomous intelligent entities, called agents. These agents are modelled with a particular behaviour approximating humans and placed in a partially observable airport environment. An overview of the agent-based system is provided in Figure 2. It shows the different types of agents and their interactions with each other and with the environment. The elements of this model are further discussed below. Section 4.1 describes the specification of the environment of the model. Section 4.2 describes the specification of the agents. Section 4.3 describes the specification of the interactions between passenger agents and the environment. Section 4.4 describes the specification of the interactions between the passenger agents. The specification of the interactions between passenger agents and operator agents is provided in [Janssen et al., 2018].

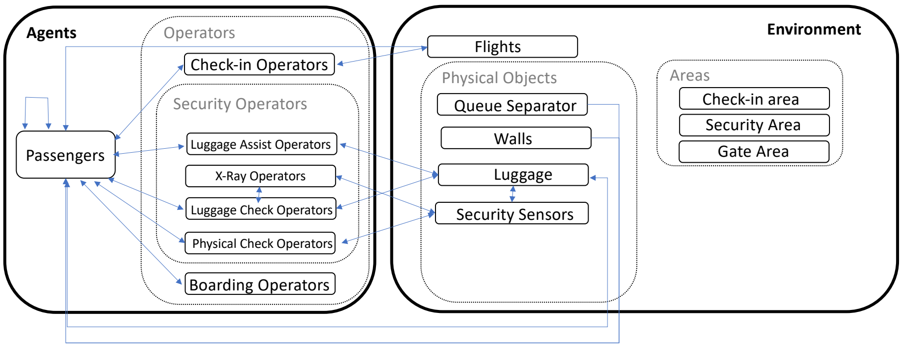

Figure 2: Overview of the multi-agent system including the different types of agents and their interactions with each other and the environment.

4.1 Specification of the environment of the model

The model's environment represents an airport terminal under COVID-19 conditions, as seen in Figure 3. It resembles an existing regional airport from the Netherlands. The environment consists of three main areas: the check-in area, the security checkpoint area and the gate area. Shops, restaurants, and restrooms are not considered in this model because these are not essential to the research study. At many airports, shops and restaurants are closed due to COVID-19.

The check-in area consists of four sets of check-in desks, each with three desks and one designated queue. There is a check-in operator (red dot), which checks-in passengers, behind each check-in desk. Three check-ins are using a common zig-zag queue. One check-in is using three single straight queues. This single queue is implemented for the purpose of the case study, explained in Section 6.1.

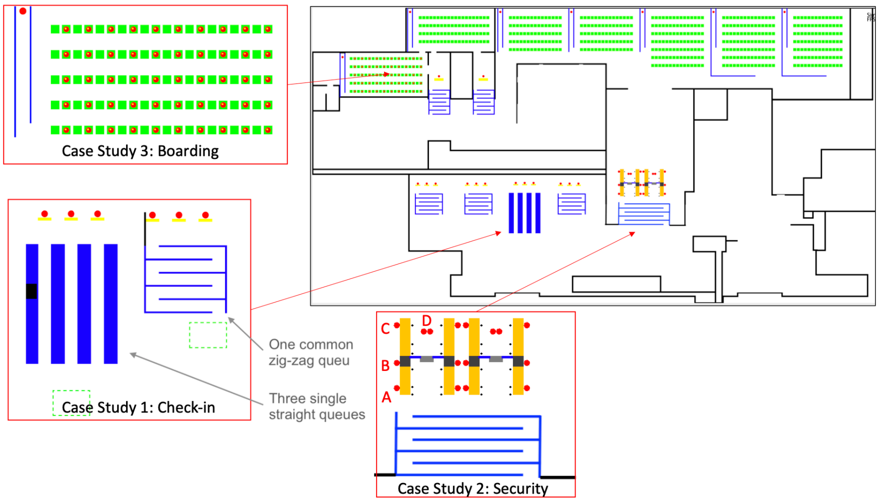

Figure 3: The environment of the agent-based model.

The security checkpoint area consists of four security lanes and one large common queue. The checkpoint lanes have a luggage belt, an X-ray sensor and a walk-through metal detector. There are four types of security operators (A, B, C, D) as indicated in the lower part of Figure 3. Operators A assist passengers in their luggage drop activity. Operators B perform the x-ray scan activity. Operators C perform the luggage check-activity and operators D perform a physical check when a passenger is suspicious. The black dots represent the luggage divest and luggage collect positions. Figure 3 shows three divest and three collect positions per lane, respectively. The number of divest and collect positions can vary depending on the input to the model.

The gate area consists of two non-Schengen gates (the two most left of Figure 3) and five Schengen gates. Each gate consists of seats, a queue for boarding and a boarding agent. The passengers can use the queue to line up before boarding. The seats can be used by the passengers when waiting before boarding. For case study 3, described in Section 6.3, only the most left non-Schengen gate is considered, which has 100 seats. Since airport operators have to guarantee physical distancing, only every second seat is available for the passengers. The other seats are marked as "blocked".

4.2 Specification of the agents

The model contains three types of agents: passenger agents adhering to COVID-19 rules, passenger agents not adhering to COVID-19 rules and operator agents. These three types all share the AATOM cognitive architecture described by [Janssen et al., 2018] and shown in Figure 4. The shaded blocks of Figure 4 show the extensions and improvements made to the baseline AATOM model.

Agents have a certain set of goals that determine their behaviour. Their goals are stored in their goal module. Using the planning module, agents can generate plans based on their goals. Besides planning, agents can perform analysis (about e.g., the environment) and make decisions (about e.g., activities). This is modelled in the analysis module and the decision-making module.

Agents can observe the environment and perceive commands using their perception module. Their observations are interpreted in the interpretation module. With interpreted observations, agents can maintain or update their beliefs (e.g., about the availability of a check-in desk).

The navigation module is used to navigate and to determine a collision-free path to the agent's goal. In the activity module, a sequence of planned activities is generated. Together with the navigation module, this sequence of planned activities is fed as a command into the actuation module. In the actuation module, the actions to complete the activities are performed. Also, the walking behaviour of the agents is modelled in the actuation module.

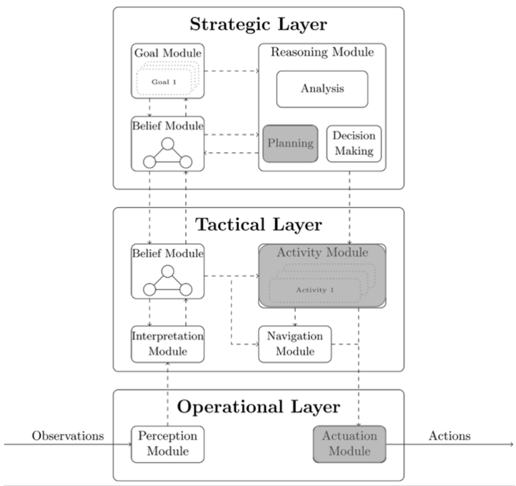

Figure 4: Cognitive architecture of AATOM

4.2.1 Specification of passenger agents

Passenger agents can complete different activities, namely: check-in, security checkpoint, gate, boarding and queue activity. They are characterised by the same mass (80 kg), colour (red) and diameter (40 cm). The mass and the diameter of the passenger agents are used in the Helbing social force model. The Helbing social force model models the passengers' movement and is explained in Section 4.4.1. Passengers adhering to physical distancing are defined by their Helbing constants, $A = 250$ Newton and $B = 0.5$ meter. These passengers have a "Queue Stop Distance value" or simply Q constant of 1.5 meters. This means that during queuing, they stop at 1.5 meters behind other passenger agents. The Q constant is used in the queue activity, explained in 4.4.2. Passengers not adhering to physical distancing have A equal to 250 Newton, B equal to 0.1 meter and Q equal to 1 meter.

4.2.2 Specification of operator agents

Operator agents need to do specific tasks in the airport, namely: check-in, luggage assist, x-ray, luggage check, physical check and boarding activity. During the boarding activity, boarding operators have the goal to board passenger agents as quickly as possible. Boarding operator agents are defined by their boarding pass check time (t_{bc}) and their boarding group size (GS). The GS is the number of passenger agents that the operator can call to come boarding at the same time. The t_{bc} is the time the boarding operator needs to check the boarding pass of a passenger agent. The rest of the activities is explained in [Janssen et al., 2018].

4.3 Specification of the interactions between passenger agents and environment

The model considers three mandatory airport terminal activities for the passenger agents: check-in activity, security checkpoint activity and the boarding activity.

During the check-in activity a passenger agent has the goal to get checked-in as quickly as possible. Depending on the passengers flight, the passenger has to check-in at a certain check-in. If the desks of the respective check-in are already occupied, then the agent can queue in the designated queuing area. At the check-in, the passenger has to wait for some time t_{ci} according to variable normal distribution. The value of t_{ci} of is dependent on the check-in operator and is given in Table 1.

During the security checkpoint activity, a passenger has the goal to pass the security checkpoint as quickly as possible. If there is a divest point available at one of the security lanes, then the passenger can start the security checkpoint activity. The passenger first drops the luggage in a certain amount of time t_d at the divest area. Then if the walk-through metal detector is free, the passenger walks through this sensor. If the alarm of the sensor goes off, the passenger is physically checked by the security operators. Hereafter, the passenger can collect the luggage in a certain amount of time t_c at one of the available collection positions. The values of t_c and t_d are given in Table 2.

During the boarding activity, the passenger has the goal to board as quickly as possible. While in pre-COVID-19 conditions passengers would board in any order (independent on their seat number) this model considers a specific boarding strategy. The procedure used in the model is called "back-to-front" procedure and is also advised by the EASA [Schultz and Soolaki, 2020]. This means that passengers are boarded by rows, starting with the last row at the back of the aircraft. As this requires some organisation, a boarding operator in the model is introduced for each gate. The boarding operator calls a specific group of passengers to start their boarding activity. The group of passengers then line up in front of the gate counter in the queuing area. The passengers board one by one. The boarding operator checks the boarding pass of every passenger. After all passengers of the boarding group are boarded, then directly a new group is called to board by the boarding operator.

4.4 Specification of the interactions between passenger agents

Physical distancing has an impact on the interaction between passengers. For this study, the movement module and the activity module of the baseline AATOM model were revised to include physical distancing between the agents when they are walking and when they are queuing.

4.4.1 Movement module: social force model

The Helbing social force model handles the movement of passenger agents [Helbing et al., 2000]. It is performed in the actuation module of the cognitive architecture presented in Figure 4. The model assumes that the passengers' movement is guided by a superposition of attractive and repulsive forces, determining the passengers' walking behaviour.

The formula to calculate the velocity change $d\vec{v}_i$ of each passenger i is given by Equation 1 and follows Newton Second Law. Each passenger i with mass m_i (in total there are N passengers) wants to move in direction of their goal $\vec{e}_i^0$ with a desired speed $\vec{v}_i^0$ (equal to 1.4 m/s). However, each passenger i needs to adapt its actual velocity $\vec{v}_i$ with time characteristic τ_i (equal to 0.5 sec) to keep distance with other passengers (j) and physical objects such as walls (W). The repulsive forces are expressed as $\vec{f_{ij}}$ and $\vec{f_{iW}}$. The repulsive forces consist out of a social repulsion force $\vec{f}_{social\ rep.}$, a pushing force $\vec{f}_{push}$ and a friction force $\vec{f}_{fric}$. The pushing force and a friction force refer to the forces when passengers collide with each other. These forces are not important for the model because passengers are not allowed to touch each other; they need to keep their distance. The social repulsion force $\vec{f}_{social\ rep.}$, on the other hand, is important for simulating physical distancing.

$$m_i \frac{d\vec{v}_i}{dt} = m_i \frac{v_i^0(t)\vec{e}_i^0(t) - \vec{v}_i(t)}{\tau_i} + \sum_{j(\neq i)} \vec{f}_{ij} + \sum_W \vec{f}_{iW} \tag{1}$$

The social repulsion force $\vec{f}_{social\ rep.}$ is modelled by Equation 2 and was calibrated in order to simulate physical distancing between the agents. It models the psychological tendency of two pedestrians i and j to stay away from each other. r_{ij} is the sum of the radii of pedestrian i with radius r_i and pedestrian j with radius j. d_{ij} is the absolute distance between the pedestrians i and j (taken from their center of mass). $\vec{n}_{ij}$ is the normalised vector from pedestrian j to i and is calculated by: $\vec{n}_{ij} = (n_{ij}^1, n_{ij}^2) = (\vec{r}_i - \vec{r}_j)/d_{ij}$. A_i and B_i are the "Helbing" constants [Helbing et al., 2000]. These Helbing constants define the distance between passengers and are therefore crucial in modelling physical distancing.

$$\vec{f}_{social\ rep.} = A_i e^{(r_{ij} - d_{ij})/B_i}\ \vec{n}_{ij} \tag{2}$$

In the baseline AATOM model, no difference was made between the social repulsion force of two agents and the social repulsion force of an agent and an object. The values of A and B for both scenarios were taken 250 [N] and 0.1 [m], respectively. However, in the model for this research study, the distinction is made between both. In this model, every passenger agent that performs physical distancing is given two sets of Helbing parameters. One set of parameters to simulate the social repulsion force of a passenger agent with the environment. Another set of parameters to simulate the social repulsion force of a passenger agent with other passenger agents. For the first set, the values of A and B were taken to be equal to the original values 250 [N] and 0.1 [m] such that emergence of the interactions is similar to the baseline AATOM model. For the second set, the B value was calibrated to represent physical distancing between agents. In Figure 5 one can see the impact of parameter B on the social repulsion force. The higher the B value, the earlier the social repulsion force is activated. The B was increased to 0.5 meter (while A remains 250 [N]). It was visually inspected by simulation that a B value 0.5 meter guarantees a physical distancing between passengers while still representing correct walking behaviour.

Figure 5: Plot of social repulsion force $f_{social\ repulsion}$ [N] vs distance between the passengers d_{ij} [m]. For both graphs A is 250 [N]. The blue graph is the social repulsion force of the baseline AATOM model (when agents are not physically distancing). The orange graph is the social repulsion force for the extended AATOM model where agents are physically distancing.

4.4.2 Activity module: queue activity

For this study, the queue activity, which is a part of the activity model, was defined. In the activity module the activities, an agent will execute, are prepared based on the inputs from the reasoning module (which is part of the strategic layer).

The queue activity is executed by a passenger agent when the next planned activity cannot be executed due to capacity limitations. For example, when an agent is at the end of the check-in queue and observes that all desks are occupied then queue activity is executed. Passenger agents also perform the queue activity when other passengers are queuing in front of them. The queue activity is modelled as a sequence of waiting periods. It ends when the passenger agent in front moves forward, or when the planned next activity is available [Janssen et al., 2018].

In the baseline AATOM model, passengers were queueing 1 meter from each other. For this research study, the distance (or Q value, explained in Section 4.2.1) was increased to 1.5 meters for passengers adhering to physical distancing.

4.5 Metrics for airport operations performance and passenger health safety

Two analysers were added to the model to analyse the passenger health safety. The agent-based model is able to identify at each time point which passenger agents are not performing physical distancing, this will be referred to as using "agents that are in contact". One analyser was implemented in the model that represents the number of passengers that are in contact at every time step. This is shown in Figure 6(a). This analyser is used to determine the contact locations.

A second analyser, presented in Figure 6(b), integrates the first and represents the total time of all passengers that were in contact. This analyser is used as a metric for results of the case studies presented in Section 7. A third analyser, in Figure 6(c), shows the summed contact time but with a distinction between 'face-to-face' contacts and 'everything-back contacts'.

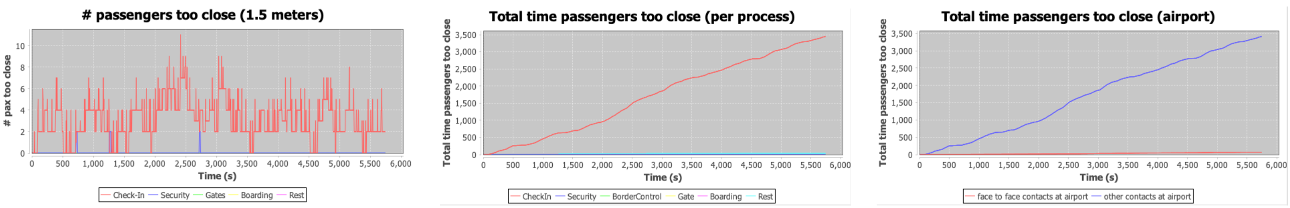

(a) Analyser showing the amount of agents that are in contact at every time step and at which location. Case study 1: scenario 5.

(b) Analyser showing summed time of all passengers that were in contact. The amount of contacts (figure on the left) are integrated over time. Case study 1: scenario 5.

(c) Analyser showing summed time of all passengers that were in contact "face-to-face" and "everything-back". Case study 1: scenario 5.

Figure 6: The passenger contact analysers

The orientation of each passenger is calculated based on the speed vector of the passenger's last movement. Using the orientation, a distinction is made between two type of contacts: "Face-to-face" contacts, shown in Figure 7(b) and "Everything-back" contacts, shown in Figure 7(c) and Figure 7(d). "Face-to-face" contacts are defined as passengers that are closer than 1.5 meter from each other and are facing each other: they are in front of each other and their difference in orientation is larger than 100 degrees. "Face-to-face" contacts are considered as the worst type of contact because virus particles can be spread more direct [Sciensano, 2021].

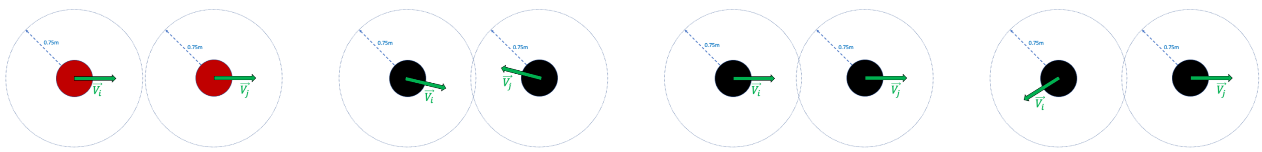

(a) Physical distancing (b) Face-to-face contact (c) Face-to-back contact (d) Back-to-back contact

Figure 7: Type of contacts

5 Verification

An essential step in the development of the agent-based model is verification. This section explains the actions taken to verify the agent-based model.

Verification is the process of determining that the agent-based model implementation correctly represents the requirements or the specification of the model. In essence, this means that we need to check if the model does what we think it is supposed to do [Ormerod and Rosewell, 2009].

Since the developments of new additions to the agent-based model was an iterative process, the verification was also iterative. All the extensions made to AATOM are visualized in the UML diagrams, Figure 1.1 and 1.2 of Supporting Work. After every addition to the model, a verification step was performed.

For the additions implemented in the movement module and the activity module, explained in Section 4.4.1 and 4.4.2, physical distancing was verified by observation. The advantage of the Graphical User Interface (GUI) option in AATOM, is that it gives you direct feedback about the model's implementation. For the verification of the implementation of physical distancing, an extra feature to the model was added; the colour of a passenger turns black when the passenger is not performing physical distancing. Several tests were performed using the model set-up explained in Section 6.1. From the observations from the simulation runs, it was verified that moving passengers were physically distancing when using the new A and B values. For the queue activity, some bugs in the model were encountered. Since the Q values were increased to 1.5 meters, passengers were sometimes ending stuck in queues. Due to the increase in Q, passengers were sometimes queuing when they didn't need to: when they observed queueing passengers at the other side of a queue wall. This bug was fixed by adding an additional algorithm to the model, presented in Chapter 1 of Supporting Work. Additions made to the code were also always verified by using print commands. For instance, to verify which activity passenger agents performed, each passenger's activity was printed, including the agent identification to easily trace errors.

The safety metrics, explained in Section 4.5, were verified by comparing the GUI observations with the model's output graphs. For example, when the colour of two passenger agents turns black (which means they are not physically distancing), the safety metric graph should increase.

The throughput metric of each passenger's handling process was verified by comparing the number of generated agents with the throughput metric's output (how many passengers passed the check-in, security and boarding). As a result, we know that the throughput metric works correctly and no passenger agents are getting stuck because the throughput matches the number of agents generated.

Lastly, the model was also verified for rare errors. Because the model is stochastic, errors in the code can still exist if one only checks for errors by running a few simulations. Therefore, the model was tested by running many simulations (over 1000 simulations per model set-up). Errors in the code could be found by checking for outliers in the output files. Since the random seed was logged for every simulation, outliers could be easily traced back to a particular simulation run.

6 Case studies

For this research, three different case studies are performed. The first three case studies each analyse one process at the airport in depth. The check-in process is analysed in Section 6.1. The security process is analysed in Section 6.2. The boarding process is analysed in Section 6.3. In each case study, different hypotheses are answered by simulating various scenarios in which different COVID-19 measures are modelled. Every scenario is simulated 450 times on the server. These three case studies all share a common goal: they aim to analyse the impact of the COVID-19 measures on the performance of the process and the passengers' health safety. The model set-up and the used metrics are explained in the following three sections.

6.1 Case study 1: check-in

In this case study only the check-in is considered, as presented in Figure 3. This case study aims to analyse the impact of three COVID-19 measures: First, the impact of physical distancing between passengers. Secondly, the impact of longer waiting times at the desk due to additional paperwork related to COVID-19. Thirdly, the impact of a different queue lay out, for instance three straight queues instead of one commong zig-zag queue.

The following three metrics are developed to analyse the effect of these measures on the system's performance and the associated health safety of the passengers:

1. Check-in throughput T_C, calculated in passengers per hour. Check-in throughput is defined as the number of passengers that were served by a check-in area in a specific time period. Note a check-in area consists out of three check-in desks, as explained in Section 4.1.

2. Average contact time per passenger C_{pax}, calculated in seconds. Contact time per passenger is defined as the time duration for which a passenger agent is not able to perform at least 1.5 meters physical distancing. For the check-in case study, two variants of this metric were designed. Namely, A) the average contact time per passenger in the check-in queue $C_{pax_{CQ}}$. This metric only considers the contact time of a passenger for which the passenger was in the queue during the check-in process. B) The average contact time per passenger at the check-in desk $C_{pax_{CD}}$. This metric is thus only calculated for the passengers that are at the desk. These two variants were implemented to understand at which location the passenger is exposed the most: in the queue or at the desk.

Using these metrics, five different hypotheses were found to be the most interesting to analyse:

- **Hypothesis 1:** Physical distancing decreases check-in throughput T_C.
- **Hypothesis 2:** Physical distancing decreases average contact time per passenger in the queue $C_{pax_{CQ}}$.
- **Hypothesis 3:** A 20% increase in check-in time t_{ci} increases the average contact time per passenger in the queue $C_{pax_{CQ}}$.
- **Hypothesis 4:** Three single straight queues (instead of one common zig-zag queue) result in a higher check-in throughput T_C.

- **Hypothesis 5:** Three single straight queues (instead of one common zig-zag queue) result in a lower average contact time per passenger $C_{pax_{CQ}}$.

These four hypotheses are tested by simulating five different scenarios. The environment for each scenario is the check-in area, as shown in Figure 3. Passenger agents are generated in front of check-in queue and they only perform the check-in activity and the queue activity. The inputs to the model for each scenario are given in Table 1.

Scenario 1 models a pre-COVID-19 situation. No COVID-19 measures are modelled in this scenario. Thus, passenger agents do not perform physical distancing. No extra paperwork is required. Therefore, the check-in time t_{ci} follows a normal distribution with a mean of 60 minutes and a variance of 6 minutes. This is based on data that is gathered before COVID-19 [Janssen et al., 2019] [Janssen et al., 2020]. Passenger agents are using a common zig-zag queue (explained in Section section 4.1). In scenario 2, the 1.5-meter physical distancing measure is modelled. Scenario 1 and 2 are used to test hypotheses 1 and 2. In scenario 3, a 20% increase in check-in time t_{ci} is modelled, thus N(72,6), in order to account for additional health questions and more paperwork related to COVID-19. This scenario is used to test hypothesis 3. In scenario 4, the measures of scenario 2 and 3 are modelled together. Lastly, in scenario 5 passenger agents use a straight check-in queue instead of a common zig-zag queue. This scenario is used to test hypotheses 4 and 5.

6.2 Case study 2: security

Case study 2 only considers the security process. This case study's environment is the security checkpoint area, as shown in Figure 3. This case study aims to analyse the impact of the COVID-19 measures on the performance of the security checkpoints and the associated passenger health safety. Similar metrics as for the check-in case study are used, namely:

1. Average security throughput T_S, calculated in passengers per hour. Security throughput is defined as the number of passengers that were served by two security lanes in a specific time period.

2. Average contact time per passenger C_{pax}, calculated in seconds. Two variants of this metric were designed to identify at which location most contacts occur. Namely, A) the average contact time per passenger in the security queue $C_{pax_{SQ}}$. B) The average contact time per passenger at the security lane $C_{pax_{SL}}$.

Also for this case study some hypotheses were found interesting to be analyzed:

- **Hypothesis 6**: An increase in luggage divest time t_d and luggage collect time t_c result in a lower security throughput T_S.
- **Hypothesis 7**: An increase in luggage divest time t_d and luggage collect time t_c result a higher average contact time per passenger $C_{pax_{SL}}$ and $C_{pax_{SQ}}$.
- **Hypothesis 8**: Less luggage divest n_d and luggage collect n_c positions result in a lower average contact time per passenger $C_{pax_{SL}}$ and $C_{pax_{SQ}}$.

To test these hypotheses seven different scenarios were designed. In each scenario, only two security lanes are open. Passenger agents are generated in front of the queue of the security checkpoint. They only perform the queue activity and the security checkpoint activity. The inputs to the model for each scenario are given in Table 2.

Scenario 1 is the baseline scenario with parameters simulating the pre-COVID19 situation, thus without any COVID-19 measures. Three luggage divest n_d and three luggage collect n_c positions are implemented per lane. Thus, passenger agents are standing there close to each other. The distributions for the luggage divest time t_d and the collect time t_c are based on [Janssen et al., 2019].

Scenario 2 considers an increase of 20% in divest time t_d and collection time t_c. From interviews with airport stakeholders it was revealed that security operators do not actively support passengers anymore during divesting which results in more time needed for passengers. When passengers place items incorrectly in the trays, operators try to minimise contact with the passengers' belongings. Therefore, they let passengers rather reorganise their items themselves which results in additional time. This scenario is used to test hypothesis 6 and 7.

Scenario 4, 5, 6 and 7 consider different number divest n_d and collect positions n_c. Since the divesting and collection area is generally very crowded, pre-COVID-19 configurations with three divest positions and three collect positions per lane do not correspond to physical distance regulations any longer. These scenarios are used to test hypothesis 8.

6.3 Case study 3: boarding

For case study 3, only boarding is considered. Only one gate area is considered as explained in Section 4.1 and shown in Figure 3. This case study aims to analyse the impact of the COVID-19 measures on the boarding procedure. For this case study, 50 passengers are considered representing a regional flight with a B737 with a load-factor of 1/3, based on expert knowledge [Dilweg, 2021]. It is assumed that 50 passengers are all sitting at the start of the simulation. For this case study two metrics are considered, namely:

1. The average time to board 50 passengers T_B, calculated in minutes. Note: the time starts when the first passenger agent starts the boarding process (when the passenger agent leaves the seat) and it ends when the last (50th) passenger agent is boarded.
2. The average contact time per passenger C_{pax}, calculated in minutes.

Using these metrics, four different hypotheses were found interesting to be analysed:

- **Hypothesis 9**: Physical distancing increases the total time to board 50 passengers T_B.
- **Hypothesis 10**: Boarding in smaller groups increases the total time to board 50 passengers T_B.
- **Hypothesis 11**: Boarding in smaller groups decreases the average time passengers are in contact C_{pax}.
- **Hypothesis 12**: A higher average boarding pass check-time t_{bc} increases the average time passengers are in contact C_{pax}.

These hypotheses are tested by simulating four different scenarios. The inputs to the model for each scenario are given in Table 3. Scenario 1 is the baseline scenario in which passengers do not maintain physical distance, they board in groups of 10 and the t_{bc} follows a normal distribution with mean 10 seconds and variance 1 second. In scenario 2, passengers board in smaller groups of 5 passengers. This scenario is used to test hypotheses 10 and 11. In scenario 3 physical distancing is modelled to test hypothesis 9. Lastly, for hypothesis 12 scenario 4 simulates the impact of a higher t_{bc} because airlines often ask health questions (related to COVID-19) before checking the boarding pass.

7 Results

In this section the results for the case studies of section 6 are discussed. To test each hypothesis also the results from the global sensitivity analysis and the Vargha-Delaney A-test are used. The coefficients of correlation and the A-test values are presented in Section 2.3 and 2.4 of Supporting Work.

7.1 Results for case study 1: check-in

Table 1 presents the results of the check-in case study, Section 6.1.

For hypothesis 1, Table 1 shows that scenario 1 and 2 result in the same check-in throughput T_C, namely 167 passengers per hour. This means that physical distancing PD does not influence the check-in throughput T_C. This was confirmed by the coefficient of correlation $\rho_{PD,T_C} = -0.11$ with p-value $= 0$. Since the $\rho_{PD,T_C} < 0.4$ (rule of thumb) we can say there is no significant correlation between these two variables. Also, A_{12}-value is close to 0.5, meaning there is no significant difference in throughput for the two scenarios. Thus, we can **reject hypothesis 1**.

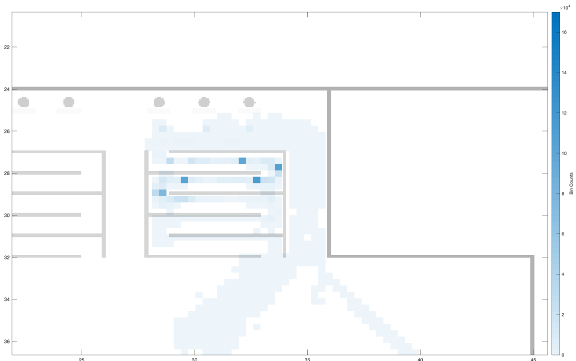

Figure 8: Heatmap scenario 2. The dark blue areas represent the hot spots of passenger contacts.

For hypothesis 2, Table 1 shows that in scenario 1 a passenger is on average 4 seconds in contact at the desk $C_{pax_{CD}}$ and 1 minute and 25 seconds in contact with other passengers in the queue $C_{pax_{CQ}}$. For scenario 2, $C_{pax_{CD}}$ is the same but $C_{pax_{CQ}}$ reduced with 41%. This means that physical distancing does decrease $C_{pax_{CQ}}$. This is confirmed by the strong negative correlation coefficient: $\rho_{PD,C_{pax_{CQ}}} = -0.9$ with p-value $= 0$. Therefore, we can **support hypothesis 2**.

For hypothesis 3, it can be deduced from scenario 3 in Table 1 that an extra 20% more check-in time t_{ci} (due to e.g., extra COVID-19 related paper work) increases the average contact time per passenger in the queue $C_{pax_{CQ}}$ by 23%. The coefficient of correlation $\rho_{t_{ci},C_{pax_{CQ}}} = +0.72$ with $p = 0$. This means there is a significant positive correlation between t_{ci} and $C_{pax_{CQ}}$. Therefore, we can **support hypothesis 3**. This is reasonable because t_{ci} also reduces the check-in throughput T_C with 16 % which results in longer waiting times for passengers in the queue.

For hypothesis 4 and 5, three single queues were implemented in scenario 5 instead of one common zig-zag queue. Table 1 reveals that straight queues increase passenger throughput with a small 3%. The coefficient of correlation ρ_{QT,T_C} equals 0.24, which is lower than 0.4, meaning there is no significant correlation. We can **reject hypothesis 4**.

The introduction of three single queues also reduced $C_{pax_{CD}}$ by 50% and $C_{pax_{CQ}}$ by 42%. The coefficients of correlation $\rho_{QT,C_{pax_{CD}}}$ and $\rho_{QT,C_{pax_{CQ}}}$ are -0.86 and -0.74. This confirms that single queues reduce the average contact time per passenger C_{pax}. **Hypothesis 5** can be **supported**. The reason for this reduction is threefold: 1. Due to the three straight queues, the passenger flow from the end of the queue towards the check-in desk is more efficient. Fewer passengers interfere with each other because there are three queue exits instead of one. 2. The absence of corners in a straight queue. Figure 8 shows that in a zig-zag most contacts occur in the corners (dark blue dots). In a straight queue, Passengers do not need to turn while queuing. When passengers are turning, they focus less on other passengers than when they walk in a straight line. 3. The model implementation: a passenger agent is programmed to stop when observing other passenger agents that are in queueing mode and are at 1.5 meters distance. At corners, the passenger's observation can be blocked by a wall which causes that other passenger agents are observed too late (when the passengers are already closer than 1.5 meters).

Table 1: Results of case study 1: check-in. PD means physical distancing, t_{ci} means time to check-in. Note that percentages are given w.r.t. the baseline scenario 1. For every scenario 450 simulations were performed.

Check-in scenario	Input to Model			T_C			$C_{pax_{CD}}$			$C_{pax_{CQ}}$		
	Queue Type	PD	t_{ci} [sec]	μ [pax/h]		σ^2 [pax^2/h^2]	μ [min:sec]		σ^2 [sec^2]	μ [min:sec]		σ^2 [sec^2]
1	One common	No	N(60,6)	167		0.3136	00:04		0.0410	01:25		1.6543
2	One common	Yes	N(60,6)	167	0%	0.3548	00:04	0%	0.0365	00:50	-41%	3.1109
3	One common	No	N(72,6)	140	-16%	0.4750	00:04	0%	0.0334	01:45	23%	1.9986
4	One common	Yes	N(72,6)	140	-16%	0.6131	00:04	0%	0.0337	01:03	-26%	6.2027
5	Three single	Yes	N(72,6)	145	-13%	0.3422	00:02	-50%	0.0194	00:27	-68%	23.773

7.2 Results for case study 2: security

Table 2 presents the results for this case study. In the baseline scenario, where the parameters from [Janssen et al., 2019] were used, the throughout for the 2 lanes T_S is 230 passengers per hour. This is equal to 1.92 passengers per minute per lane, which is in line with the findings of [Janssen et al., 2019]. As for the check-in case study, we observe from scenario 3 that physical distancing PD does not influence the security's throughput. Because the physical distancing is already analysed in the previous case study, no further analysis is needed.

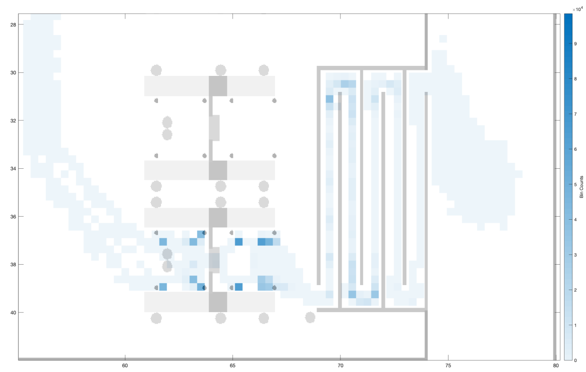

Figure 9: Heatmap scenario 3. The dark blue areas represent the hot spots of passenger contacts.

For hypotheses 6 and 7, scenario 1 and 2 can be compared. In scenario 2, a 20% increase in divest t_d and collect t_c time was implemented (because operators do not actively support passengers to diminish the interactions). Table 2 shows that an increase in t_d and t_c has a negative influence on the throughput T_S. Throughput reduces by 10%. This reduction is supported by the coefficient of correlation $\rho_{t_d,T_S} = \rho_{t_c,T_S} = -0.51$ with a p-value of 0. Therefore **hypothesis 6** can be **supported**. The average contact time per passenger at the security lane $C_{pax_{SL}}$ and in the queue $C_{pax_{SQ}}$ increased by around 13% and 15%. The coefficients of correlation are 0.42 and 0.39. Since this is lower than 0.4 (rule of thumb), we can't say there is a significant correlation. Therefore, we need to **reject hypothesis 7**.

From Figure 9, it was observed that most contacts happen at the luggage divest and collect area of the security system, therefore different number of luggage divest n_d and collect n_c positions were implemented. For Hypothesis 8 we can compare scenario 4, 5, 6 and 7 in Table 2. Table 2 shows that a reduction in n_d and n_c lowers the average contact time per passenger at the security lane $C_{pax_{SL}}$. This correlation is confirmed by the coefficients: $\rho_{n_d,C_{pax_{SL}}} = 0.9$ and $\rho_{n_c,C_{pax_{SL}}} = 0.76$ (both with $p = 0$). **Hypothesis 8** can be **supported**.

However, Table 2 also shows that a reduction in n_d and n_c lowers the security throughput T_S. To find an optimal between the positive influence of n_d and n_c on the C_{pax} and the negative influence on T_S, some more analysis of the scenarios is needed:

Comparing scenario 4 with scenario 5 shows that a "one divest position less" measure improves the $C_{pax_{SL}}$ better than "one collect position less". From this, we can conclude in the luggage divest area more passenger contacts happen than in the collect area. Both measures have almost the same impact on security throughput T_S, around 160 passengers per hour.

In scenario 6, one divest position less (scenario 4) and one collect position less (scenario 5) were implemented together. Table 2 shows that throughput reduces to 137 passengers per hour. The contact time at the security lane is reduced to 9 seconds per passenger, which means that almost no contacts occur at the security lane.

Lastly, in scenario 7 only 1 divest position and 1 collect position per lane was implmented. For this scenario, the throughput T_S dropped even further to only 69 passengers per hour. The average contact time per passenger at the security lane dropped to 2 seconds per passenger while the contact time in the queue increased to 4 minutes and 20 seconds.

From this comparison, my recommendation to airport managers is to have only two divest and two collect positions per lane (as simulated in scenario 6) to adequately diminish passenger interactions. However, as this measure reduces the throughput to only 137 passengers per hour, opening of an additional lane should be considered to decrease queueing time.

Table 2: Results of case study 2: security. PD means physical distancing, t_d luggage drop time, t_c luggage collect time, n_d number of divest positions per lane and n_c number of collect positions per lane. Note that percentages are given w.r.t. the baseline scenario 1. For every scenario 450 simulations were performed.

Security scenario	Input to Model					T_S			$C_{pax_{SL}}$			$C_{pax_{SQ}}$		
	PD	t_d [sec]	t_c [sec]	n_d	n_c	μ [pax/h]		σ^2 [pax^2/h^2]	μ [min:sec]		σ^2 [sec^2]	μ [min:sec]		σ^2 [sec^2]
1	No	N(54, 36)	N(71, 54)	3	3	230		15.9250	01:05		3.1485	01:52		4.9035
2	No	N(65, 36)	N(85, 54)	3	3	206	-10%	12.9633	01:13	13%	2.9601	02:09	15%	3.2523
3	Yes	N(65, 36)	N(85, 54)	3	3	206	-10%	15.0640	01:13	12%	4.9906	01:13	-35%	31.879
4	Yes	N(65, 36)	N(85, 54)	2	3	165	-28%	13.8631	00:28	-57%	7.6131	01:36	-15%	68.954
5	Yes	N(65, 36)	N(85, 54)	3	2	155	-33%	16.8833	00:59	-9%	7.9570	01:51	-1%	75.153
6	Yes	N(65, 36)	N(85, 54)	2	2	137	-40%	10.1974	00:09	-86%	3.9940	02:01	8%	78.221
7	Yes	N(65, 36)	N(85, 54)	1	1	69	-70%	17.7884	00:02	-97%	0.2418	04:20	132%	559.09

7.3 Results for case study 3: boarding

In case study, 3 different boarding strategies were analysed. In total 5 scenarios were simulated. The results are shown in Table 3.

For hypothesis 9, scenario 2 and 3 are compared. Scenario 2 in Table 3 shows that when passengers are not performing physical distancing PD, the time to board 50 passengers T_B is 4 minutes and 49 seconds. When passengers are performing physical distancing the time to board 50 passengers is 4% higher. This is also confirmed by the coefficient of correlation ρ_{PD,T_B} equal to 0.61 and the *p*-value equal to 0 which means there is a significant positive correlation. Thus **hypothesis 9** can be **supported**. This makes sense because passengers need more time to organise themselves in the queue, especially at the beginning of the queue.

For hypotheses 10 and 11, scenario 1 and 2 are compared. Scenario 2 shows that when passengers are boarding in smaller groups GS (five passengers instead of ten) the time to board 50 passengers T_B increases by 12%. The average contact time per passenger C_{pax} decreases by 52%. This is also reflected by the coefficients of correlation which are $\rho_{GS,T_B} = -0.8$ (*p*-value of 0) and $\rho_{GS,C_{pax}} = 0.9$ (*p*-value of 0). Therefore **hypothesis 10 and 11** can be **supported**. We can conclude that splitting a boarding group in two does not imply that the total boarding time doubles. This finding is important for airports with limited space at gates for queueing.

Since some airlines ask additional questions related to COVID-19 during scanning of the boarding pass, passengers need to wait longer at the gate counter. Therefore, an increase of 10 seconds in boarding pass check time t_{bc} was implemented in scenario 4. To check hypothesis 12, scenario 3 and scenario 4 can be compared. Scenario 4 in Table 3 shows that an in increase in boarding check time t_{bc} increases the average time a passenger is in contact C_{pax} with 4 seconds. The coefficient of correlation $\rho_{t_{bc},C_{pax}} = 0.6$ with a *p*-value of 0. Therefore, **hypothesis 12** can be **supported**. Moreover, it can also be seen from Table 3 that the total boarding time T_B significantly increases. Thus, the waiting time at the gate counter should be minimised as much as possible because it significantly influences the total boarding time and the average contact time per passenger. We can recommend that administrative questions should be asked in advance, for example, during online check-in.

Table 3: Results of case study 3: boarding. GS means boarding group size, PD means physical distancing and t_{bc} means boarding pass check time. Note that percentages are given w.r.t. the baseline scenario 1. For every scenario 450 simulations were performed.

Boarding scenario	Input to Model			T_B			C_{pax}		
	GS	PD	t_{bc} [sec]	μ [min:sec]		σ^2 [sec^2]	μ [min:sec]		σ^2 [sec^2]
1	10 pax	No	10	10:45		10.9984	01:04		1.1028
2	5 pax	No	10	12:03	12%	21.5824	00:31	-52%	1.2914
3	5 pax	Yes	10	12:28	16%	24.4984	00:08	-88%	5.6517
4	5 pax	Yes	20	20:49	94%	25.3051	00:12	-81%	18.645
5	1 pax	Yes	20	34:25	220%	37.7517	00:00	-100%	0

8 Discussion

The proposed agent-based model simulates the main airport handling processes of passengers at an airport under COVID-19 circumstances. The purpose of the model is to understand the impact of the COVID-19 measures on airport operations' performance and the associated health for passengers. The model is an extension of the baseline AATOM model and includes a redefined passenger dynamics model based on the social force model of Helbing to simulate physical distancing. The agent-based model also consists of a new model environment (check-in, security and boarding infrastructure) to represent realistically an airport under COVID-19 conditions. The metrics to assess the health safety of the passengers are based on existing studies regarding COVID-19 transmission. Because of the COVID-19 pandemic, passenger safety has become an essential item/topic on airport operators' agenda. With the possibility of new pandemics arising, this study is not only relevant for today but also for the future. This study can help airport operators in their decision-making and make airports more resilient for future crises.

The results from the three case studies are airport specific because the parameters used were specific to a particular regional airport. Data was taken from [Janssen et al., 2019] [Janssen et al., 2020] to calibrate the parameters for the case studies done with the model. As every airport has different distributions of passenger types and different infrastructure and personal, the used parameters can thus not per se be copied to represent other airports. Also, since there is not much work done in the field of agent-based models used for both the analysis of the airport operations performance and for the associated passenger health safety. It is difficult to compare the results with other studies. However, as explained in related work, there exist studies regarding these two fields considered separately. The obtained results for the throughput metric of the baseline scenario for the check-in case study and the security case study are in line with the results presented in the [Janssen et al., 2019] [Janssen et al., 2020].

Regarding the results of the average contact time per passenger metric, there exists no research study to the best of the author's knowledge that uses this metric to assess passengers' health safety. However, there exist other papers with which the results can be qualitatively compared. Desart and Kohse also identified that the divest and collect area at the security lanes are critical [Desart and Kohse, 2020]. They found similar to this research study that security lanes can have no more than two divest and collect positions because otherwise, passenger health safety cannot be guaranteed. They also recommended reducing the amount of drop off and collect position to only two per lane. This paper also identified that the COVID-19 measures significantly impact the boarding procedure and specifically the total required boarding time. They also recognised that capacity at the gates for many airports is critical. It frequently does not facilitate enough space for passengers to sit and line up for boarding safely.

Although this study has proven to be useful in analysing the impact of the COVID-19 measures, this study also made some assumptions. The contact time metric used in this research study takes into account distance (a contact happens when passengers are closer than 1.5 meter from each other) and time (the time of a contact). However, the model does not distinguish between contacts that happen at 1 meter and contacts that happen at 1.4 meters. Both situations will result in the same output. However, in reality a closer contact would result in a higher risk of transmission. Additionally, the model does not take the vulnerability of passengers into account, e.g., older people

The model assumed that only 95% of the passengers are willing to perform physical distancing. In reality, the actual percentage of people adhering to rules varies and depends on many factors. For example, in some countries people adhere to rules better than people in other countries. The percentage can, however, easily be changed in the model.

The model assumes that every passenger is travelling alone. In reality, people can also travel in a group, for instance, a travelling family. The influence of travelling groups on health safety is thus not taken into account by the model. A travelling group can also imply an additional requirement for the boarding procedure. For example, when parents need to stay with their children, they need to be in the same boarding group. The model assigns passengers to a boarding group purely based on the aircraft's seat and does not consider additional requirements, such as a travelling family. Moreover, the model assumes that passengers are reacting immediately when they are called to board. However, in reality passengers sometimes do not pay attention or do not correctly understand the announcement.

Lastly, the model only considers check-in desks staffed with operators. However, in reality many airports have self-check-in desks as these can spread over the passenger demand and decrease costs. This research study does not consider how self-check-in desks can contribute to safer operations for passengers.

9 Conclusions and future work

This study aimed to analyse the impact of COVID-19 restrictions on airport operations' performance and the associated health safety of the passengers. An Agent-based Airport Terminal Operations Model (AATOM) was used for this research study. AATOM covers the main handling processes of passengers and it was expanded to include COVID-19 restrictions and to include passenger health safety analysers. To include the COVID-19 measures, the environment and the agents of the model were redefined. The agent-based model was used to explore three different case studies to analyse the impact of these measures on the check-in, the security and the boarding process, respectively. The measures' effects were all tested in different scenarios for each case study by analysing the maximum throughput and the average contact time per passenger for check-in and security. For the boarding case study, the time to board 50 passengers was analysed and the associated average contact time per passenger.

The results show that physical distancing during queueing does not affect the throughput of the check-in and the security process. Physical distancing does lead to passengers being less in contact with each other, and it also decreases the capacity of queues. Therefore, airport operators should expand their queueing area where possible because a shortage of queueing space could lead to overspilling queues with passengers being too close as a consequence.

The implementation of single queues instead of one common queue had a positive impact on the throughput of the check-in and the passengers' health safety. The flow towards desks is more efficient (with less interfering flows of passengers), and it is easier for physical distancing in single queues because no turning is required.

Furthermore, it was shown that in a pre-COVID-19 security lane set-up many passengers are too close at the luggage divest and collect area. The case study results showed that a decrease from three luggage divest and collect positions per lane to two positions of each per lane leads to a significant positive impact on passenger health safety while the throughput is still acceptable. However, to obtain the same throughput with one drop off and one collect position less it is advised to open an extra security lane. Implementing only one divest and one collect position per lane is unnecessary because it does not appropriately improve passenger health safety. Thus, two passengers per divest area and two per collect area is perfectly possible. Then, passengers can move without being closer than 1.5 meters from each other.

The boarding case study results showed that boarding in smaller groups positively impacts the average contact time per passenger. In contrast, it negatively affects the total boarding time. The results also showed that physical distance has a relatively small impact on the total boarding time because the organisation of the passengers lining up during queueing takes a bit more time.

Lastly, the results showed that extra paperwork due to COVID-19 at, e.g., the check-in desk should be minimised whenever possible. Additional paperwork leads to a higher waiting time, and this negatively affects the throughput. A lower throughput results in more people queuing and being exposed to each other. Therefore airport operators should advise passengers to perform as much paperwork as possible before entering the airport. For example, check-in and online questionnaires related to COVID-19 can be filled in online.

Future work on this topic involves improving the model further to represent reality better. Firstly, the movement module and the queueing activity of the AATOM model can be further calibrated to represent a more realistic walking behaviour of the passengers. Moreover, the boarding activity of the AATOM model can be further defined.

References

[Blue and Adler, 2001] Blue, V. and Adler, J. (2001). Cellular automata microsimulation for modeling bi-directional pedestrian walkways. *Transportation Research Part B Methodological*, 35:293–312.

[De Herdt, 2020] De Herdt, C. (2020). Massa mensen afgelopen weekend op luchthaven van Charleroi, viroloog Steven Van Gucht reageert verbaasd: "Jammer dat dit gebeurt". `https://www.nieuwsblad.be/cnt/dmf20201221_98258870`. Accessed on 2021/03/21.

[Desart and Kohse, 2020] Desart, B. and Kohse, U. (2020). Impact Assessment of Covid-19 Measures on Airport Operations & Capacity. Technical Report 1, Airport Research Center GmbH, Aachen.

[Dilweg, 2021] Dilweg, A. (2021). Interview with rotterdam the hague airport for msc thesis gregory. Personal Communication.

[EASA, 2020] EASA (2020). Covid-19 aviation health safety protocol - operational guidelines for the management of air passengers and aviation personnel in relation to the covid-19 pandemic. Technical report, European Union Aviation Safety Agency.

[Gipps and Marksjö, 1985] Gipps, P. G. and Marksjö, B. (1985). A micro-simulation model for pedestrian flows. *Mathematics and Computers in Simulation*, 27(2):95–105.

[Helbing et al., 2000] Helbing, D., Farkas, I., and Vicsek, T. (2000). Simulating dynamical features of escape panic. *Nature*, 407(6803):487–490.

[ICAO, 2020] ICAO (2020). Covid19 airport status. `https://www.icao.int/safety/Pages/COVID-19-Airport-Status.aspx`. Accessed on 2021-02-14.

[Janssen et al., 2018] Janssen, S., Knol, A., and Blok, A.-N. (2018). AATOM - An Agent-based Airport Terminal Operations Model. `http://stefjanssen.com/AATOMarchticeture.pdf`. Accessed on: 2021-02-19.

[Janssen et al., 2019] Janssen, S., Sharpanskykh, A., and Curran, R. (2019). Agent-based modelling and analysis of security and efficiency in airport terminals. *Transportation Research Part C: Emerging Technologies*, 100:142–160.

[Janssen et al., 2020] Janssen, S., van der Sommen, R., Dilweg, A., and Sharpanskykh, A. (2020). Data-Driven Analysis of Airport Security Checkpoint Operations. *Aerospace*, 7(6).

[Kierzkowski and Kisiel, 2020] Kierzkowski, A. and Kisiel, T. (2020). Simulation model of security control lane operation in the state of the COVID-19 epidemic. *Journal of Air Transport Management*, 88.

[Løvås, 1994] Løvås, G. G. (1994). Modeling and simulation of pedestrian traffic flow. *Transportation Research Part B: Methodological*, 28(6):429–443.

[Ma, 2013] Ma, W. (2013). *Agent-based model of passenger flows in airport terminals*. PhD thesis, Queensland University of Technology, Brisbane, Australia.

[Müller et al., 2020] Müller, S. A., Balmer, M., Neumann, A., and Nagel, K. (2020). Mobility traces and spreading of COVID-19. *medRxiv*, pages 1–22.

[Okazaki and Matsushita, 1993] Okazaki, S. and Matsushita, S. (1993). A Study of Simulation Model for Pedestrian Movement with Evacuation and Queuing. *Engineering for Crowd Safety*, 432.

[Ormerod and Rosewell, 2009] Ormerod, P. and Rosewell, B. (2009). Validation and Verification of Agent-Based Models in the Social Sciences BT. In Squazzoni, F., editor, *Epistemological Aspects of Computer Simulation in the Social Sciences*, pages 130–140, Berlin, Heidelberg. Springer Berlin Heidelberg.

[Ronchi and Lovreglio, 2020] Ronchi, E. and Lovreglio, R. (2020). Exposed: An occupant exposure model for confined spaces to retrofit crowd models during a pandemic. *Safety Science*, 130:104834.

[Schultz and Soolaki, 2020] Schultz, M. and Soolaki, M. (2020). Analytical approach to solve the problem of aircraft passenger boarding during the coronavirus pandemic. *Transportation Research Part C: Emerging Technologies*, page 19.

[Sciensano, 2021] Sciensano (2021). FACT SHEET COVID-19 disease (SARS-CoV-2 virus). `https://covid-19.sciensano.be/sites/default/files/Covid19/COVID-19_fact_sheet_ENG.pdf`. Accessed on: 2021/03/03.

[Teknomo et al., 2016] Teknomo, K., Takeyama, Y., and Inamura, H. (2016). Review on Microscopic Pedestrian Simulation Model. *arXiv e-prints*, page arXiv:1609.01808.

II

Literature Study
previously graded under AE4020

1 Introduction

1.1. Impact of COVID-19 on aviation

Since the outbreak of the COVID-19 virus governments have taken actions to mitigate the spread of the virus and to reduce COVID-19 deaths. As such, many countries closed their borders and people needed to stay at home. The passenger demand (in revenue passenger kilometer or RPK) of April 2020 has plunged 94.3 percent compared to April 2019. This is a rate of decline never seen in the history of IATAs traffic series, which dates back to 1990 [36].

A vaccin is currently considered as the only solution to completely eradicate the spread of COVID-19. Fortunately, there is a large global effort to develop vaccines and as of June 2020, at least ten vaccine candidates have already entered clinical trials, including phase II trials [75]. However, the European Medicines Agency (EMA) expects that it may take at least one year before a vaccine is approved and available for widespread use in the EU [23].

Even the situation remains very critical, the spread of the COVID-19 virus in many European countries decreased. As such lift mobility restrictions have been lifted in many countries. Also, business confidence is improving in key markets such as China, Germany and the US, according to Alexandre de Junac, IATA's Director General and CEO [36]. However, passenger demand at airports is still low compared to before COVID-19. Rotterdam The Hague Airport (RTHA) handled in June 2020 only 9.545 passengers, compared to the 244.450 passengers in June 2019 [58] [59]. Roland Berger, a global consultancy firm, predicts that it will take at least three to four years for the demand to recover back to the 2019 values. This prediction is in line other literature found. [48]

Thus airports are very slowly starting up. However, it is important that operations are executed safely and efficiently. Therefore in Europe, the European Aviation Safety Agency (EASA) has released guidelines for airports and airlines with measures to protect public health while at the same time allowing for viable air services to help the European economic recovery [35]. Some examples of restrictions are: Physical distancing, entry/exit temperature screening measures, prevent queuing, the use of personal protective equipment and many more.

These measures are actually also adopted in other public places such as restaurants, supermarkets, train station etc. Physical distancing and face masks are becoming accepted by the majority of citizens and are becoming part of daily life. It seems that we are entering a "new normal".

However, for airport operators it is still unknown what the impact will be on airport operations when passenger demand is rebounding back. In this master thesis, the impact of the COVID-19 restrictions on the terminal operations are assessed using the AATOM simulator, designed by Stef Janssen [66]. AATOM is an agent-based model to simulate movement and operations in the airport terminal. This model will be adjusted to incorporate the COVID-19 health measures and the output will be used to evaluate the safety of the passengers the airport. Also, the model will be used to identify bottlenecks in the airport and can serve as a validation of the measures for the airports.

During the literature study, it has been found out that currently there is a lack of models to simulate the airports under COVID-19 restrictions and to evaluate the performance in terms of safety and efficiency. This literature study investigates the different ingredients needed in order to make a model that fills the research gap.

1.2. Report Structure

The literature study starts with explaining the advised COVID-19 measures for airports in chapter 2.
Then terminal operations are more looked into in chapter 3. An analysis is made about the current practices in an airport terminal. This is important because this gives insight about how the advised restrictions will affect the current practices.

Secondly, the modelling methodology is explained. Agent Based Modelling (ABM) paradigm is explained in chapter 4. This chapter includes why this paradigm is very suitable for modelling the problem. Then a discussion of the architecture of AATOM is given in section 4.2, 4.3 and 4.4. An understanding of the AATOM architecture is needed to further adjust the model when the thesis is in a further stage. Pedestrian dynamics is discussed in chapter 5. In order to understand the necessary adjustments to implement physical distancing, first different pedestrian dynamics models are explained and compared in section 5.3. Then the necessary modifications of the Helbing model are given in section 5.5. Also decision-making is discussed in chapter 6. As the airport terminal is a highly complex environment, it is important to understand how humans make decisions. Also, decision-making is used in anticipation mechanisms to optimise resource allocation. Then after implementing physical distancing and decision-making, the results of the modified AATOM model will be used to do a model output analysis. This is discussed in chapter 7. The analysis will focus on the safety of the passengers and a model to analyse safety is proposed. To optimise safety and efficiency at the airport relevant resources, such e.g. opening a check-in desk, will be to be allocated in an optimal way. Theory is discussed in section 7.6.

The conclusion is given in chapter 8 and lastly, the research proposal and the project plan are given in chapter 9.

2

COVID-19 Restrictions

Fortunately, the aviation is slowly starting back up as countries are easing the travel restrictions and opening their borders. In order to restart aviation in an safe and efficient way, the European Aviation Safety Agency (EASA) has published guidelines for airports and airlines to restart their operations. In this chapter these guidelines are summarised and discussed. Also, the potential impact on the performance of the airport is analysed.

In EASA, IATA's and ACI's latest pressreleases [22] [1] [34] they listed several practices to which airports and airlines should adhere to. These measures are aimed to minimize the risk of transmission. The most relevant ones for the airport operations are listed below. Note, that as the current situation is very dynamic situation it is likely that advised measures will be adjusted. EASA states that "the recommended measures will be regularly evaluated and updated in line with changes in scientific knowledge of risk transmission as well as with development of other diagnostic or preventive measures (including technical) and evolution of the pandemic" [22]. Therefore a thorough follow up on these measures is of utmost importance.

This is a summary of the measures that are advised by European Union Aviation Safety Agency (EASA). As it seems that the published reports of IATA and ACI are based on this.

1. Implementing physical distancing (1.5 meters between individuals) (page 5 of [22]). Individuals travelling together as part of the same household are not required to maintain physical distance (page 3 of [22]).

2. Airport operators in cooperation with airline operators and other stakeholders where applicable, are encouraged to take appropriate measures to prevent queuing in high passenger concentration areas as much as practicable, in order to reduce the risk of contamination posed by unnecessary human interaction. In such queues floor markings 1.5 metres apart can assist passengers in maintaining physical distancing. (page 5 of [22]).

3. Access to airport terminals should be limited to passengers, crew members and staff. Accompanying persons should only be provided access in special circumstances, e.g. persons with reduced mobility (page 5 of [22]).

4. Contact and touching of surfaces should be minimised. The use electronic alternative processes is proposed (e.g. mobile check in, non-contact boarding) (page 5 of [22]).

5. Although, airport thermal screening equipment has proven to be inefficient in detecting individuals with COVID-19 [54] [22] (Annex 1). Still this technology is advised by EASA as it may help dissuade ill persons from travelling and enhance public confidence [22] (Annex 1). As such EASA advises to locate the equipment before check-in (ideally before the entrance of the terminal) for departing passengers and before baggage reclaim for arriving passengers.

6. EASA also advises passengers, staff and other stakeholder to use personal protective equipment (PPE). Passengers are advised to bring a mask from home and if that is not possible they should be able to buy or get one at the airport. Therefore airport operators are advised to install e.g. vending machines or other distribution channels [22].

7. EASA strongly recommends airport operators to enhance their cleaning activities and to provide disinfection for passengers, staff and other stakeholders. [22]

8. If passenger traffic permits, no adjacent security lines can be operated at the same time such that 1.5 meter physical distance between passengers is maintained [2].

Of all these recommendations, I personally think that the physical distancing will have the biggest impact on the performance of the airport. Because physical distancing will induce longer waiting times and the passenger throughput of the airport will decrease [11]. Generally, bottlenecks are usually the security checking areas and the check-in desks. Imposing physical distancing, will make it even more challenging. On the other hand, it is believed that the use of personal protective equipment, such as face masks, will have a negligible influence on the passenger throughput of the airport.

3
Airport Characteristics

This chapter discusses the airport characteristics. The passenger flow at airports is treated by explaining the process for departing passengers, then for arriving passengers and lastly for transferring passengers.

3.1. Overview of Passenger Flows at an Airport Terminal

Passenger flow can generally be categorised into three types: departing passengers, arriving passengers and transferring passengers. And each category of passengers use the airport in a specific way. For example, departing passengers do not make use of the luggage claim area while the arriving passengers do use the check-in desks. Below a picture of the ground plan of a regional airport can be found.

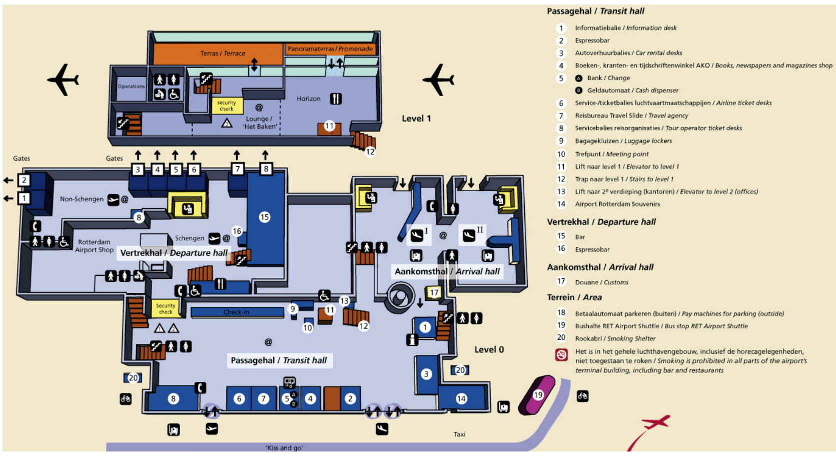

Figure 3.1: Ground plan of the Rotterdam The Hague Airport

The figure above shows the ground plan of Rotterdam The Hague Airport (RTHA). This is a regional airport as it mainly serves domestic and small continental traffic. It serves as a feeder for hubs for charter and origin and destination (O&D) airlines. In 2019, it handled 2.1 million passengers in total. However, due to the covid-19 outbreak RTHA handled only 453 passengers in April, 1113 passengers in May and 9945 in June [4]. Numbers are thus slowly increasing back. The airport terminal can be divided into three parts: the transit hall, the departure hall and the arrival hall.

The transit hall is the area where departing passengers enter the airport and arrived passengers leave the airport. In this area the departing passengers can check in at the check-in desks or make use of other facilities such as shopping or restaurants.

The transit hall and the departure hall are connected by the security check area. In this area, passengers are checked for illegal items such as e.g. weapons, flammable fluids or other dangerous goods. This is in order to prevent any threats and dangerous situations happening at the airport or aircraft and illegal goods entering a country. The screening of passengers and their luggage is done by both detection machines (e.g.

X-ray machines) and manual checks by security agents. After the security check, departing passengers can directly go to their gate or can first go shopping or eat a restaurant. Also, passengers with a Non-Schengen destination need to go through an additional security check - immigration or passport control. So, generally European airport departure halls can be divided into a Schengen and a Non-Schengen area. At the gate, there are usually seats where passengers can wait before boarding.

The arrival hall is solely used by arriving passengers (and connecting passengers). For arrived passengers from a Non-Schengen area they first need to go through immigration. Then the passengers are able to collect their baggage in the baggage reclaim area. Hereafter, normally Non-Schengen passengers also need to go through customs, where their baggage is inspected. Lastly, passengers can go to the transit hall and exit the airport.

3.1.1. Departing Passengers

Airports usually advice departing passengers to arrive at the airport 2 hours prior their flight-time for flights within the Schengen zone and 3 hours for long-haul flights [12]. Then, usually the process is as follows: check-in, security control, boarder control (for Non-Schengen) and boarding [47]. This is depicted in the figure below:

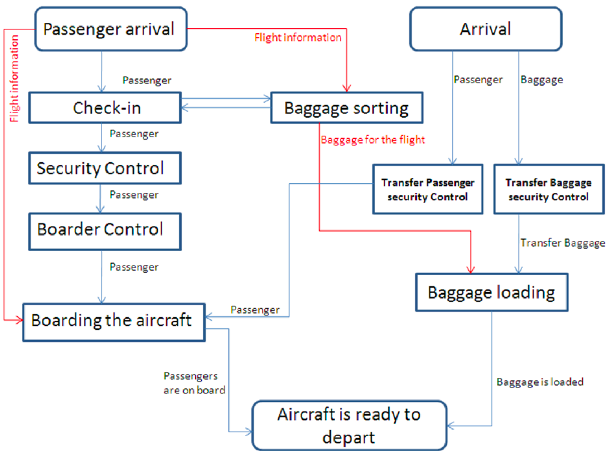

Figure 3.2: Process at terminal for departing passengers, from [47].

In the figure above, the flow of the baggage is depicted in red. Passengers can hand-over their baggage at the check-in and from there on the baggage is sorted, checked and loaded in the aircraft baggage compartment.

Note, that now due to COVID-19 many airports implemented an extra procedure: a temperature check before entering the airport terminal. Anyone whose temperature exceeds 38řC is screened a second time. If during this second screening the body temperature is again found to be higher than 38řC the passenger is directed to medical staff. The medical staff assesses this passenger further on COVID-19 symptoms. The medical staff may then refuse this passenger to enter the airport terminal if necessary. [12].

For the check-in some airports also provide self-check-in desks, where passengers can check-in without the help of check-in operators. As a result, decreasing the pay-roll costs of the airlines and decreasing the check-in time. Also now with the COVID-19 situation, the European Union Aviation Safety Agency (EASA) advises the use of self-check-in desks to decrease the risk of COVID-19 transmission.[22]

Also many airports already implemented systems for passenger guidance, such as queue counting indicators. With this system, passengers are able to see how many passengers are currently waiting in the queue and this thus helps the passengers in choosing which queue to join. This is also done in order to spread passengers more evenly out and increase the passenger throughput.[47]

Moreover, business passengers usually are more familiar with the airport procedures. They know better which items are prohibited to bring with them and now better how the security checks work, e.g. they know they need to take out their metal keys out of their pockets etc. Therefore, they usually pass the security check faster than leisure passengers [62]. Therefore, many airports provide priority lanes for business travellers.

It is believed that in high peak hours, the security control and boarder control have the longest waiting time and are the bottlenecks [47]. Therefore, it is important to monitor these areas closely such that they do not become hot-spots for COVID-19 transmissions.

3.1.2. Arriving Passengers

When an aircraft arrives at the gate, the passengers are disembarked and are guided to the arrival hall. Now due to COVID-19 situation before entering the terminal hall, the passengers need to pass a temperature check (the same as for departing passengers).

After the temperature check, if the passenger is arriving from a Non-Schengen zone then the passenger first needs pass immigration before collecting baggage at the baggage reclaim area.

After collecting the luggage, the passenger can exit the terminal. The procedures and the flow of the baggage (in red) are presented in the figure below:

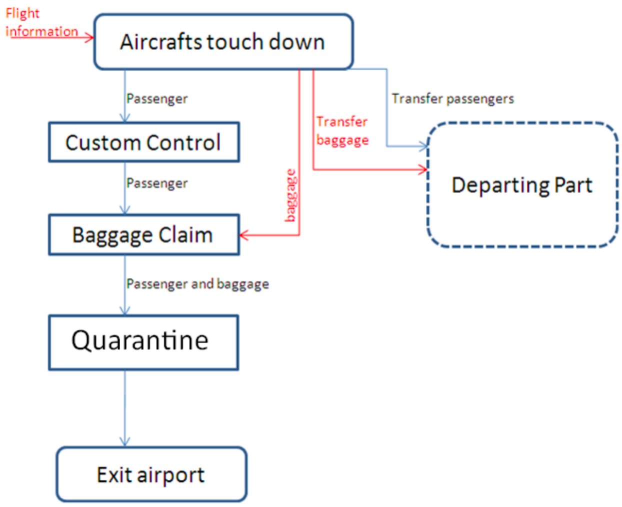

Figure 3.3: Process at terminal for arriving passengers, from [47].

3.1.3. Transferring Passengers

For passengers that need to transfer to another aircraft the procedure at the airport is a bit more complicated. The procedure is different depending on if baggage self-delivery is provided by the airport and the airline. If baggage self-delivery is provided then the baggage of the transferring passengers is forwarded to their final destination without passengers needing to reclaim and check-in again their baggage. Hereafter, they need to pass security control again to enter the departure hall. Then, they can directly go to their gate or make use of the facilities such as shops, restaurants or other services before boarding the aircraft. The process is presented in Figure 3.4.

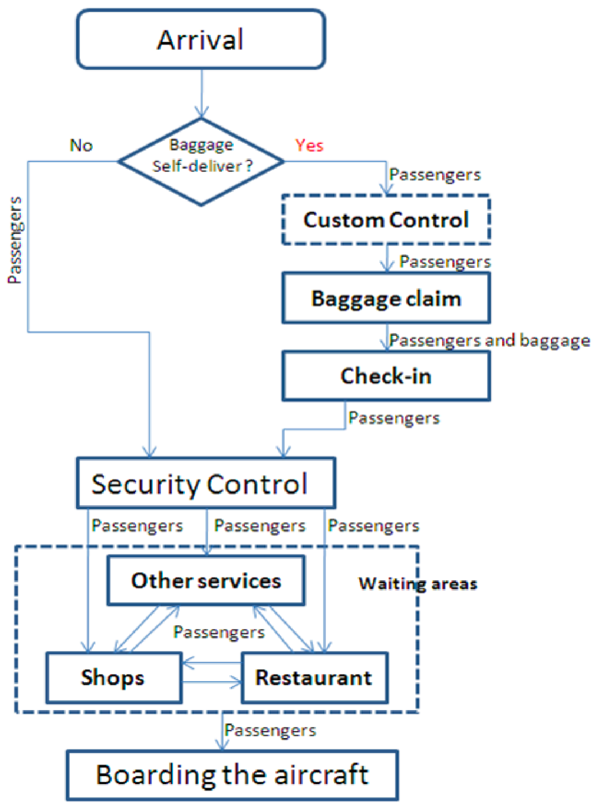

Figure 3.4: Process at terminal for transferring passengers, from [47].

4

Agent Based Modelling and AATOM

This chapter addresses the modelling methodology, which is agent-based modelling. Firstly, the modelling paradigm: Agent Based Modelling is explained in section 4.1. Secondly, the existing AATOM model is explained section 4.2, 4.3 and 4.4.

The scope of the research is to make a model that is both able to asses airports their efficiency and safety performance for the passengers. As explained earlier in the report, the airport is complex socio-technical system. The passengers need to follow a sequence of procedures in the airport. Considering also that passenger characteristics vary and influence their behaviour makes the system even more complicated. Also, the COVID-19 situation is dynamic as restrictions are modified regularly we need a model that is able to capture this highly complex system and is able to adapt to varying conditions.

The agent-based AATOM model developed by the PhD student S.A.M Janssen seems to satisfy these requirements.

4.1. Introduction to Agent Based Modelling

Agent based modelling is a good method to model and study complex socio-economic systems, such as airport operations [29]. It uses as bottom-up modelling approach. The passengers and airport staff are programmed as autonomous intelligent entities, called agents. These agents are modelled with a certain behaviour approximating humans and placed in a partially observable environment (the airport). The behaviours and interactions of the agents may be formalised by equations, but also more generally by (decision) rules (e.g. if-then kind of rules). As a result the modelling approach is very flexible [29]. In this way it allows to produce characteristics of the system emergence without having to make assumptions in advance regarding the system as a whole [29]. The simulation fills the gap between the individual behaviour of the passengers and the collective outcome on the airport operations performance. Also, the behavioural rules of agents can be varied ("heterogeneity") or random influences can be incorporated ("stochasticity"). Agents characteristics can be varied. For example: gender, age, business vs leisure and the walking speed (findings from chapter 3 can be integrated). Also agent-based simulation is ideal to study interdependencies between agent types and model emergences [29], for example which passenger type has a higher risk of COVID-19 infection. Agent based models are also very suited to study the resilience of the system [29], e.g. what the effect is of a sudden disruption in the flight schedule on the airport operations.

Finally, agent-based simulations are suited for detailed hypothesis-testing, more in particular to study the consequences of ex-ante hypotheses such as the interactions of agents and the emergence of the system as a whole [29]. It can be considered as a sort of magnifying glass to understand the reality better [29].

In the next section AATOM is discussed.

4.2. Introduction to AATOM

AATOM, the Agent-based Airport Terminal Operations Model simulator is designed by PhD student S.A.M Janssen. It is agent-based and contains calibrated templates of basic airport terminal configurations that can be easily adjusted and used for analysis of airport operations [39]. The model simulates the main handling processes for departing passengers in the airport terminal, this includes check-in, security checkpoint and border control. The model also includes facilities such as, bathrooms, restaurants and shops. The usefulness of the AATOM simulator has already be proven by several case studies, e.g. airport security [41], gate assignment [65] and resilience [10]. Agents in this simulator follow the AATOM architecture, an activity-based architecture for human airport agents [39]. The framework is explained in the next section.

4.3. AATOM Architecture

The AATOM simulator consists out of three layers, as depicted in Figure 4.1.

The top layer is called the "strategic layer". This layer is responsible for the strategy of the agent. This includes determination of goals, updating and maintaining a belief and reasoning [66]. Management of the agent's goals is done by the goal module. The agent's goal can be in three states: "not completed", "failed" and "succeeded". They all start as "non completed" and if they are met the goal state is updated to "succeeded" and if it cannot be met (before a certain time point or before another activity) then it is updated to "failed" [66]. The reasoning module includes three other modules which are the planning module, the analysis module and the decision making module. The analysis of the agent's current state is done in the analysis module. Using the planning module, agents can generate their plans based on their goals. These goal are translated in an ordered sequence of activities in order to maximise the completion of as many goals possible [66]. Decision making is done in the decision making module. An example can be the determination of which queue area to choose if there are multiple. [66]

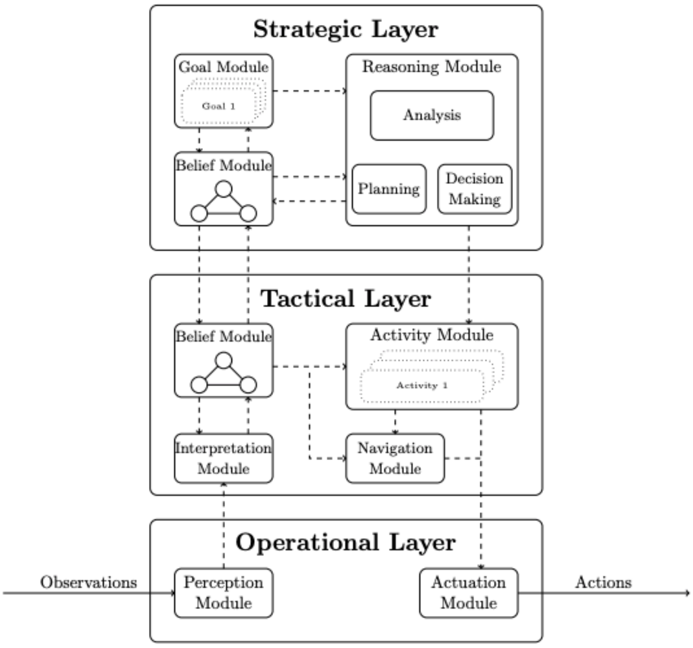

Figure 4.1: The AATOM architecture, from [66].

The middle layer is called the "tactical layer". The tactical layer is connecting the strategic layer and the operational layer. It is responsible for interpreting the perceived information from perception module and feeding this into the belief module of the strategic layer. Using the belief module, the agents are able to update and maintain their belief (e.g. characteristics, interpretation, activity and action state, plans) [66]. The activity and action state is updated when the status of the activity and actions has changed. Also, the belief module of the strategic layer automatically updates when a change is made. The activity module and the navigation module are able to access the information in the belief module in order to work accordingly [66]. The navigation module is used to navigate and to determine a collision free path to the agent's goal using path finding algorithms (e.g. A* [72] and Jump Point Search [28]). The determined path is a sequence of reference points and it is saved into the "path" variable [66]. In the activity module a sequence of planned activities is generated. This sequence of planned activities, together with the navigation module, is fed as a command into the actuation module. [66]

The bottom layer is called the "operational layer". It is responsible for the lower interaction with the

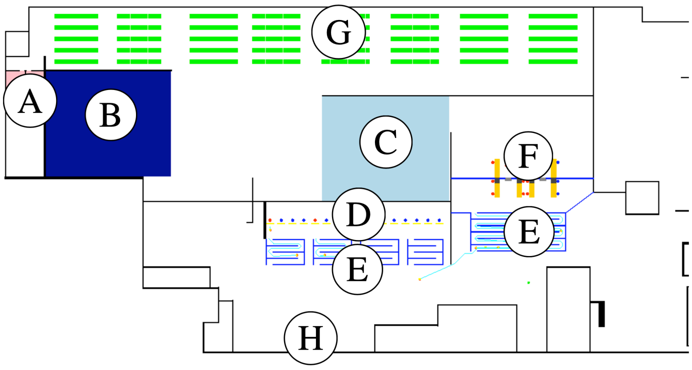

Figure 4.3: A visualisation of the AATOM environment with indicators showing the different areas [39]. Representation of Rotterdam the Hague Airport (RTHA).

environment and the agents [66]. Using the perception module, the agents receive the input from the environment and from other sensory information. There are three types of agents in AATOM: passenger agents, operator agents and orchestration agents. The perceived information is specific to the three agent types. Using the actuation module, the agents can perform the actions that were generated in the tactical layer [66]. An example of an action is communicating with other agents etc. [66] Also the walking behaviour of passenger agents is modelled in the actuation module. The walking mechanism is based on the Social Force Model developed by Helbing et al. This is further explained in section 5.4.

In summary, the sequence of operations is performed in the AATOM architecture: observation - perception - interpretation reasoning - activity control - actuation - action [66].

4.4. AATOM Model Specification

The AATOM model can be explained by dividing it into three parts. Firstly, the specification of the environment is addressed in subsection 4.4.1. Then, the specification of the agents is addressed in subsection 4.4.2. Lastly the specification of the interactions (between agents and between agents and the environment) is addressed in subsection 4.4.3.

4.4.1. Specification of the Environment

AATOM contains different templates to simulate the operations at airport terminals, examples are Rotterdam The Hague Airport (RTHA) or Eindhoven Airport. AATOM is designed such that the model can be easily modified to also simulate any other airport. To describe the environment of AATOM it can be divided into three: "physical objects", "flights" and "areas". The hierarchy of the environment is shown in Figure 4.2. The differences are explained in the following sections.

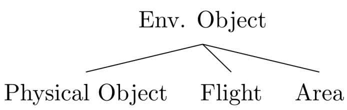

Figure 4.2: The division of the different objects in the environment.

The environment is actually made out of areas which are accessible to the passenger and operational agents. These areas are a two dimensional polygon that are bounded by e.g. walls. There are different types of areas. These can be seen in Figure 4.3. In this figure A, B and C are facility areas. D is the check-in area and E are queuing areas. F is the checkpoint area, G is the gate area and H is the entrance area [39].

Physical objects and flights are also part of the environment. Examples of physical objects include: luggage, seats, a queue separator, a belt, a desk or a sensor like a Walk Through Metal Detector sensor (WTMD sensor). [66]

Each passenger agent is related to a specific flight. The flight defines to which check-in desk and to which gate the agent has to go at a certain time point. Passengers are generated as input for the system and they disappear with their departing flight after going through the required terminal processes. [66]

4.4.2. Specification of the Agents

This section addresses the specification of the agents. AATOM considers three agent types: "passenger agents", "operator agents" and "orchestration agents". This section explains the differences between them.

Passenger agents are generated as input for the system. Their end-goal is to catch their flight. They move using the movement module, which is based on the Social Force Model of Helbing explained in section 5.4. Before boarding, the passenger agents are able to visit shops, restaurants or toilets. They disappear with their departing flight after going through the required terminal processes.

The operator agents have a job to do. Two types of operator agents are defined in AATOM: security agents and check-in agents. Security agents are standing at the security check points and need to perform a certain task e.g. monitoring x-ray, check travel document, physical check. Check-in agents are located behind the check-in desk. They need to check-in the passenger agents.

The passenger agents and the operator agents are both human agents. They are represented in AATOM by a circle of certain radius r.

The orchestration agents are left general on purpose and can be adapted to different case studies. They can be implemented such that they are able to monitor the overall performance of the airport and to co-ordinate the operations. An example, is the MSc Thesis of Anne-Nynke Blok [9], where she implemented orchestration agents that were able to make changes in the environment (opening or closing security lanes) to improve the operations. For this research orchestration agents can be used for example in order to optimise safety of the passenger agents, as explained in section 7.6.

4.4.3. Specification of the Interactions

There are different sort of interactions possible in AATOM. Firstly, check-in operators are able to interact with the environment, especially the flights. For example, they can update the state of a certain flight that everyone has checked-in [66].

Secondly, operators can interact with each other. For example, operator responsible for X-Ray scanning and the operator responsible for luggage checking can communicate with each other.

Thirdly, operators and passenger agents can interact with each other. For example, a check-in agents can order a passenger to wait for a specific time at the check-in desk.

Lastly, a orchestration agent can be implemented for coordination of terminal operations, such as optimising physical distance between agents. In order to allow for coordination, the orchestration agent can be designed to interact with operators, passengers and the environment. [66]

5

Pedestrian Dynamics

The movement of the passengers in the AATOM simulator is modelled using the Social Force Model of Helbing [30]. As explained earlier in chapter 2, safety agencies such as EASA require airport operators to take COVID-19 measures to facilitate a safe and efficient journey for the passengers. The key measure is social distancing. Social distancing, also called physical distancing means maintaining a minimum distance of 1.5 meters between yourself and other people who are not from your household. This should be performed where ever is possible at the airport [22].

In order to implement this measure in AATOM it is important to understand how movement of passengers is modelled. In this chapter, the Social Force Model [30] is looked further into and how it can be adapted such that social distancing is simulated. The outlook of this chapter is the following. First microscopic and macroscopic models and the limitations of macroscopic models are explained in section 5.1. Then, different microscopic models are explained. These models are generically compared to the Social Force Model in section 5.3. Hereafter, an detailed analysis is given of the Social Force Model [30] and the necessary modifications of the Social Force Model are analysed and how these could work in order to facilitate social distancing in section 5.4 and 5.5.

5.1. Explanation on Macroscopic and Microscopic Models

Pedestrian simulation models are used in many fields these days to simulate crowded places. Examples are: football stadiums, train stations, airport terminals. There is wide variety in different pedestrian models. Each model has its advantages and disadvantages. The choice of the modelling method depends on the intended application. Generally pedestrian models can subdivided into two categories: macroscopic models and microscopic models. In the following section the differences between these two are explained.

5.1.1. Difference between Macroscopic and Microscopic Models

Macroscopic models model pedestrian flow as a whole without considering the behaviour of the individual pedestrians. Microscopic models on the other hand, model pedestrians in great detail. It distinguishes the behaviour of the individuals and their interactions. [64]

Microscopic models are slow and computational demanding but they are highly precise. Contrary, macroscopic models are very fast but not good in representing the behaviour of the agents. They can be used in applications, where the human interaction is not important. [64]

5.1.2. Limitation of Macroscopic Models

Although macroscopic models are applicable to evaluate the macro outcomes of the pedestrian flow while being computational efficient. The biggest disadvantage is the incapability of analysing how pedestrians react in crowd due to the lack of individual behaviour consideration [47]. Also the incapability of analysing how the pedestrians react with changes in the environment [47]. However, this feature is very much needed in the AATOM simulator. Therefore, an exclusion of the use of a macroscopic model has been made. In the next section, different microscopic models are discussed.

5.2. Microscopic Models

In this section five different microscopic models are discussed. The section starts with explaining the Benefit-cost Cellular model.

5.2.1. Benefit-cost Cellular Model

The Benefit Cost Cellular Model is one of the earliest approaches for modelling pedestrian movement. It was first proposed by Gipps and Marksjo in 1985 [27]. It simulates pedestrians as particles that occupy a cell. The program proposed by Gipps and Marksjo used interactive colour graphics to display the model. But, many researches state that this model is computational inefficient and therefore the applicability for modelling passengers in a terminal environment is limited. [47]

The model works as follows. Every cell can be occupied by maximum one pedestrian. Cells surrounding a pedestrian (including the cells that is occupied with a pedestrian) are assigned with a score. This score is used to represent the progress of the pedestrian towards the destination. The repulsive effect between pedestrian is calculated by the following formula [70]:

$$Score = \frac{K(S_i - X_i)(D_i - X_i)|(S_i - X_i)(D_i - X_i)|}{|S_i - X_i|^2 |D_i - X_i|^2} - \frac{1}{(\Delta - \alpha)^2 + \beta} \tag{5.1}$$

where S_i is the vector location of target cell. X_i is the vector location of the pedestrian. D_i is the vector location of the destination. Δ is the distance between cell and the pedestrian. K, α and β are constants.

When a cell is neighbouring two pedestrians, the score of the cell is the sum of the score generated by the 2 pedestrians. The pedestrians move towards the next cell that has the maximum net benefit.

The downside of the model is that the constants K,α and β are chosen rather arbitrary and do not have a physical meaning. Thus, in order to model realistic interactions and characteristics of pedestrians, these parameters need to calibrated rather arbitrary. However, many researchers state that it is difficult and sometimes impossible to obtain identical interactions and characteristics when different environments are modelled. Also, the link between the action of the pedestrians and the environment is sophisticated and hard to explain [70].

5.2.2. Magnetic Force Model

Prof. Okazaki and Matsushita developed the magnetic force model [50]. This model is based on the magnetic field theory to simulate pedestrian movement. In the model pedestrians and obstacles are modelled as positive poles such that they are repelled from each other. The goal of the pedestrians is modelled as the negative goal such that the pedestrian is attracted to the goal. There are two magnetic forces that act on the pedestrians. The first one F is the one formulated by Coulombs law, where the magnetic force depends on the distance between the pedestrians, from [50]

$$\vec{F}_{ij} = \frac{k q_i q_j}{|\vec{r}_{ij}|^3} \vec{r}_{ij} \tag{5.2}$$

where F_{ij} is the magnetic force between pedestrian i and an other pedestrian j or an object j. k is a constant (in the original law this was the Coulomb's constant). q_1 is the intensity of the magnetic load of a pedestrian i and q_j is the intensity of the magnetic load of an other pedestrian j or an object j. $\vec{r}_{ij}$ is the vector between pedestrian i and an other pedestrian j or object j and $|\vec{r}_{ij}|$ is the distance in between. The parameters k, q_i and q_j can be trimmed such that the desired emergent behaviour is obtained. Generally the intensity of the negative pole (the goal) is set much larger in value than the positive poles (objects or other pedestrians that need to be avoided) because the pedestrian's priority is to reach their goal. [70]

The other force acts such that a pedestrian avoids collision with other pedestrians or obstacles and exerts an acceleration that is calculated by, from [50]:

$$\vec{a}_i = \vec{V}_i cos(\alpha) tan(\beta) \tag{5.3}$$

where $\vec{a}_i$ is the acceleration that acts on pedestrian i to modify its direction $\vec{RV}_i$ to $\vec{AC}$ (see figure below). Line $\vec{AC}$ is the line of contact going from pedestrian i to the intersection with the circle around pedestrian j. The choice of the value of the radius is up to the user.

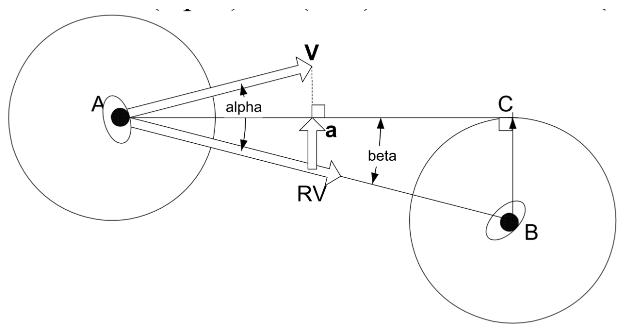

Figure 5.1: Additional Repulsive Force on Magnetic Force Model, from [70].

The repulsion and attraction forces are superimposed such that the pedestrian attempts to arrive at their goal.

Below a demonstration is given of the superposition of these forces.

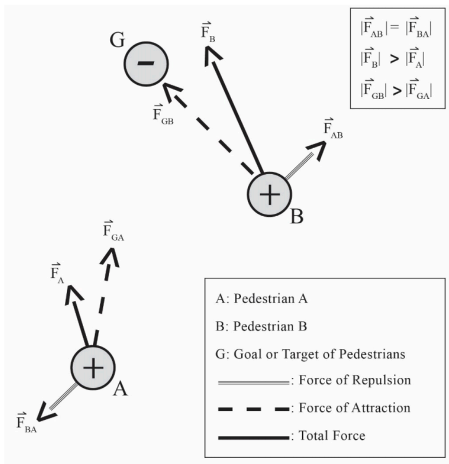

Figure 5.2: The magnetic forces presented

Although the model involves certain physical meanings of real pedestrian movement, it still deviates from the true sense to some extent. Also the load of the forces have an effect on both the distance between the pedestrians and the velocity of the pedestrians. These cannot be controlled separately which is a disadvantage. [47]

5.2.3. Cellular Automata Model

The Cellular Automata Model builds a bit further on the Benefit-Cost Model. It was first proposed in 1998 by Victor Blue. Also, like the Benefit-Cost Model the Cellular Automata Model is discrete. This means that the simulated environment is discretised in a grid cell structure. Each agent is placed on one cell. They decide about their their direction of movement based on the status of the neighbouring cells and they decide on their target cell depending on their interpretation about their surrounding. The movement of all the pedestrians is updated when all the conflicts of the system are solved. In the original model (Victor Blue 1988), the movement of all pedestrians are updated in parallel and the differences in velocity are visible by the decision to move during a time step [21].

There exist many modifications of the cellular automate model, such as for example the on of Michael Schultz proposed in [61]. In which he proposed this model to simulate the pedestrian dynamics during emergency situation in airport terminals. This model also contains the social-force-based repulsion and friction forces.

The methodology of the model looks as follows. The terminal environment is discretised in square cells. Each cell has two states, namely occupied or free. This can be seen in the left part of Figure 5.3.

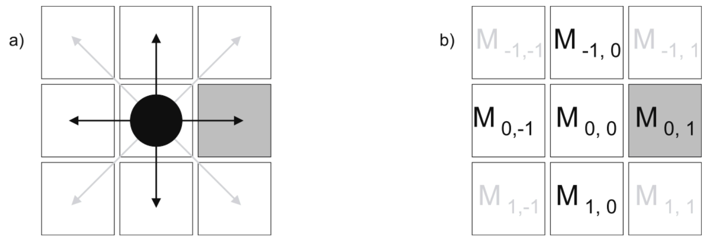

Figure 5.3: (a) shows the grid stucture with the black dot representing a passenger and the arrows indicate the possible direction. (b) shows the preference matrix, from [61].

The passenger can move to their neighbouring cell depending on its state and on the transition probability which is stored in a preference matrix $M_{q,p}$ which is shown in the right part (b) of Figure 5.3. Details regarding the calculation of the preference matrix is presented in [61].

5.2.4. Social Force Model

The Social Force Model is developed by Helbing, Molnar and Viscek in 1991 [30] and it has aspects which are similar as those of the Magnetic Force Model.

The movement of a pedestrian is simulated by a superposition of different forces. Firstly there is the attraction force, which acts as the force that drives the pedestrian to its goal. Then there is the social repulsion force, by which agents are repelled from each other such that they keep distance and don't enter into the social space of an other pedestrian. Than lastly, there are contact forces and friction forces which simulate the behaviour when pedestrians touch each other. These forces are summed together in the right side of the following equation:

$$m_i \frac{d\vec{v}_i}{dt} = m_i \frac{v_i^0(t)\vec{e}_i^0(t) - \vec{v}_i(t)}{\tau_i} + \sum_{j(\neq i)} \vec{f}_{ij} + \sum_{W} \vec{f}_{iW} \tag{5.4}$$

The first term $d\vec{v}_i/dt$ represents the motivation of pedestrian i to reach its goal at a certain target time with a desired speed. More details about the formulas are explained in section 5.4.

This model is the most popular microscopic pedestrian model and has been implemented in many specific pedestrian simulations [47]. Also, the parameters in the equations have a physical meaning and they do not need to be calibrate for every new environment which is an advantage [47]. Disadvantages are that the model lacks the ability to include for emotions and it can produce unrealistic backward motions of agents when they get repulsed by the preceding ones [47].

5.2.5. Queuing Network Model

The Queuing Network Model is a network model proposed by Lovas in 1994 [45]. There exist extended versions of the Queuing Network Model, an example is SimPed proposed by Daamen in 2002 [19]. This section focuses on the the queuing network of Lovas [45] as the characteristics are similar to the other modified models.

This model discretizes the environment into links and nodes. The rooms in the environment are modelled as nodes and the area connecting adjacent rooms are connected by links. The movement of the pedestrians is stochastic because it uses Monte Carlo simulation. Therefore a number of simulations need to be made to be statistically significant and represent the motion of a crowd.

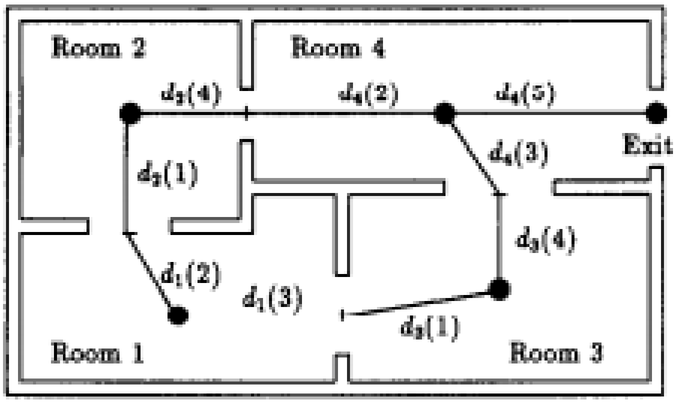

Figure 5.4: A representation of the modelled environment. Each room is represented as a node and are connected by links. From [45]

Each pedestrian departs from a starting node, in our case this would be the entrance of the terminal, and it queues on a link to go to another node. It has the goal to go the gate, which is the end node. When the pedestrian arrives at a node, it makes a weighted-random choice to choose the next link. The weight is dependent on the amount of pedestrians in the room.

One main criticism for the Queuing Network Model is that the queues are uni-dimensional and therefore it is not so realistic because pedestrians walk bi-dimensional. Also, some researchers state that the Queuing Network Model can not deal with high density scenarios [49]. Also, this model lacks the ability to analyse the interactions between the different agents.

5.3. Comparison of the Microscopic Models

In order to simulate the behaviour of the passengers it was chosen to use a microscopic model because macroscopic models are not able to present the individual behaviour of the passengers. In this section the microscopic models are compared.

As already discussed earlier, the thesis considers to analyse the impact of the COVID-19 restrictions on the airport performance. Therefore, the reality of the simulated passenger flow and interactions is very important. The Social Force Model is very suitable for this research as the parameters have a more concrete physical meaning and therefore they can be easier measured [47]. The table below shows a comparison of the five discussed models.

	Benefit-Cost Model	**Magnetic Force Model**	**Cellular Automata Model**	**Social Force Model**	**Queuing Network Model**
Pedestrian Movement	Discreet	Continuous	Discreet	Continuous	Discrete
Movement to Goal	Gain Score	Positive and Negative Magnetic Forces	Min (gap, max speed)	Desired Velocity	Weighted Random Choice
Repulsive	Cost Score	Positive and Negative Magnetic Forces	Gap or Occupied Cell	Interaction Forces	Queues
Value of the Parameters	Arbitrary	Physical Meaning	Arbitrary	Physical Meaning	Physical Meaning

Table 5.1: Comparison Microscopic Pedestrian Simulation Models, based on [70].

The main disadvantages of the Queuing Network Model are that it only considers uni-directional motion, it lacks the ability to model interactions between the agents and it cannot deal with high density crowds [49]. This is considered to be very limiting and therefore this model was already discarded as a choice.

The Benefit-Cost Model and the Cellular Automata Model were also discarded early because of their low capability to capture realistic pedestrian behaviour as they are discrete. Also the values of the constants of these two models are arbitrary and this limits validation possibilities. The Cellular Automata Model is also not able to generate the self-organisational emergences such as stop and go-waves as the Social Force Model [21].

The Social Force Model was chosen over the magnetic force model because for the magnetic force model the load forces effect both distance between pedestrians and their velocity and thus distance and velocity cannot be controlled separately [47]. Therefore the Social Force Model was considered to be the model for this thesis.

5.4. Social Force Model Mathematical Explanation

Now the social force model has been chosen to further use in the AATOM model, a more mathematical analysis can be done. In section 4.3 the AATOM architecture was explained. The different layers and modules were explained. As you can remember, passengers (agents) make observations using the operational layer. Based on their observations, the passengers calculate a collision free path to their activity locations in the navigation module [38]. Using the action module, the passengers follow their generated path. The movement along the path is calculated using the Social Force model defined by Helbing [30]. In this section, the mathematics of the model is further explained.

The model assumes that movement of the passengers is guided by a superposition of attractive and repulsive forces, determining the behaviour of the individuals. The model is continuous and each passenger is treated as an individual which means that this is a microscopic model. One could say that the system searches for the lowest amount of energy/interaction it can achieve [21]. The formula of the force model is given in Equation 5.5. It assumes a mixture of socio-physical and physical forces that influence the crowd movement: each pedestrian i with mass m_i (in total there are N pedestrians) wants to move in direction $\vec{e}_i^0$ with a desired speed $\vec{v}_i^0$. However pedestrians needs to constantly adapt their actual velocity $\vec{v}_i$ with time characteristic τ_i in order not to bump in to other pedestrians and to keep velocity-dependent distance to walls and other pedestrians. The "interaction" forces are expressed as $\vec{f}_{ij}$ and f_{iW} [30]. The change in velocity of each pedestrian i, expressed as $d\vec{v}_i/dt$, is given in the following Equation 5.5, from [30]:

$$m_i \frac{d\vec{v}_i}{dt} = m_i \frac{v_i^0(t)\vec{e}_i^0(t) - \vec{v}_i(t)}{\tau_i} + \sum_{j(\neq i)} \vec{f}_{ij} + \sum_W \vec{f}_{iW} \tag{5.5}$$

The position of each pedestrian i can be calculated by integrating $d\vec{v}_i$ over time.

The social force model designed by Helbing et al. was first designed to simulate the dynamical features of escape panic of pedestrians but it became used many other fields. In this model, each pedestrian exerts two kind of forces, "social" and "physical", on the other pedestrians and the environment. The "social" force is the physiological force of not colliding with other pedestrians or the environment. For example, if a pedestrian sees an other pedestrian closely than it is going to slow down in order to not collide. The "physical" force refers to the fact that this force deals with the physical contact between pedestrians and with the environment. When pedestrians are too close to each other, pedestrians are often forced to collide. As a result, the pedestrians exert pushing and friction forces on each other. A mathematical form of the force that pedestrian i exerts on pedestrian j is the following:

$$\vec{f}_{ij} = \vec{f}_{social\ repulsion} + \vec{f}_{pushing} + \vec{f}_{friction} \tag{5.6}$$

where

$$\vec{f}_{social\ repulsion} = A_i e^{(r_{ij}-d_{ij})/B_i}\ \vec{n}_{ij} \tag{5.7}$$

$$\vec{f}_{pushing} = kg(r_{ij} - d_{ij})\ \vec{n}_{ij} \tag{5.8}$$

$$\vec{f}_{friction} = \kappa g(r_{ij} - d_{ij})\Delta v_{ji}^t \vec{t}_{ij} \tag{5.9}$$

The psychological tendency of two pedestrians i and j to stay away from each other is modelled by a "social repulsion force" expressed as Equation 5.7. Here, d_{ij} is the absolute distance between the pedestrians i and j (taken from their center of mass). $\vec{n}_{ij}$ is the normalised vector going from pedestrian j to i and is calculated by: $\vec{n}_{ij} = (n_{ij}^1, n_{ij}^2) = (\vec{r}_i - \vec{r}_j)/d_{ij}$. A_i and B_i are constants.

Note that if the distance between the pedestrians d_{ij} is smaller than the sum of radii of both pedestrians $r_{ij} = r_i + r_j$ then the pedestrians are touching each other. If this is happening then $g(x)$ in Equation 5.8 and Equation 5.9 is set equal to argument x (otherwise $g(x)$ is zero). Then there are two additional forces (according to Helbing inspired is by granular interactions [30]).

First, there is the "pushing force" which counteracts the body compression. The mathematical form is presented by Equation 5.8. Here k is a constant.

Second, there is the "friction force", which is presented by Equation 5.9. In this function, $\vec{t}_{ij} = (-n_{ij}^2, n_{ij}^1)$. This is the tangential direction and $\Delta v_{ij}^t = (\vec{v}_j - \vec{v}_i) \cdot \vec{t}_{ij}$ is the tangential velocity difference. Here κ is a constant.

So in summary, we have seen the "social repulsion force" and two additional forces (in case the two pedestrians touch each other $g(x) = x$): the "pushing force" and the "friction force".

We also have the same three interaction forces between a pedestrian i and the wall W.

$$\vec{f}_{iW} = \vec{f}_{social\ repulsion} + \vec{f}_{pushing} + \vec{f}_{friction} \tag{5.10}$$

where

$$\vec{f}_{social\ repulsion} = A_i e^{(r_i - d_{iW})/B_i}\ \vec{n}_{iW} \tag{5.11}$$

$$\vec{f}_{pushing} = kg(r_i - d_{iW})\ \vec{n}_{iW} \tag{5.12}$$

$$\vec{f}_{friction} = \kappa g(r_i - d_{iW})(\vec{v}_i \cdot \vec{t}_{iW})\vec{t}_{iW} \tag{5.13}$$

$$\vec{f}_{iW} = \{A_i exp[(r_i - d_{iW})/B_i] + kg(r_i - d_{iW})\}\vec{n}_{iW} + \kappa g(r_i - d_{iW})(\vec{v}_i \cdot \vec{t}_{iW})\vec{t}_{iW} \tag{5.14}$$

So, in this case d_{iW} is the distance from pedestrian i to the wall W, $\vec{n}_{iW}$ is the direction from pedestrian i perpendicular to the wall W and $\vec{t}_{iW}$ is the direction from pedestrian i tangential to the wall W.

In the original version of AATOM [66] the constants are set to the following values:

1. Helbing constant A = 250 N
2. Helbing constant B = 0.1 m
3. Acceleration time constant τ = 0.5 sec
4. Elasticity constant k = 1.2e5 kg/sec^2
5. Coefficient of sliding friction κ = 2.4e5
6. Average mass of passenger is m_i = 80 kg. (found in modelbuilder)
7. Shoulder width of passenger is 0.5 meter. (passengers are modelled as circles with radius 0.25 meter)
8. Desired velocity v_i^0 can be more than 5 m/s and can go up to 10 m/s moving to the exit.
9. Identical parameters for all pedestrians because of not having to deal with calibration and to increase robustness.

5.5. Modifications needed for the Helbing Movement Module

There are many papers that propose modifications to the social force model designed by Helbing et al. [30]. A paper that proposes some useful modifications is the paper of Lakoba et al. [42]. This paper deals with some issues of the social force model which can be related to introducing physical distancing.

Lakoba et al. [42] addresses two issues with the social force model [30].

Firstly, the social and physical repulsion forces defined in Equation 5.7 and 5.8 do not guarantee that pedestrians do not overlap each other. By overlapping, the authors mean the following. A pedestrian can be squeezed in unrealistically (greater than s_{max}). The pedestrians are modelled as circles with a radius r_i and the maximum allowed magnitude of squeezing is s_{max}, which taken equal to 20 percent of the circle radius r_i. Although, the thesis actually deals with implementing physical distancing. This paper is dealing with sort of a similar problem: imposing a maximum value on the magnitude of squeezing and hence eliminating the pedestrians of overlapping each other. Frankly, I have been running the AATOM simulator multiple times and I have never seen the issue of overlapping passengers. Actually, this is because the value of the elasticity constant k in the original version of AATOM [66] and the model of Helbing et al. [30] was taken very high, k = 1.2e5 kg/sec^2. This results in modelling the passenger into very rigid structures that are not squeezable at all, therefore also overlapping is eliminated. Lakoba et al. pointed out that for such a high value of k the contact forces are also too high, e.g. 2 passengers squeezed by 5 cm would result in a contact force of 6000N, which is 7 times their weight (80 kg). Therefore, authors addresses the research question: can we eliminate the possibility of pedestrian overlapping with at the same time using a more realistic value of k which thus needs to be significantly lower [42]. Although, the overlapping is for the thesis no big concern since the passengers are actually need to keep 1.5 meter distance. Still this paper, provided interesting insights in how physical distancing could be implemented in AATOM.

The paper suggests multiple ways of solving this problem. First they propose a solution which take the form of a contact force that creates an impenetrable potential barrier between pedestrians i and j. However, as they explain in section 2.1, using such a force would cause substantial numerical difficulties in the simulations [42]. Therefore other solutions are further explored in the report.

The second issue of the social force model [30] that Lakoba et al. addressed has to do with the choice of the numerical values. In [30] the value of A in Equation 5.7 was taken 2000 N and the value of B was taken 0.08 m. However Lakoba et al. states that this value of B, called the "fall-off length", is too small. A fall-off length of only 8 cm meter would mean tat the social forces are close to zero when the passengers are not the order if 8 cm apart. He proves this with with the following equation of motion 5.15 and 5.16. Assuming a 80 kg pedestrian moving straight towards a wall with a preferred speed of 1.5 m/sec and acceleration time constant τ equal to 0.5 sec.

$$\frac{dx}{dt} = v \tag{5.15}$$

$$\frac{dv}{dt} = -\frac{v - v_0}{\tau} - \frac{A}{m} e^{-|x|/B} \tag{5.16}$$

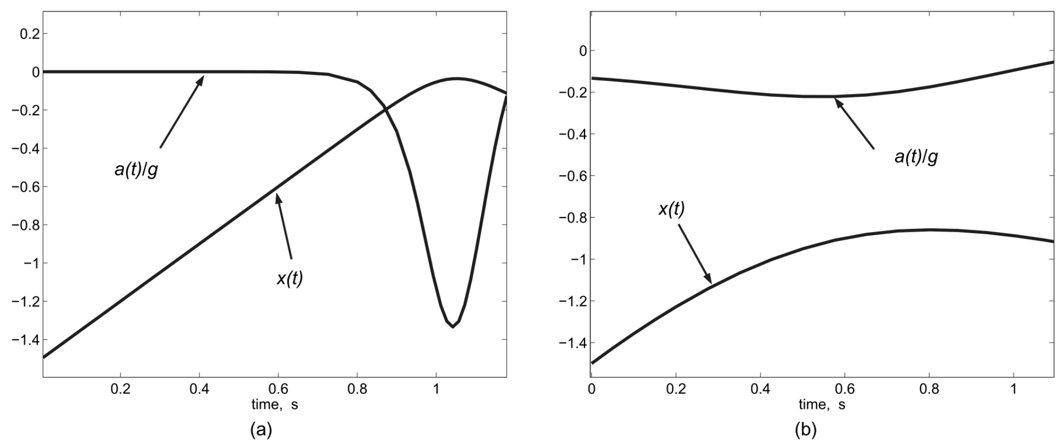

Figure 5.5: Results of solution of Equation 5.15 and Equation 5.16 with A = 2000 N and B = 0.08 m (a) and 0.5 m (b)

As you can see in Figure 5.5, in the case (a) with the B equal to 0.08 m the deceleration peaks at -1.4 m/s^2. This seems unrealistic because this is higher than the acceleration of gravity by almost 40 percent. In case (b) with B equal to 0.5 meter and everything else the same, the acceleration peaked at -0.3 m/s^2. This seams far more realistic. Thus for the second issue the authors addressed the following: will the model still produce realistic simulations with the value of B taken to be 0.5 m instead of 0.08 m? [42]

When the authors changed the parameter B alone, the simulation of the crowd behaviour produced unrealistic elements. For example, when passengers were grouping before the exit to leave the other new-coming passengers would turn away instead of joining the group. This can be seen in Figure 5.6. To solve this, the authors found out two solutions. First, the model should take into account that the social force should vary with crowd's density. Second, the model should distinguish face-to back and face-to-face social repulsion forces [42].

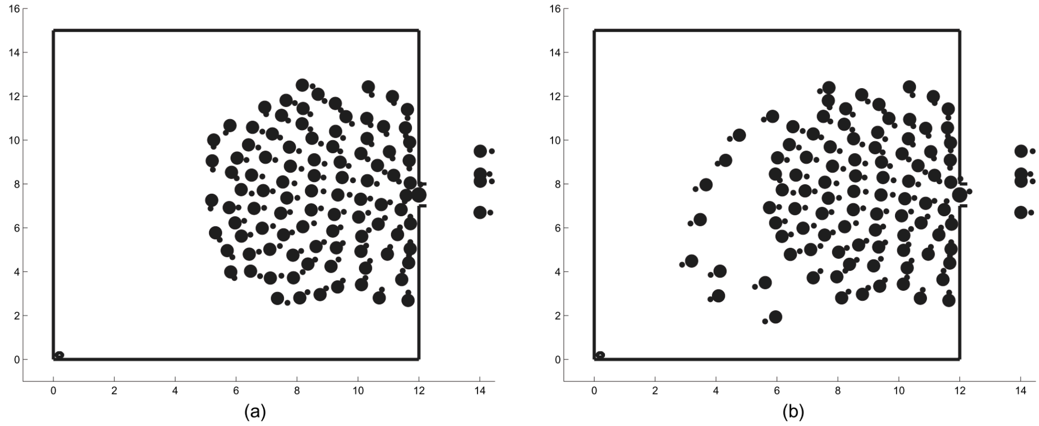

Figure 5.6: Snapshots crowd just before (a) and a few seconds after (b) when a new-coming group at the back turns away and leave. [42]

More information regarding the implementation of these 2 solutions is discussed in section 3.1, 3.2 and 3.3 of [42].

Regarding the relevance of the paper of Lakoba et al. [42]. I think especially the last part is quite helpful to implement social distancing in AATOM. Although for the original version of AATOM [66] the values A and B are calibrated differently, namely they were set to 250 N and 0.1 meter. Especially, the B is lower than the suggested 0.5 meter by [42]. My hypothesis, regarding which method is the easiest to implement social distancing in AATOM is to increase B from 0.1 meter to 1.5 meter. However, this will probably result in some undesirable side effects, e.g. such as Figure 5.6. And this will require some extra additions to the model to eliminate these side effects. Just like Lakoba et al. did in their study [42]. Increasing the fall-off length B to 1.5 meter will probably also result in passengers not fitting anymore in queues. This was observed by experimenting with the AATOM simulator, depicted in Figure 5.7.

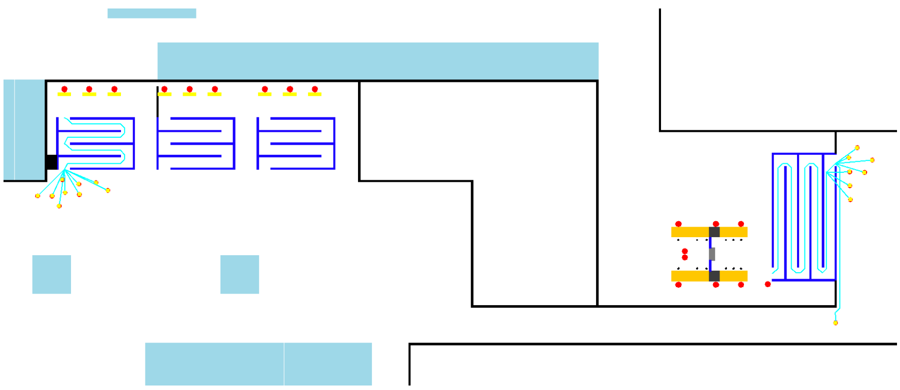

Figure 5.7: Snapshot of AATOM simulation of passenger behaviour at Eindhoven airport using fall-off length B = 1.5m. Note Passengers are stuck at the beginning of the queue and one passenger is stuck at the corner.

The figure above shows a snapshot of an AATOM simulation of the passenger behaviour at Eindhoven airport using fall-off length B = 1.5m. As one can see, using a bigger value of B the passengers are keeping 1.5 meter distance from each other. This is because of the social repulsion force which is now activated earlier, referring to Equation 5.7.

Figure 5.8: Plot of social repulsion force $f_{social\ repulsion}$ [N] vs distance between the passengers d_{ij} [m]

The reason why the passengers are now stuck at the beginning of the queue is probably because the implemented social force model in AATOM does not distinguish the repulsion forces between passengers only and between passengers and objects. Probably a modification should be made in AATOM such that two fall-off lengths are considered: one for the distance between passengers and objects and one for the distance between passengers only.

5.6. Air Passenger Characteristics

In order to model the passenger flow at airport terminals it is important to also understand the influence of passenger characteristics on their behaviour. These characteristics are also important to calibrate the parameters of the pedestrian dynamics model, which are discussed previously.

5.6.1. Passenger characteristics vs walking speed

Schutz Michael et al [62] did research in analysing behaviour of passengers (in more particular their walking speed) in airport terminals by using an a video surveillance system. They observed a significant difference between business and leisure related passengers. They also concluded that the influence of carry-on baggage on the maximum speed is very small but the size of the passenger group has large impact on the walking speed. The results were provided as statistical distributions. These statistical distributions can be used in AATOM. Because now, the original AATOM model does not distinguish different passenger types (they are all the same) and they travel alone. The results of [62] are further presented in the following paragraphs.

Firstly, one can relate the expected walking speed to the age structure of the passenger. Figure 5.9 shows that the walking speed for 20 year old is the highest (1.6 m/s or 5.76 km/h) compared to passengers of other ages. From that point, the walking speed almost linearly decreases with increasing age. Also in [62], the percentages of passengers per age category were given. This is very handy because together with graph presented in Figure 5.9 it can be used in AATOM.

Secondly, the interdependencies between gender and walking speed were analysed. It was found that on average male walk 10 percent faster than female. The average speed of a male passenger was found to be 1.4 m/s (or 5.4 km/h) (with a standard deviation of 0.22 m/s) and the average speed of a female passenger was found to be 1.27 m/s (or 4.57 km/h) (with the same standard deviation as for male passengers) [62]. The distribution can be found in Figure 5.10.

Thirdly, a link was made between the walking speed of passengers and their travel purpose. It was found that business passengers walk in general 24 percent faster than leisure passengers. The average speed for business passengers is 1.36 m/s (with a standard deviation of 0.22 m/s) and for leisure passengers is 1.0 m/s (with a standard deviation of 0.23 m/s) [62]. This can be seen in Figure 5.11.

Lastly, the authors observed a dependency between the group size of passengers and their walking speed. Currently, AATOM assumes that every passengers walks alone but this could be further elaborated to groups. Therefore this observation can be useful. It was found that walking speed is 22 percent faster alone than in a group of two passengers and 30 percent faster than a group of 3 passengers. The average speed of someone walking alone was found to be 1.36 m/s (std of 0.23 m/s), for a group of 2 passengers it is 1.06 m/s (std of 0.21 m/s) and for a group of 3 passengers it is 0.96 m/s (std of 0.19 m/s).

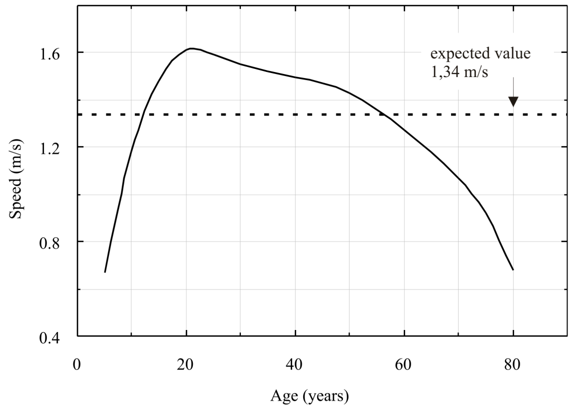

Figure 5.9: Relation between passenger age and walking speed, from [62]

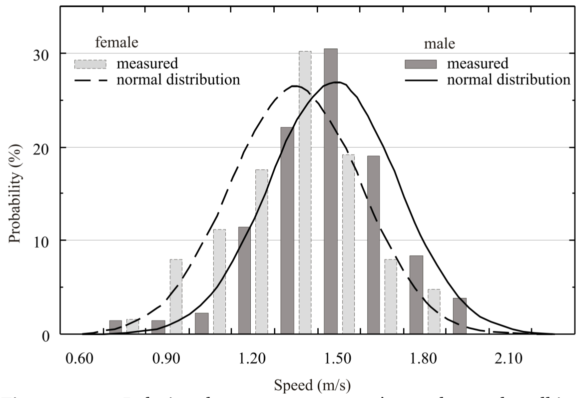

Figure 5.10: Relation between passenger's gender and walking speed, from [62]

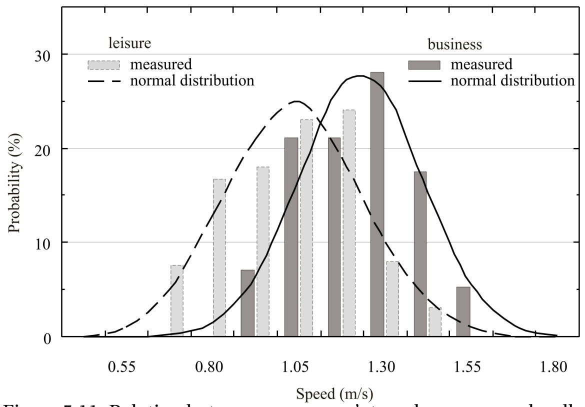

Figure 5.11: Relation between passenger's travel purpose and walking speed, from [62]

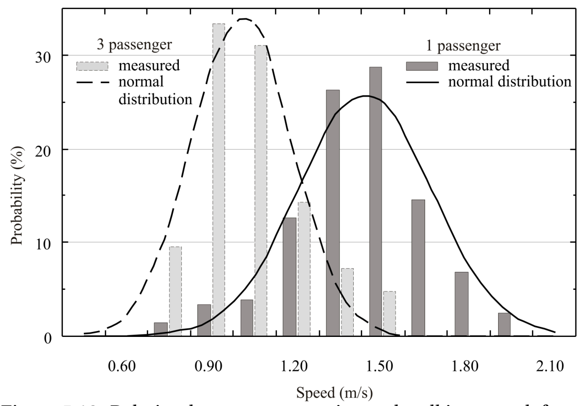

Figure 5.12: Relation between group size and walking speed, from [62]

Note that these data measurements were taken in normal conditions prior to the COVID-19 situation when physical distancing was not mandatory. Therefore, it is expected that the walking speed of passengers are lower because passengers need to be more careful and need to take more distance with respect to others. This research will need to find out what the impact is of physical distancing on passenger walking speed. However, it is expected that the interdependencies which were shown above still hold.

The findings of Schultz et al. are considered to be credible because data was obtained from many different airports such that the data is statistically significant. Airports include Frank-furt, Berlin-Tegel, Berlin-Schönefeld, Hamburg, Munich, Hannover, Dresden, statistical data from German Airports Association and airline data from SWISS [62].

The findings of the authors are considered also to be very useful for the thesis because they can used for implementing different passenger types in AATOM. In the output analysis, these different passenger types can then be used to observe which type of passenger is more vulnerable to a COVID-19 infection due to his or her behaviour.

6
Cognitive Decision-Making

It is commonly acknowledged that cognitive and affective aspects have an important role in human decision-making [63]. In a recent study of K. O'Connell et al. [53] based on the data of Blagov P. [8] an analysis was done in the relation between personality traits and their tendency to take risks, their meanness, and lack of restraint. They found that individuals reporting high levels of antisociality engage in fewer social distancing measures. For example these people left their homes more frequently and stand closer to others while outside [53]. In order to account for these different personality traits of different passengers and the impact on their behaviour it is important to consider these cognitive aspects in the literature study. This chapter discusses the neurological principles and theories and provides a deeper understanding of decision-making.

In the past, literature on decision-making was mainly dominated by the economic utility-based theories [74], [25] [71]. However, lately these utility-based theories have been critizised by many experts as these theories do not incorporate emotions and biases that play a role in decision-making. As a result these theories are considered unrealistic and have a limited applicability, e.g. for decion making cases that only require an idealised rational approach where no emotions play no role [33].

To incorporate for emotions, a number of decision-making models have been developed [63], [60], [68]. The paper 'Adaptive modelling of social decision-making by agents integrating simulated behavior and perceptions chains' by Sharpanskyk'h [63] incorporates theory of the OCC model developed by Ortony, Clore and Collins [51], 'simulation' theory of Hesslow [31] and Damasio's theory on somatic markers [33]. In the following sections the theory is further looked into.

6.1. Simulation Hypothesis Theory of Hesslow

One key process involved in decision-making is the generation of options and evaluating their outcome. These options are generally a sequence of actions. The simulation hypothesis developed by Hesslow G. in 1994 [31] tries to scientifically explain this generation and evaluation of options in terms of basic perceptual and motor functions. It relies on the following three core assumptions, from [31]:

1. *Simulation of actions.* We can activate pre-motor areas in the frontal lobes in a way that resembles activity during a normal action but does not cause any overt movement.

2. *Simulation of perception.* Imagining that one perceives something is essentially the same as actually perceiving it, but the perceptual activity is generated by the brain itself rather than by external stimuli.

3. *Anticipation.* There are associative mechanisms that enable both behavioural and perceptual activity to elicit other perceptual activity in the sensory areas of the brain. Most importantly, a simulated action can elicit perceptual activity that resembles the activity that would have occurred if the action had actually been performed.

Based on these assumptions Hesslow identifies the following behavioural chain how long sequence of responses responses and consequences can be simulated. This is presented in Figure 6.1.

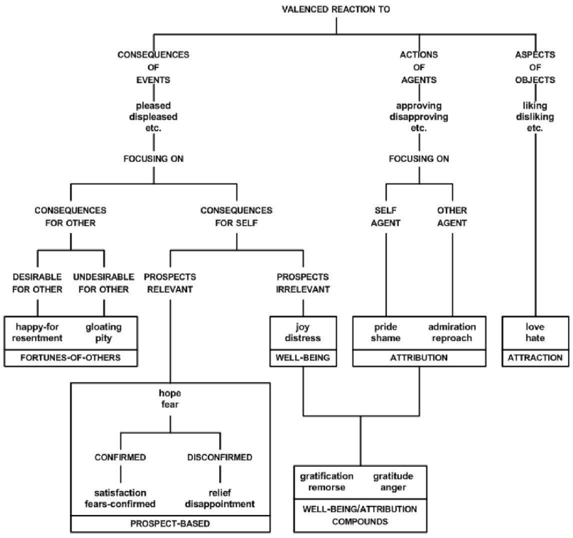

Figure 6.2: The original structure of emotions of the OCC model from [52].

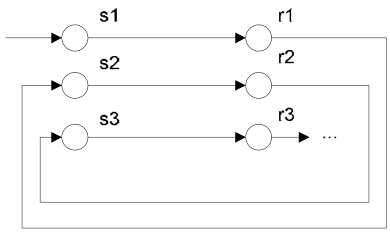

Figure 6.1: Representation of internal simulation proposed by Hesslow, from [31].

Figure 6.1 shows the simulation of a behavioural chain proposed by Hesslow. Supposing that someone has experienced the following situation in the past: a response R1 to a certain situation S1 usually results in other certain situation S2 which in turn usually result in certain situation response R2 and so on. As such this regularity can be learned and so when performing the neural activity r1 in the presence of s1, elicits the expected activity s2. This sensory state may serve as a stimulus for a new response, and so on. And as such one is able to imagine a long chain of of responses and situations without even performing those actions [31].

This theory is also used in the section 7.6 regarding anticipation. Using this theory, the agents can generate an action plan to the information they perceive.

6.2. Damasio's Somatic Marker Hypothesis

Contrary to the utility-based theories, Damasio observed that people with damage in the brain region related to the regulation of emotions have a poor decision-making behaviour. He introduced in 1994 the theory known as the Somatic Marker Hypothesis [33]. He defines somatic markers as feelings in the body that are associated with emotions (e.g. anxiety). According to Damasio these somatic markers depend on past experiences and affect decision-making [33].

Damasio argues these somatic markers are induced by the sensory state of the person and it can be described by the the following causal chain [63]:

sensory state →preparation for the induced bodily response →induced bodily response →sensing the bodily response →sensory representation of the bodily response →induced feeling

6.3. OCC

The OCC Model is a model developped by Ortony, Clore and Collins (OCC) in 1988. The OCC model presents a structure that clusters 22 emotion types as presented in Figure 6.2.

The hierarchy is branched down into three: (1) emotions due to consequences of events (e.g., fear), (2) emotions due the actions of agents (e.g., admiration) and emotions due to the aspects of objects (e.g., love). Some of the emotions are clustered together, e.g. joy and distress are clustered together in the well-being group. These three branches (events, actions and objects) make the OCC model suitable for implementation in agent-based models [67].

Later experts have identified ambiguities regarding the structure of the OCC model and regarding the applicability for the field of Artificial Intelligence. Steunebrink B. R. revisited the OCC model and constructed a new hierarchy [67]. This effort seems to formalise the emotions in a more logic way which makes it easier for the implementation in agent-based models.

7
Model Output Analysis

The purpose of this thesis is to provide insight in the impact of the COVID-19 restrictions on the airport operations performance using the AATOM simulator. In order to do so, AATOM should provide the relevant outputs to make conclusions about the impact on the performance.

7.1. Current Outputs

There are already several analyzers made in AATOM by Stef Janssen, which can be used. These can be visualised in the graphs tab, as can be seen below in Figure 7.1. Examples of analyzers are: QueueAnalyzer, TimeInQueueAnalyzer, ActivityDistributionAnalyzer, TimeToGateAnalyzer, AgentNumberAnalyzer, MissedFlightsAnalyzer, DistanceAnalyzer.

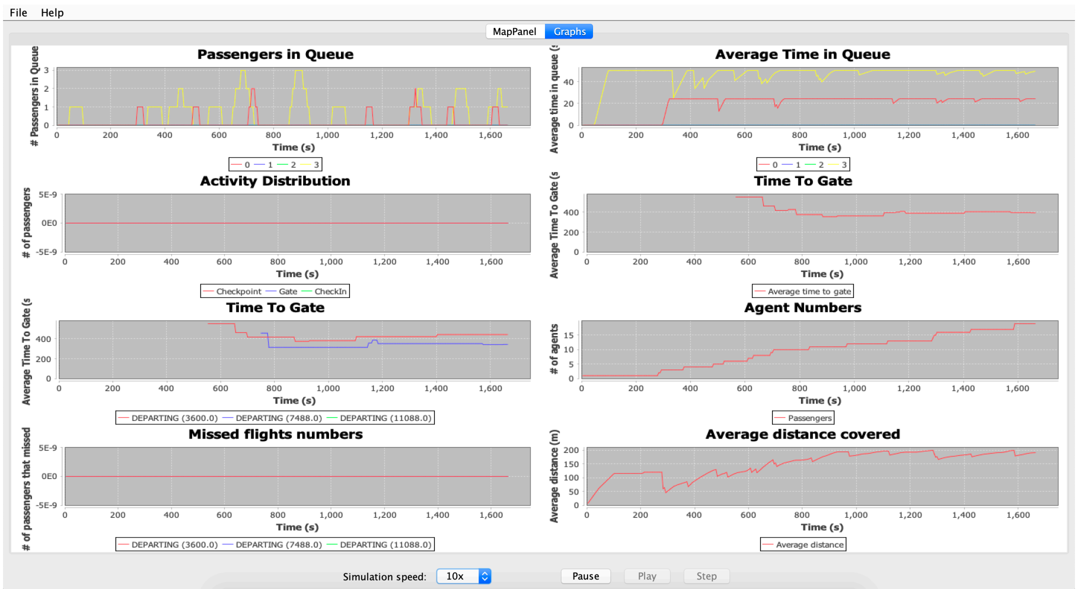

Figure 7.1: Snapshot of AATOM graphs for Eindhoven Airport

The QueueAnalyzer and TimeInQueueAnalyzer (the two graphs in in top of Figure 7.1) show the amount of passengers in a queue and the average time a passenger spends in a queue. The red colour in these graphs refers to the most left check-in queue. The purple colour refers to the middle check-in queue. The green colour represents the right check-in queue. Yellow represents the security queue. The ActivityDistributionAnalyzer shows the amount of passengers distributed over the 3 sections of the airport, namely checkpoint, gate and check-in. The TimeToGateAnalyzer shows two graphs. Namely, the average time passengers takes to the gate and the average time passengers (filtered per flight) take to arrive at the gate. The AgentNumberAnalyzer shows the amount of passengers at the airport. The MissedFlightAnalyzer shows the amount of passengers that missed their flight. Lastly, the DistanceAnalyzer shows the average distance covered of the passengers.

Unfortunately, these outputs only give an indication about the performance of the airport. They don't give any indication about the safety of passengers, e.g. what the average distance between passengers is. Due to the COVID-19 situation, passenger safety is also very important. A trade-of between airport efficiency and passenger safety needs to be made.

7.2. Why Safety KPIs are needed

Due to the COVID-19 situation airports are obliged to take measures to ensure safety for the passengers. Many airport consulting companies, such as Crowdvision [18], think that safe separation KPIs will be as important for airports as passenger experience and efficiency KPIs. They have the vision that only those airports that focus on passenger safety and pandemic risk reduction will emerge the fastest and strongest from the current crisis [18]. Recently, the Airport Council International ACI started the airport health accreditation (AHA) programme. This is a programme which gives airports with an assessment of how aligned their health measures are with the ACI Aviation Business Restart and Recovery guidelines and ICAO Council Aviation Restart Task Force recommendations along with industry best practices.

Other key reasons to implement Safe Separation KPIs are, from [69].

To secure the right to operate: Airports can use this to tool to demonstrate to regulators, staff unions, insurance companies and other stakeholders that they are prioritizing health and safety in a measurable, established manner and risk management strategies have been implemented.

To win confidence: Airports can prove to the passengers that a safe environment is created and that the necessary measures to reduce the risk of disease transmission have been taken.

To rethink the airport layout: This tool can be used to assess the safety of an airport and to determine possible bottlenecks and unsafe spots. By analysing and comparing the best layout, processes and practices can be chosen to define the new normal.

To compete: Airports will compete which each other in terms which of safety and passenger experience. With the use of this tool airports can differentiate from other airports.

To be future proof: we are entering a new normal, with more attention to passenger safety. Like the terrorist attack of 9/11 changed aviation in terms of passenger security, COVID-19 will change aviation in terms of passenger safety and health. This tool will enable airports to sustain beyond COVID-19 and to be prepared when new pandemics arise in the future.

7.3. Translating Risk into KPIs

In order to know how we can eliminate the disease transmission one should first understand how the disease is transmitted. If this is known, one can design KPIs that present useful information in order to monitor the risk.

The transmission of the respiratory syndrome corona-virus 2 (COVID-19) virus is not fully understood yet. Many experts assume that the spread is found by physical contact, droplets and airborne routes [76]. Also the average number of virus particles needed to get infected (also known as the infection dose) is not known yet. But given, the rapid spread, it is likely to be low around the order of a hundred to a thousand particles - according to Willem van Schaik, professor microbiology and infection at the University of Birmingham [26]. Keeping in mind that for example a single sneeze can release about 3000 droplets, the infection dose is thus really low. Thus, one could get infected by inhaling a 1000 infected viral particles in one breath by someone standing in front of him or her. Or one could get infected by inhaling 100 viral particles over 10 breaths. Also one could get infected by being in contact with a highly contaminated object. All of the these situations could lead to an infection [24]. The risk of infection is thus related to the infection dose, which is a relation between the exposure mechanism to the virus (e. g. how close you are standing to an infected person and if you are standing face-to-face to each other) and for how long (in a long period of time you can inhale more particles). Also the risk of infection is dependent on the vulnerability of the people. Persons at a age above 55 years are generally at a higher risk of acquiring COVID-19 than those younger [55]. The risk can be translated into a multivariable equation with key parameters: Exposure Mechanism, Exposure Time and Vulnerabiility of the individual [24] [55].

In order to minimise the risk of transmission in the airport terminal one should therefore increase the distance between the passengers (spread out) and decrease the time people are exposed to each other (speed up). It has thus two dimensions and can be seen in Figure 7.2.

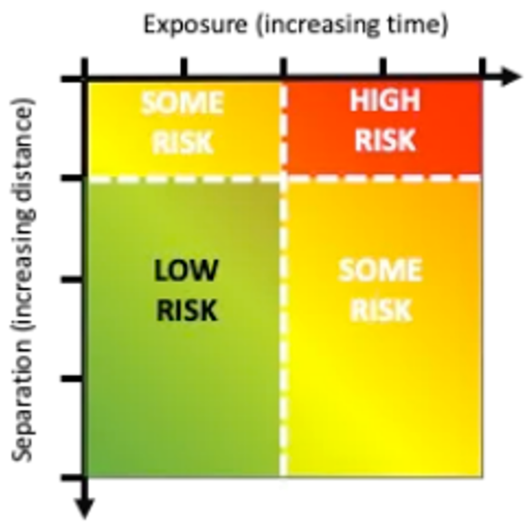

Figure 7.2: To minimise the risk of transmission should increase the distance between the passengers (spread out) and decrease the time people are exposed to each other (speed up) [17].

7.4. Risk Analysis Models

There are different options to asses the passenger risk to get infected by the COVID-19 pandemic. An simple option could be to keep it simple and to assess basic characteristics, such as the average distance between the agents. A more advanced option could be to couple the model with a epidemiological model, such that more insight is gathered how the disease would spread in the terminal.

An example of such an epidemiological model is the SIR model [7]. This model was developed in 1920 to study disease spread. It divides the people into three types: Susceptible, Infectious and Recovered. This model is nowadays still used often. Especially now during the COVID-19 situation, it is used by policy makers to support decisions, such as e.g. the physical distancing measures to mitigate the spread of COVID-19. Also many modifications of the SIR model exist. An example is the SEIR model [43], which includes and extra type: Exposed. Other models are stochastic transmission models and mean-field epidemiological models.

Although these models provide great insight insight and help decision makers to predict the spread of the disease, there are two issues with these models [56].

Firstly, these existing epidemiological models are macroscopic and therefore they do not fully consider the individual behaviour of the people and their interactions [56]. Therefore these models are unsuitable to analyse the impact of a social distance measure.

Secondly and more importantly, these models rely on specific assumptions and initial conditions which are linked to the specification of the disease. Namely, how many people are infected initially. Without knowing these input parameters these models can not be used for AATOM.

Therefore we need to look at more universal models to assess the safety of the passenger.

7.5. EXPOSED Model

An example of such an universal model is EXPOSED [56]. This is a model-agnostic, which means that it can use any microscopic crowd model that is able to simulate pedestrian movement and to provide outputs regarding the location of the agents in the simulated environment over time [56]. Therefore it very suitable for AATOM because the implementation is easy.

The EXPOSED model, designed by Ronchi E. and Lovreglio R. [56] is using a general formulation instead of relying a specific disease transmission. It is therefore very universal and can be tailored to new pandemics when there is no compelling understanding in the transmission of the pandemic. Adaptions to the model can be made by changing the exposure assumptions (e.g. distance between passengers, face-face or face-back). These assumptions will be explained next.

The model does a quantitative analysis of the exposure of passengers to disease transmission. It assumes a direct transmission from passenger to passenger by physical contact, droplets and airborne routes. It does not take into account contaminated surfaces.

7.5.1. Exposure Mechanisms

The authors consider six exposure mechanisms. These are explained in the following paragraph and presented in Figure 7.3:

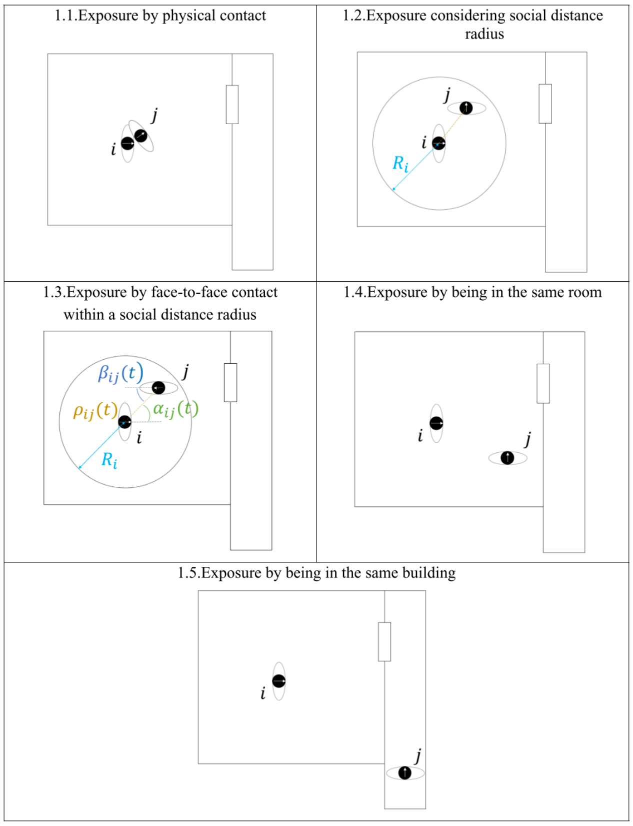

Figure 7.3: Six different exposure mechanisms [56]

Firstly, a passenger can be exposed by physical contact with an other passenger. Since passenger are modelled as circles, it is therefore possible to easily detect if passengers touch each. This assumptions requires the passengers location over time. But this is easily stored in the log files of AATOM.

Secondly, a passenger can be exposed by an other passenger being too close (less than 1.5m). This assumption is calculated in the same way as first mechanism and requires the same information.

Thirdly, the previous mechanism can be advanced by incorporating the heading of the passengers. Since passengers that are headed towards each other, are exposed more than for e.g. when these passengers were face-to-back. Therefore a distinction could be made. This assumption requires to the location and heading of passengers over time. To simplify calculations, Ronchi proposes to use polar coordinates.

Lastly, Ronchi addresses the two other mechanisms namely: exposure by being in the same room and exposure by being in the same building. I don't think this mechanism needs attention because it is not very applicable to a terminal environment. A terminal environment is one big area.

Of all these six different mechanisms, the EXPOSED model can implemented with one or more of these mechanisms. One can also run the EXPOSED model for the different mechanisms separately and then observe to which exposure mechanism passengers are exposed the most. The methodology of the model is explained in the next section.

7.5.2. EXPOSED Methodology

The methodology of the EXPOSED model is as follow:

There are n agents in total and each agent i can be exposed to a certain number of other agents at each time-step $\vec{t} = \{t_0, t_1, ..., t_q, ..., t_f\}$. The number of people k to which agent i is exposed to at each time step t_q can be expressed by the vector $\vec{e}^{\,i}$.

$$\vec{e}^i = \{e_{t0}, e_{t1}, ..., e_{tq}, ..., e_{tf}\}\ \forall i \tag{7.1}$$

where e_{t_q} is the number of agents k to which agent i is exposed at time point t_q.

If we create this vector for all the n agents, we can make a matrix E_t^i with implementing on every row this vector of respective agent.

$$E_t^i = \begin{bmatrix} \vec{e}^1 \\ \vdots \\ \vec{e}^i \\ \vdots \\ \vec{e}^n \end{bmatrix} = \begin{bmatrix} e_{t0}^1 & \cdots & e_{tq}^1 & \cdots & e_{tf}^1 \\ \vdots & \ddots & \vdots & \ddots & \vdots \\ e_{t0}^i & \cdots & e_{tq}^i & \cdots & e_{tf}^i \\ \vdots & \ddots & \vdots & \ddots & \vdots \\ e_{t0}^n & \cdots & e_{tq}^n & \cdots & e_{tf}^n \end{bmatrix} \tag{7.2}$$

Note, that it is possible to add a weighting constant to each row that considers the vulnerability of each agent. For example if different types of agents are implemented such as older and younger agents than these weights could compensate for the vulnerability of the older agents.

From the E_t^i it is possible to obtain the time T_k^i each agent i has been exposed to a given number of agents k by summing the time-steps t_q at which agent i was exposed to k number of agents. This is formalised by Equation 7.3.

$$T_k^i = \sum_{t_0}^{t_f} t_q^i\ \forall i, k \tag{7.3}$$

If we calculate Equation 7.3 for all the n agents and for all k. Then it is possible to group the exposure times corresponding to the given number of agents k and observe the distributions with a mean μ_k and standard-deviation σ_k.

$$T_k(\mu_k, \sigma_k^2) \tag{7.4}$$

The distributions can give insight in the passenger exposure and also in:

- The maximum number of agents that agents are exposed to a the same time.
- The longest time agents are exposed to other k agents at the same time.
- The mean and variance of these exposure times and how they are distributed among the different number of agents k.

If we sum the exposure times T_k^i of all agents that have been exposed to a given number of agents k, we can perform a cumulative exposure assessment. This is formalised with Equation 7.5, with C_k is the indicator of how long all the passengers have been exposed to k other passengers (at the same time.)

$$C_k = \sum_{i}^{n} T_k^i \tag{7.5}$$

To perform a global assessment one can sum all C_k multiplied with a weighing factor γ_k. This weighting factor can for example be linearly increased with increasing k because being exposed to more people is less desirable (and therefore it should increase the exposure output). A formalisation is presented in Equation 7.6

$$G = \sum_{k=1}^{m} \gamma_k C_k \tag{7.6}$$

The choice of the values of γ_k is up to the user and can be changed.

For an example how the EXPOSED model is presented in section 5 of [56].

7.5.3. Advantages and Disadvantages

The advantage of EXPOSED is that it is:

1. It is very universal because it is an model-agnostic and therefore only needs the outputs of any pedestrian dynamics model, which is able to provide information concerning the location of the agents throughout time.

2. It does not rely specific assumptions that depend on specific disease characteristics. It also does not require specific initialisation parameters, e.g. how many infected passengers enter the terminal.

3. It is very flexible and can be adapted to use different transmission mechanisms and assumptions. It is therefore also future-proof in the case a new pandemic arises.

The downside of this model:

1. The result is very much depended on the accuracy of the pedestrian dynamics model. If the pedestrian dynamic model does not provide realistic outputs, such as the location of the passengers over time, then the safety analysis wont be credible.

2. It is a rather simple model. The output is not very advanced. This model does not give information, at which location the passengers are exposed the most and thus observing where bottlenecks are. One could however, make some simple modifications to enable this feature.

7.6. Anticipation on the allocation of resources

The airport is a complex socio-technical system that is dynamic due to a varying flight schedule and is exposed often to internal and external disruptions.

One can make a distinction between disruptions on their probability of occurrence. First, there are exceptional disruptions such as a terrorist attack, as the one in March 2016 at Brussels Airport. These kind of disruptions have mostly catastrophic effects and unfortunately they are very hard to predict.

Secondly, there are disruptions that happen on a regular basis but fortunately they are easier to predict. An example are delays and cancellations of flights due to bad weather. Also, striking personnel (e.g. security personnel [32]) can happen. Resulting in larger queues because of the reduced capacity. More importantly, now with COVID-19, it is very common that flights get cancelled because for example governments suddenly closing their boarders or countries that are getting a negative travel advise.

F. Jimenez Serrano and A. Kazda [40] made a list of different disruptions including their predictability, the main elements disrupted and its propagation along the operations of the airport. As they state that state that even small disruptions such as small error in flight schedules can propagate further in the flight schedule it is an important step in understanding the disruption management process.

Disruptions are often associated with a high cost. Disruptions in aviation cost airlines and their customers up to 60 billion dollar per year, or about 8 percent of worldwide airline revenue according to Amadeus [37]. Not only the economical costs are of concern but more importantly these disruptions can impact the safety of the passengers. Disruptions such as a change in flight schedule can result in overflowing waiting queues and people being exposed to the risk of COVID-19 infection. Therefore in order to minimze the impact of these events one should implement an mechanisms in AATOM that is able to predict disruptions and is able to act accordingly such that operations can continue as smooth as possible.

7.6.1. Risk management versus disruption management

The analysis of disruptions and abnormalities in airport operations involves two main streams of research: risk management and disruption management. "Risk management" deals with: risk identification, risk quantification (quantify the the probability of occurrence and the impact) and risk mitigation (defining actions to mitigate the risk) [6]. Disruption management on the other hand deals with disruptions after they have happened including: disruption discovery, disruption recovery and network redesign and learning [6]. Thus, risk management is more about predicting and anticipating on probable disruptions [6]. The rest of this section will consider risk management, focusing on anticipation.

7.6.2. Different types of anticipation

Rosen was one of the first that defined anticipation in artificial systems in 1985 [57]: An anticipatory system is a system containing a predictive model of itself and/or of its environment that allows it to change current state at an instant in accord with the model predictions pertaining to a later instant.

Butz [13] identified four types of anticipation: implicit anticipation, payoff anticipation, sensory anticipation, and explicit anticipation. However, implicit anticipation can not be considered as anticipation according Rosen's definition because it does not make a prediction about the future and the actions are reactive.

Payoff anticipation evaluates the expected benefits associated with each possible action and executes the action with the highest benefit [16]. In this case, the decisions are thus based on the utility of the predicted results. [20]

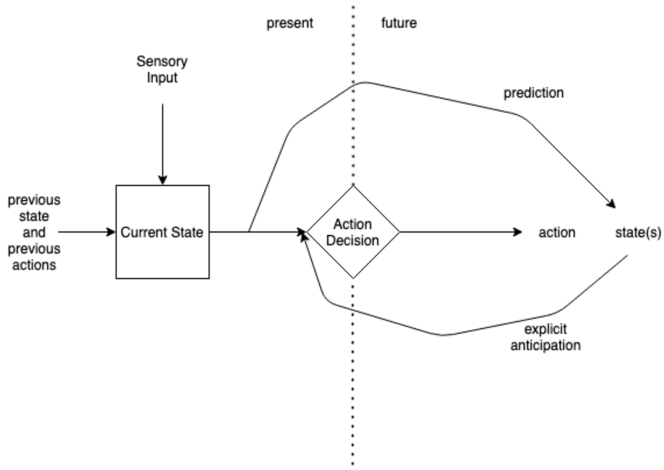

Figure 7.4: A schematic representation of explicit anticipation. Decision making is directly influenced by future state predictions and the current state of the agent can be influenced by previous actions and sensory input, from [13].

In sensory anticipation the predictions have an influence on behaviour of the agents. The decision-making is however not only influenced by the current state of the system and not by the predictions. An example is the model of Castelfranchi et al. [15] agents tend to modify their perceptions and their behavior (for example anxiety) in relation to occurring events.[20]

In explicit anticipation combines both mechanisms of payoff anticipation and sensory anticipation. The predictions influences perceptions and decision-making simultaneously [20]. A schematic representation of explicit anticipation is presented in Figure 7.4.

The figure shows that decision-making is directly influenced by future state predictions and their utility regarding the predicted results. The current state of the agent is influenced by previous actions and sensory input. Sensory input can also trigger the generation of predictions about future state(s) [14].

7.6.3. Conceptual Model

As explained earlier, there are three type of agents in AATOM: passenger agents, operator agents and orchestration agents. The orchestration agent was left general by S. A. M. Janssen to be adapted depending on the case study. Therefore the orchestration agent can be used as the anticipation agent. The orchestration agent can be modelled with the function to observe and monitor the passenger agents and the environment such as disruptions in the flight schedule as well as the KPIs explained in chapter 7. Based on these observations the orchestration agent can then make predictions about the future state of system and identify potential risks. A potential risk should be defined as the system exceeding a certain threshold of one the KPIs explained in chapter 7. The orchestration agent can be modelled with the function to generate a set of actions based on the predictions, such as opening or closing extra set of security lanes, check-in desks, or other resources. Other actions could be ordering an operator agent to attend passenger agents on social distancing. Then predictions are made of the action effects. All predictions are computed by forward simulation of the agent-based simulator as explained in chapter 6. These actions are evaluated by the orchestration agent regarding the utility of the results using the defined safety KPIs as a metric. At the same time, costs associated with the actions (activation of the extra resources) opening extra security lanes should also be taken into account in the evaluation. Using these valuations, the orchestration agent can then decide on what action to perform.

Considering the architecture of AATOM explained in Figure 4.1 and the discussion above a conceptual model for the orchestration/anticipatory agent is proposed. The model is represented in Figure 7.5.

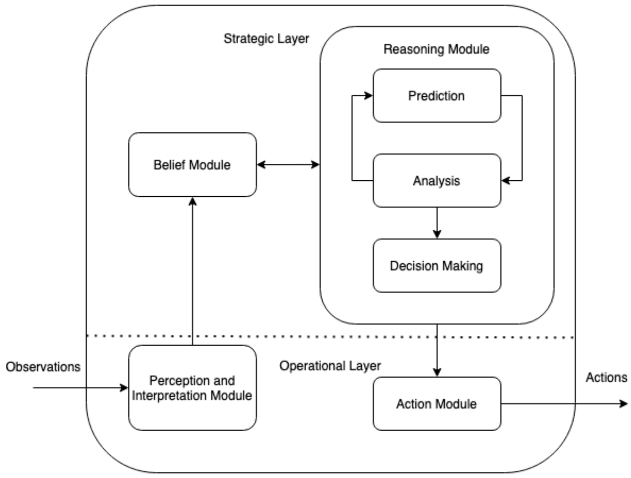

Figure 7.5: Model architecture for the orchestration agent, from [9].

The proposed model in Figure 7.5 is different compared to the model for the passenger and operator agents (see Figure 4.1 regarding the strategic layer and the absence of the tactical layer. The architecture and its modules is explained below.

Using the perception and interpretation module the orchestration agent is able to observe the environment (examples include disruptions in the flight schedule, queue lengths) and the metrics defined in chapter 7. It is then able to interpret these observations, such that it is aware of the changes in the environment and possible risks that triggers anticipation. It is comparable to the sensory input shown in Figure 7.4.

Based on these interpretations the belief module is updated. The belief module stores all the information that it gathered from the perception module, information includes the activity and action states. Hence an update in the belief can also trigger the activation of the reasoning module. But also the output of the reasoning module is fed back into the belief module such as the predicted outcomes of the proposed set of actions.

Using the interpretation of the environment which is stored in the belief module the reasoning module makes predictions about the future state of the system. It analyses this future state and can identify potential risks based on the Hesslow simulative theory, see chapter 6. It then generate a set of possible actions and predicts their utility. These actions are then evaluated regarding the utility to decide on what action to perform.

This action is then send to the action module. In the action module the selected action is executed.

8 Conclusions

In this chapter, the final conclusions are presented, which aim to summarise the most significant aspects of the analysed literature.

COVID-19 restrictions - Due to the COVID-19 virus many countries closed their borders to mitigate the spread of the virus and to reduce COVID-19 deaths. As a result, global passenger demand of April 2020 (in revenue passenger kilometer or RPK) plunged with 94.3 percent compared to last year. A vaccine is considered as the only solution to completely eradicate the spread of COVID-19. However, the European Medicines Agency (EMA) expects that it may take at least one year before a vaccine is approved and available for widespread use in the EU. Fortunately, most (European) countries have successfully flattened the curve of the first COVID-19 wave but the situation remains critical since many countries are now entering a second wave. Fortunately, countries have slowly lifted mobility restrictions and passenger demand is slowly rebounding. Thus airports are slowly starting up again. The European Aviation Safety Agency (EASA) therefore released guidelines for airports and airlines with measures to protect public health. During the literature study these measures where investigated. It was concluded that the most important restrictions for the airports are the following: social distancing, entry/exit temperature screening measures, queuing prevention and the use of personal protective equipment. Of all these restrictions social distancing is considered to have the greatest impact on the airport operations. Social distancing, also known as physical distancing, is defined as passengers needing to maintain at least 1.5 meter distance from each other. However, passengers from the same household are not required to maintain physical distance. As in normal operations and conditions, waiting lines are generally long at check-in desks and security check points imposing the social distancing rule will make airport operations even more challenging when passenger demand gets back to normal. Therefore EASA advises airports to implement floor markings 1.5 meters apart that can assist passengers in maintaining physical distance. Also it was noted that as the COVID-19 situation is highly dynamic measures will be adjusted. Therefore a thorough follow up is needed. Also the model needs to be easily adjustable. An agent-based model therefore seems the perfect modelling choice.

Airport Operations - Operations at an airport were also investigated in this literature study. It was concluded that the airport is a highly complex socio-economic system as it consists out of many different processes that are linked with each other. The passenger flow can be generally split up in departing passengers, arriving passengers and connecting passengers. It was also found that an airport terminal generally consists out of three areas: the transit hall, the departure hall and the arrival hall. The transit hall is the area where departing passengers enter the airport and arrived passengers leave the airport. In this area the departing passengers can check in at the check-in desks or make use of other facilities such as shopping or restaurants. The transit hall and the departure hall are connected by the security check area. In the departure hall the gates are located where the departing passengers can wait for their flight. The arrival hall is solely used by the arriving passengers (and connecting passengers).

Passenger Characteristics - In chapter 3 he passenger characteristics were investigated. Based on the work of Schultz M. [62] it was found that the passenger characteristics have an impact on their walking speed. It was concluded that passenger speed is significantly influenced by age, gender, group size and travel purpose (business or leisure). The results of the interdependencies between passenger speed and passenger characteristics were given by Schultz et al [62] in the form of statistical distributions. These distributions will be implemented in AATOM such that different passenger types are created. Then also a risk-analysis will be done in the model output analysis to observe which type of passenger is more vulnerable to a COVID-19 infection due to his/her behaviour.

Agent Based Modelling and AATOM - As it was concluded that the airport operations is a complex socio-economic system and that the COVID-19 situation is highly dynamic as the restrictions will change when more scientific evidence is found, there is a need for a flexible and easily adaptable modelling approach. The AATOM, Agent-based Airport Terminal Operations Model simulator, designed by the PhD student S. A. M. Janssen seems to satisfy these criteria. It contains calibrated templates of basic airport terminal configurations that can be easily adjusted and used for analysis of airport operations. The model simulates the main handling processes for departing passengers in the airport terminal, this includes check-in, security checkpoint and border control. AATOM is agent based. It is a bottom-up modelling approach as passengers and airport staff are programmed as autonomous intelligent entities, called agents and their behaviour is formalised by equations, more generally decision rules (e.g. if-then kind of rules). As a result the modelling approach is very flexible [29]. In this way it allows to produce characteristics of the system emergence without having to make assumptions in advance regarding the system as a whole. Agent-based simulation is ideal to study interdependencies between agent types and model emergences [29]. It is also suited for detailed hypothesis-testing, more in particular to study the consequences of ex-ante hypotheses such as the interactions of agents and the emergence of the system as a whole [29]. It can be considered as a sort of magnifying glass to understand the reality better [29].

Pedestrian Dynamics - During the literature study different pedestrian dynamics models were investigated because this information is necessary to implement physical distancing between the agents (one of the restrictions posed by EASA). First the differences between macroscopic and microscopic models were analysed. It was concluded that macroscopic models are not suitable for the purpose of the thesis because of their lack in detailed crowd behaviour thus not giving insights in the distances and interactions between the agents. Therefore macroscopic models were directly excluded for further analysis. Five different microscopic models were analysed: the benefit-cost cellular model, the magnetic force model, the cellular automata model, the social force model and the queuing network model. In the end, the five models were compared with each other and it was concluded that the social force model of Helbing et al. [30] was the most suitable for simulating passengers. Key reasons were that the social force model is a continuous and therefore the simulations look more realistic and it is able to simulate more emergent properties. The values of the parameters have also a physical meaning and therefore calibrating these parameters for social distancing will be easier.

Modifications Social Force Model - After the social force model was chosen to be considered to further work with in the AATOM, a deeper analysis was done in the mathematics of the model. It was found that the movement of the pedestrians are simulated by the superposition of three forces: the social repulsion force, the pushing force and the friction force. The social repulsion force is the force by which agents are repelled from each other such that they keep distance and dont enter into the social space of an other pedestrian. The mathematical expression for the social repulsion force is the following:

$$\vec{f}_{social\ repulsion} = A_i e^{(r_i - d_{ij})/B_i}\ \vec{n}_{ij} \tag{8.1}$$

This is an exponential function. As two agents i and j are coming closer to each other the social repulsion force is increasing exponentially such that the agents are repelled from each other. r_i is the radius of agent i as agents are modelled as circles. d_{ij} is the absolute distance between the two agents. n_{ij} is the normalised vector going from agent j to agent i. A and B are Helbing constants. A represents the maximum value of the social repulsion force when the agents are almost touching each other, expressed in Newtons. B represents the fall of length expressed in meters. A higher B value activates the social repulsion force earlier, such that agents automatically take more distance between each other.

Cognitive Decision-Making - During the literature study cognitive decision-making was investigated. It was found that there is a strong relation between personality traits and their tendency to take risks, their meanness and lack of restraint. It was found that individuals with high levels of anti-sociality engage in fewer social distancing rules. Therefore decision-making was considered to be an important part of the literature study. Three relevant theories regarding decision-making were investigated, namely Simulation Hypothesis Theory of Hesslow [31], Damasio's Somatic Marker Hypothesis [33] and OCC model [67]. Firstly, it was concluded that using the theory of Hesslow agents are able to imagine a long chain of of responses and situations without even performing those actions. This theory will be used in the anticipation mechanism. Secondly, it was concluded based on Damasio's Somatic Marker Hypothesis that passengers their decision-making is depended on the their feelings. Damasio's defined these feelings as somatic markers and these depend on past experiences and affect decision-making. Lastly, it was concluded that the OCC model is a suitable representation how emotion types can be clustered in a logic way in order for easy implementation in AATOM.

Model Output Analysis - The outputs of the current AATOM model were investigated. It was found that these output indicators are purely performance based, as examples include "amount of passengers in queue", "average time in queue" and others. They don't give any indication regarding the safety of the passengers. However, it was concluded that there is a need for safety indicators due to the COVID-19 situation as the ACI is issuing a new health accreditation programme. This is a merit-based programme for airports to be recognised by passengers, staff, regulators, and governments for prioritising health and safety measures [3]. Also since currently the transmission of the respiratory syndrome corona-virus 2 (COVID-19) virus is not fully understood yet. Many experts assume that the spread is found by physical contact, droplets and airborne routes[76]. Therefore there is a need for a flexible model that does not rely on specific assumptions of the disease and initial condition's (e.g. how many infected people enter the terminal). It was concluded that generally the health risk can be translated into a multivariable equation with key parameters: Exposure Mechanism, Exposure Time and Vulnerabiility of the individual [24] [55]. The EXPOSED model, designed by Ronchi E. and Lovreglio R. [56], was investigated. This model is a model-agnostic and can be used with AATOM. It is a universal model as does not rely on a specific disease transmission and can therefore also be tailored new pandemics when there is no compelling understanding in the transmission of the pandemic. The model has also some downsides. As the model does not give at which location the passengers are exposed the most and it thus not give insights where bottle necks at the airport are. Also, it does not show if passengers are always exposed to the same passengers or to many different passengers. However, this model is considered to be useful and can serve as a foundation to be further adapted.

Anticipation on Allocation of Resources - Earlier it was already stated that the airport can be considered as a complex socio-technical system that is dynamic due to a varying flight schedule and is exposed often to internal and external disruptions. Also, as even small disruptions such as small error in flight schedules can propagate further in the flight schedule. As a result, disruptions can have a significant impact an the health risk of the passengers as queues can overflow and passengers not being able to keep distance. Therefore it was concluded that mechanisms should be implemented in AATOM to be able to predict these disruptions and to act then accordingly. First, a investigation was made in the difference between risk management and disruption management. It was concluded that disruption management handles disruptions after they have happened. While, risk management is more about predicting and anticipating on probable disruptions [6]. Four types of anticipation mechanisms were identified: "implicit anticipation", "payoff anticipation", "sensory anticipation" and "explicit anticipation" [14]. "Explicit anticipation" is considered the most advanced mechanism as it combines all the aspects of the other types mentioned: decision making is directly influenced by future state predictions and their predicted utility. The current state of the agent is influenced by previous actions and sensory input [14]. This anticipation mechanism is considered to be the most applicable for AATOM. Finally, a conceptual anticipation model based on the work of [9] was proposed. This model can be implemented in the orchestration agent of AATOM.

9
Research Proposal

This chapter presents the research proposal. This includes the objective and research questions in section 9.1, the work packages required for the thesis in section 9.2 and the project planning presented in a Gantt chart in section 9.3.

9.1. Objective and Research Questions

The main goal of the thesis is:

The research objective is to analyze the impact of current (COVID-19) and future pandemic-related measures on airport terminal operations and to identify plans that airport management agents can take to control the flow of passengers in a safe, efficient, secure and resilient way.

To reach this objective, answers will be sought to the following research questions:

1. *How does the current process at airport terminals look like? Which other COVID-19 measures besides physical distancing are required in airport terminals? How can these measures be implemented in AATOM?*

   This first research question aims at defining a clear view on the conditions at which airport terminals need to operate currently and what the expectations are in the near future (seen from the standpoint of airport operators?). Relevant sub-questions are posed below. The sequence of these questions will guide to answer the research objective.

   (a) What is current passenger demand at airports? And what is expected in the near and long term future?

   (b) What current measures are introduced at airports to facilitate a safe and efficient journey to the passengers? What measures are expected in the future?

   (c) Do some processing activities (e.g. check-in or security) take more time?

   (d) How are passenger flows currently controlled? How are crowded areas in the airport avoided? Are problems expected regarding the passenger safety (exposure to COVID-19 transmission) when passenger demand is rebounding back?

   In order to answer these research questions, these questions will be asked to the operators and representatives at Rotterdam The Hague Airport (RTHA).

2. How can the measures identified (in 1) be implemented in AATOM? Which modifications are required in the Helbing Movement Module of the AATOM agent-based model in order to implement social distancing?

   This research questions aims at linking the previous question with the next one. The next research question is regarding defining the impact of the identified COVID-19 measures on the airport operations. To answer this research question, first the agent-based AATOM model will need to be modified in order to implement these COVID-19 measures. This research questions aims at defining how these identified measures can be implemented in the current existing AATOM model.

3. What will be the impact of the identified COVID-19 measures (physical distancing and other important measures) on the airport operations? Which processes at the airport need to be revised? Where at the airport will bottlenecks occur?

   If the previous research question is answered then, the modified AATOM model can be used to run simulations and to identify the impact of the measures on airport terminal operations. This research question aims at defining what kind of impact one should be looking for, namely are bottlenecks occurring or are there airport processes that need to be revised because of a lack of efficiency or safety for passenger?

4. How can passenger safety be translated into new indicators? How can these new indicators be implemented in AATOM?

   In the current AATOM model the indicators are purely performance based, as they show for example the amount of waiting passengers in queue or the average walking distance to the gate and other indications. However, the research goal of the thesis is also to analyse the safety of the passengers. Therefore, new indicators related to passenger safety need to be implemented in AATOM. This research question aims at defining what these indicators should present in order to be representative for passenger safety.

5. What measures and plans for airport management agents can be implemented to control the flow of passengers in a more safe, efficient, secure and resilient way?

   After the COVID-19 measures and the new indicators have been implemented in AATOM one can observe the new emergencies in the airport terminal operations. Then one should know what resources are available at an airport before one can come up with strategy plans and control mechanisms to improve efficiency and safety. This research question aims to define what the available resources are and what strategy plans can be made.

6. What disruptions are present at the airport? What is the impact on the resilience of airport terminal operations under COVID-19-related measures and the health risk of the passengers to sudden changes of flight schedules and the disruptions identified?

   In order to assess the resilience of the airport operations under COVID-19 restrictions it is crucial to know what disruptions events can be present at the airport. This research question aims at defining what disruptions can be present now at airport terminals and at defining what the impact is on the resilience of the aiprort and the health risk of the passengers.

7. How does the implementation of control mechanisms with regard to managing resources and the passenger flow in the airport terminal, influence the efficiency and resilience of the airport and the health risk of the passengers?

   (a) How to develop the adaptive resource control model?
      i. Which resources in the airport terminal can be controlled and how often can the allocation be adjusted?
      ii. What input data is needed for the control model?
      iii. How to predict the passenger flow?
      iv. How to determine the optimal resource allocation?

   (b) How to validate the model?

   (c) Which case studies should be performed (what disturbed conditions) in order to understand the adaptive capacity of the system?

   (d) How to analyse the results?

9.2. Work Packages

In this section the different work packages are defined.

9.2.1. Initial Phase (12 weeks)

The initial phase of the thesis is regarding the initiation of the research, the development of the model and data analysis. The initial phase is considered to take around 12 weeks. The initial phase consists out of different work packages that need to be completed, they are explained below.

WP1: Defining Research Scope and Orientation Eclipse and AATOM (2 weeks)

This part has two scopes. Firstly, it is aimed at obtaining a clear view on the conditions in which airport terminals currently operate and what the expectations are in the near future. In more particular, a physical visit to RTHA or Skype meeting needs to be planned with a representative (depending on what is possible). During this meeting, information needs to be obtained regarding the current way of operations (what is different compared to pre COVID-19 situation), the COVID-19 measures that are implemented, the current and expected passenger demand, the need for simulators to assess the safety of airports. Note, much of this information has already been gathered during the literature study but this meeting is regarded as validation. Secondly, a meeting is needed with Adin for a quick introduction to Eclipse and AATOM. Before the meeting, I should prepare by exploring AATOM more and by listing my questions. Questions will be regarding the general structure of AATOM (e.g. what the input is in AATOM. How the goals of the agents are created. How the path of the agents are created, How to change the indicators in the output analysis). These are general questions to obtain generally insight in AATOM and thus how and in which module the COVID-19 measures will need to be implemented. Also, since I have no experience with JAVA. During this work package I need to learn more about JAVA. During the literature study relevant sources to learn JAVA (internet websites such as W3schools.com, the introduction paper written by Stef Janssen) already have been gathered. Specific relevant modules of a course from Udemy will be chosen and will be executed in parallel.

WP 2: Implementation of the COVID-19 measures (4 weeks)

The second work package is regarding the implementation of the identified COVID-19 measures in AATOM. During the literature study, I have already been experimenting to implement physical distancing between the agents. It worked but I some other undesired emergences aroused such as vibrating agents. Undesired phenomena needs to be clustered according to similarity and then troubleshooted. Again, one or two meetings need to be planned with Stef and/or Adin during the execution of this work package for some tips for fast and efficient implementation. Lastly, the new emergences of the model should be verified and validated. Also during this work package, relevant modules to learn JAVA will be executed.

WP 3: Defining and Implementing new Safety KPI Indicators (3 weeks)

Firstly, new indicators need to be defined regarding the safety of the passengers. More in particular what the indicators should present in order to represent passenger safety? The work of Ronchi [56] can serve as a base to extend further. Then these defined indicators need to be implemented in AATOM. Hereafter, the indicators need to be verified and validated by visual inspection. A small case study can be executed to see where bottle necks at the airport are occurring using the new defined and implemented indicators.

Additionally, also different passenger types can be defined using the literature explained in chapter 3 and also extra literature should be gathered. These different passenger types need to be implemented. Their emergence need to be verified and validated. Hereafter one can observe if the different passenger types are influencing the indicators.

WP4: Defining conceptual control mechanism to optimise allocation of resources (2 weeks)

This work package is regarding the resource control mechanism.
Firstly, it should be defined what resources (e.g. amount of check-in desks, security check points etc.) can be controlled. Moreover, how often these resources can be changed should be defined first. For example, the amount of security check points can not be changed every 15 minutes due to available personnel and the start up of the systems and other factors. Also, all relevant disruptive events (such as delays in flight schedule) should be mapped and identified.

Then a a control model can be defined using the previous identified information based on relevant research and existing control models (references from the literature study can be used).

Steps for the development of the control model are the following:

- Conceptual model development based on literature found (making a structure)
- Formalising the model

WP5: Preparation for the Mid Term Meeting (1 week)

This work packages is regarding the work that needs for the Mid Term Meeting.

- Define key findings and progress made during the initial phase.

- Make a good PowerPoint deck.
- Prepare text for during the presentation.
- Try presentation a few times
- Prepare for Q & A

9.2.2. Final phase (12 weeks)

During the final phase, first the comments from the mid-term meeting need to be incorporated. Then the defined model to allocate the resources needs to be implemented. Hereafter, the case studies needs to be defined and executed. Lastly, the results need to be verified and validated and need to be reported in the thesis report. The final phase ends with the green light meeting. The final phase is considered to take around 12 weeks in total.

WP6: Implementation of midterm comments (1 week)
During this week the comments that were made during the midterm review will be implemented.

WP7: Implementation of the control mechanism to optimise allocation of resources (5 weeks)
After successfully executing the aforementioned work packages, the defined control mechanism (WP4) can be implemented. The steps are the following:

- Implementing the formalised conceptual model in AATOM.
- Verifying and validating the model
- Comparing the model to the previous AATOM model, verifying if the model is doing better in terms of the defined .

WP8: Defining and Executing Case Studies, Analysing Simulation Results, Local Sensitivity and Global Sensitivity Analysis (4 weeks)
In this work package, first different case studies need to be defined (e.g. what (disturbed) scenarios are considered). Then simulations are done using the new AATOM model. Then simulation results are analysed. A local and global sensitivity analysis is done.

WP9: Focus on Draft version thesis report (1 week)
At the end of the final phase, I will focus on the writing the draft version. Note that during whole final phase, report writing is done in parallel but during the work package an extra effort will be done in order to

WP10: Preparation for Green Light Meeting (1 week)
First, the draft version of the thesis report needs to be handed in.

- Define key findings and progress made during the final phase.
- Make a good PowerPoint deck.
- Prepare text for during the presentation.
- Try presentation a few times
- Prepare for Q & A

9.2.3. Final Thesis and Defence Phase (4 weeks)

After the green light meeting, we enter the final thesis and defence phase. The Final Thesis and Defence Phase is considered to take around 4 weeks in total.

WP11: Implement Feedback from Green Light Meeting (1 week)
First, the comments from the green light meeting need to be implemented. This is considered to take around 1 week depending on the amount of comments.

WP12: Finalise Thesis (1 week)
Then, I will focus on finalising the thesis. For example, the report will be checked for grammar mistakes, spellings errors, lay-out will be improved etc. This is considered to take 1 week.

WP13: Defence preparation (2 weeks)
Finally, preparation is needed for the defence. The following steps are needed.

- Define key findings of the thesis.

- Make a good PowerPoint deck.
- Prepare text for during the defence.
- Try presentation a few times.
- Prepare for Q & A

9.3. Project Planning

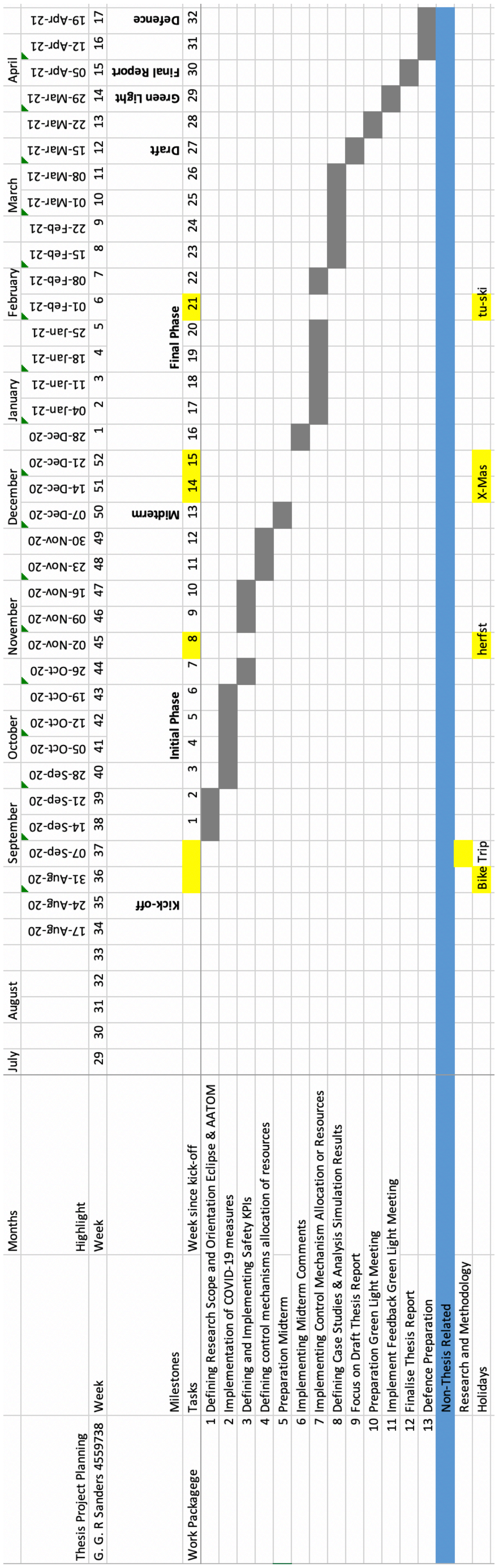

Figure 9.1: Gantt Chart of the project planning for the thesis

III

Supporting work

1 Model Elaboration

Figure 1.2 and Figure 1.1 present a UML diagram which shows the extensions made to the baseline Agent-based Airport Terminal Operations Model (AATOM) [39]. The figures are shown on the next two pages. In the next paragraph the modified code for the queueActivity is presented, this is discussed in Section 5: Verification of the paper.

The **QueueActivity.java** code is modified in order to change the distance between the passengers when they are queuing. One can change the value of "QueueStopDistance" of each passenger in order to have more or less distance between the passengers. Note that in order to let this piece of code work an additional code (line 23-24) was inserted that makes sure that passengers are only set in queuing mode when there is no physical object between them:

```
1   //This is the new modified piece of code.
2   @Override
3   public boolean canStart(int timeStep) {
4      // if we're the first one in queue, we can certainly start.
5      if (inFrontOfQueue) {
6         return true;
7      }
8      // We determine if there is an agent in front of us that we don't want to push.
9      Position position = movement.getPosition(); // own position
10     Position newPos2 = navigationModule.getGoalPosition(); // goal position
11     double angle2 = getAngle(newPos2, position);   // angle
12     if (isInQueue()) {
13        Collection<PhysicalObject> closeObjects =
              Utilities.getMapComponentsInNeighborhood(position, 10,
              map.getMapComponents(PhysicalObject.class));
14        // Observe other agents.
15        Collection<Passenger> agents = observations.getObservation(Passenger.class);
16        for (Passenger other : agents) {
17           if (other.isQueuing()) {
18              if (!other.getPosition().equals(movement.getPosition())) {
19                 // within range
20                 if (other.getPosition().distanceTo(position) < ((Passenger)
                       agent).getQueueStopDistance()) {
21                    // if other agent is in field of view/walking direction
22                    if ((inRange(getAngle(other.getPosition(), position), angle2, 45 / 2))) {
23                       // if other agents is not obstructed by physical object
24                       if (!Utilities.isLineCollision(position, other.getPosition(),
                             closeObjects)) {
25                          // then put agent in queing mode
26                          return true;
27                       }}}}}}}
28     return false;}
```

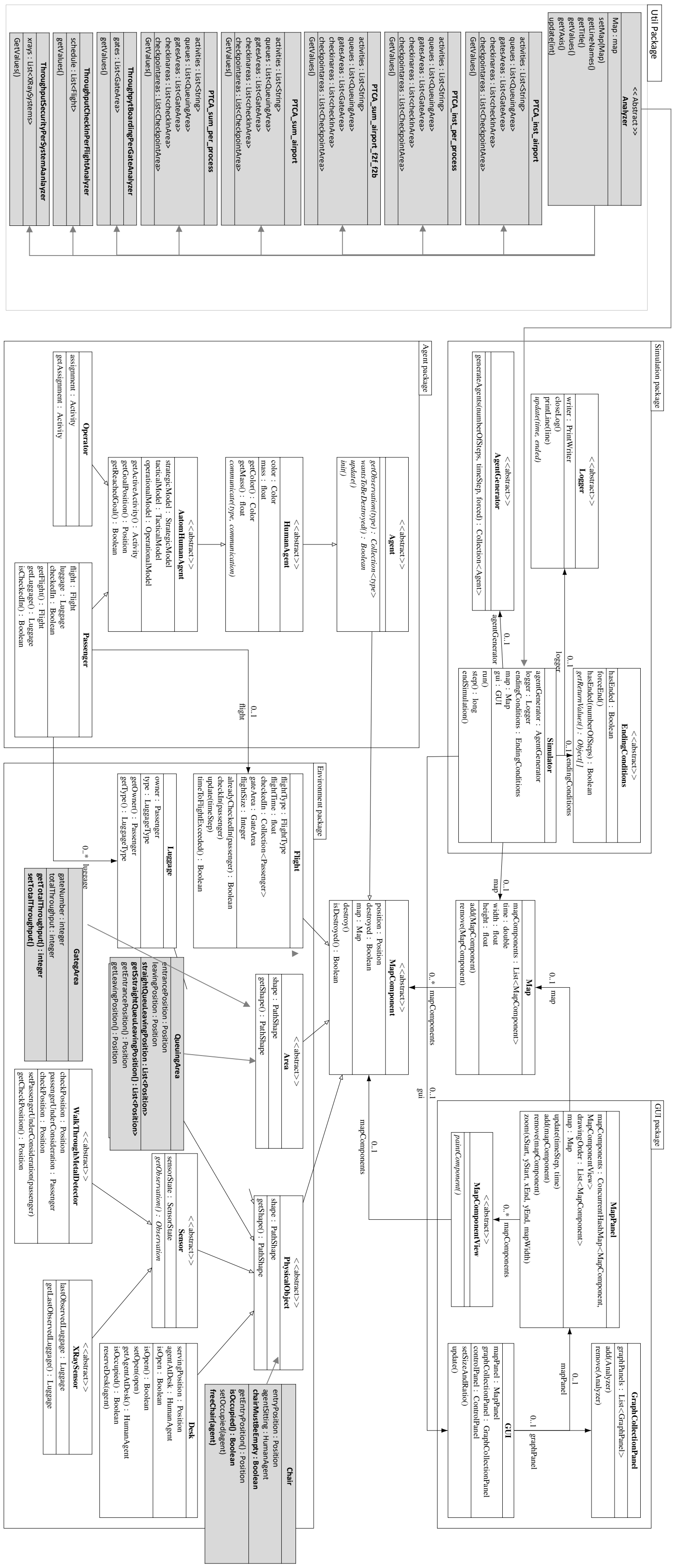

Figure 1.1: The UML class diagram of AATOM. The shaded blocks are the extensions made to the baseline AATOM. Based on [39]

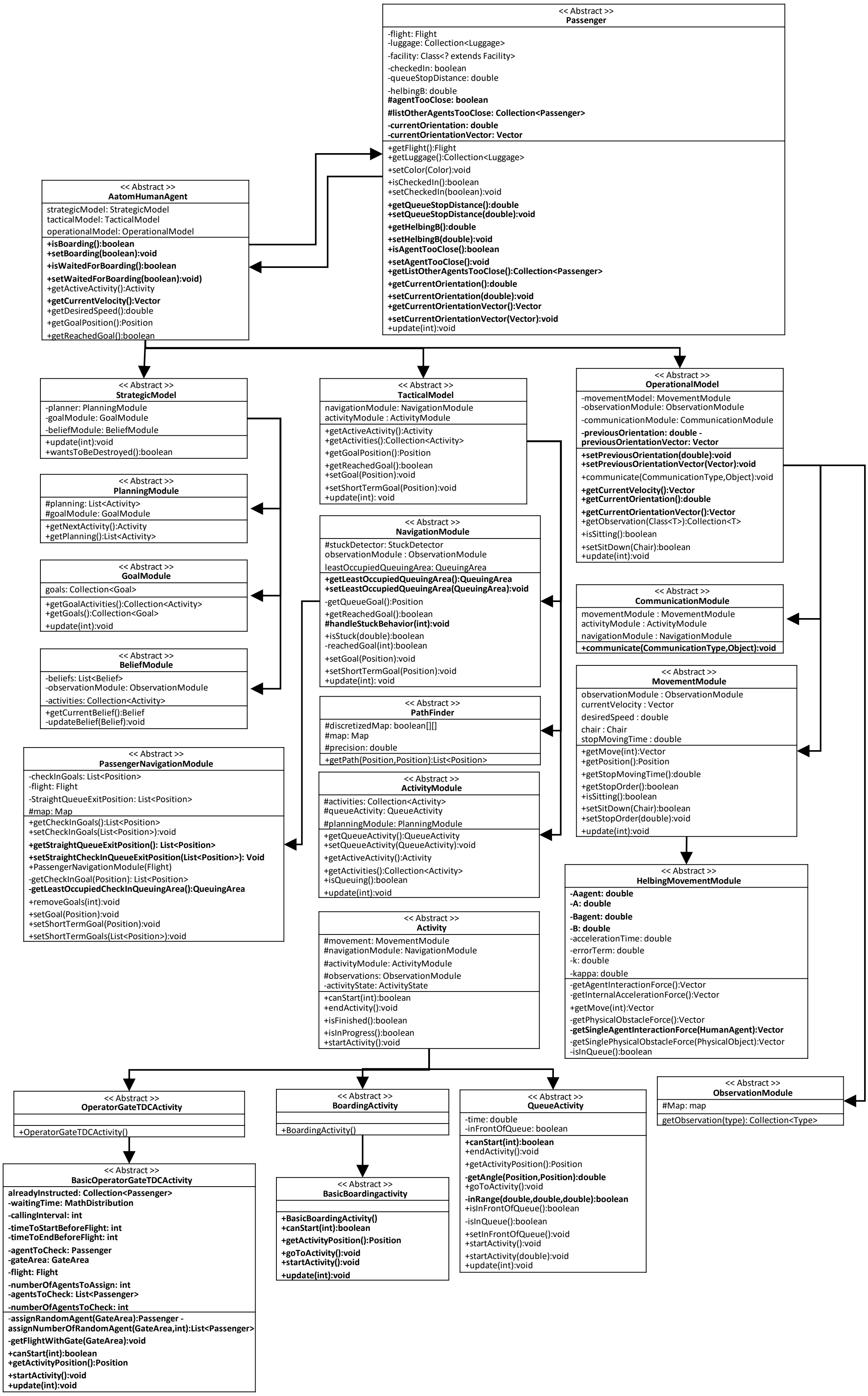

Figure 1.2: The UML class diagram of AATOM. The attirbutes and operators shaded in bold are the extensions made to the baseline AATOM. Based on [39]

2

Results Elaboration

2.1. Boxplots

In this section the results of the three case studies are presented in boxplot format. On each box, the central red mark indicates the median, and the bottom and top edges of the box indicate the 25th and 75th percentiles. The whiskers extend to the most extreme data points (not considering the outliers). The outliers are plotted individually using the red '+' symbol. The results of the check-in case study are presented in Section 2.1.1. The results of the security case study are presented in Section 2.1.2. The results of the boarding case study are presented in Section 2.1.3.

2.1.1. Check-in case study

These are the boxplots of the check-in case study.

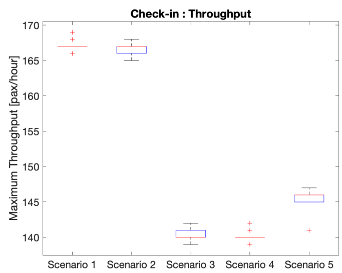

Figure 2.1: Boxplot check-in throughput T_C

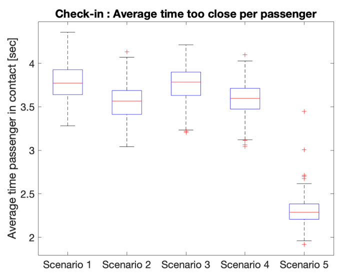

Figure 2.2: Boxplot check-in average contact time per passenger at check-in $Cpax_{CD}$

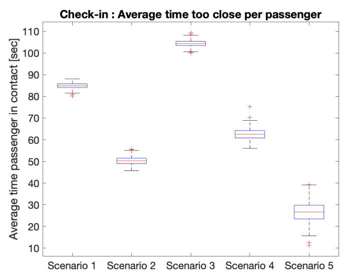

Figure 2.3: Boxplot check-in average contact time per passenger in queue $Cpax_{CQ}$

2.1.2. Security case study

These are the boxplots of the security case study.

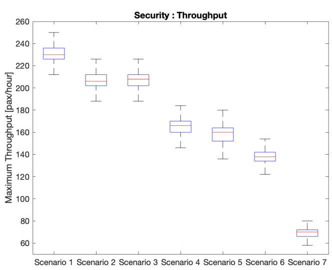

Figure 2.4: Boxplot security throughput T_S

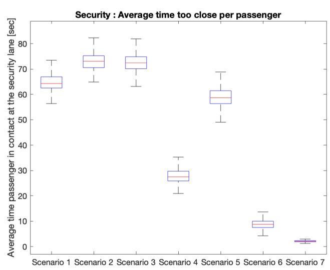

Figure 2.5: Boxplot security average contact time per passenger at security lane $Cpax_{SL}$

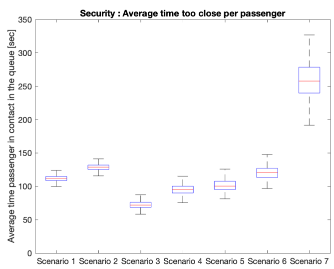

Figure 2.6: Boxplot security average contact time per passenger in queue $Cpax_{SQ}$

2.1.3. Boarding case study

These are the boxplots of the boarding case study.

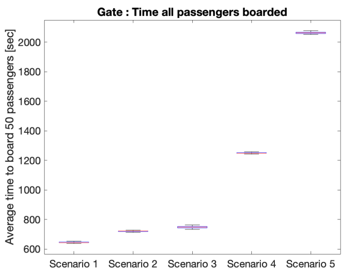

Figure 2.7: Boxplot boarding total time to board 50 passengers T_B

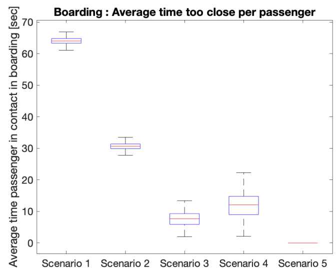

Figure 2.8: Boxplot boarding average contact time per passenger C_{pax}

2.2. Coefficient of Variation

The coefficient of variation plot was used in order to determine the number of simulations needed to have statistically significant results for the three case studies, as suggested by Lorscheid [44].

For scenario with a certain number of simulation runs, the mean of the output $\mu(o)$ and the standard deviation of the output $\sigma(o)$ were computed. The coefficient of variation is then defined as stated in Equation 2.1.

$$c_v = \frac{\mu(o)}{\sigma(o)} \tag{2.1}$$

The values of c_v were then plotted against the number of simulation runs for every scenario. The coefficient of variation plots are shown in figures 2.9 to 2.54.

In Figure 2.10 one can see that the coefficient of variation already stabilizes after 100 simulation runs while in Figure 2.21 coefficient of variation stabilizes after 250 simulation runs. To have a safety margin, 450 simulations were performed for every scenario to have statistically significant results for every metric.

In Section 2.2.1 the coefficient of variation plots for the check-in case study are presented. In Section 2.4.2 the coefficient of variation plots for the security case study are presented. In Section 2.4.3 the coefficient of variation plots for the boarding case study are presented.

2.2.1. Check-in case study

In this section the coefficient of variation plots of the check-in case study are presented.

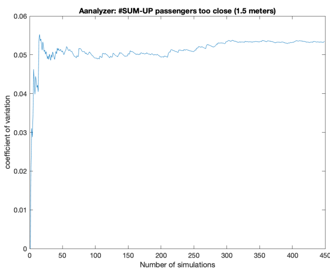

Figure 2.9: Coefficient of Variation for Metric 2 of scenario 1

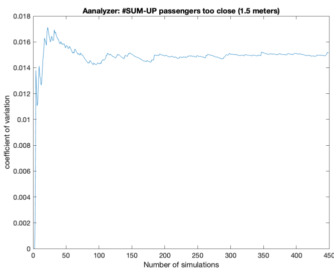

Figure 2.10: Coefficient of Variation for Metric 3 of scenario 1

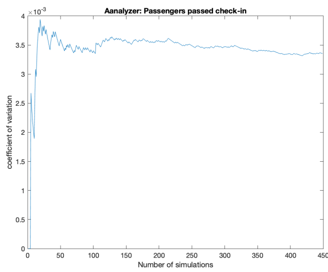

Figure 2.11: Coefficient of Variation for Metric 1 of scenario 1

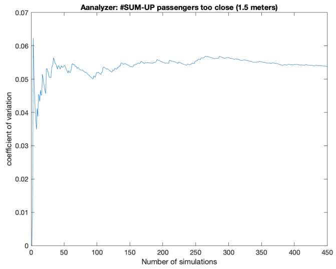

Figure 2.12: Coefficient of Variation for Metric 3 of scenario 2

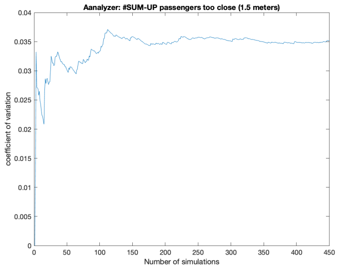

Figure 2.13: Coefficient of Variation for Metric 2 of scenario 2

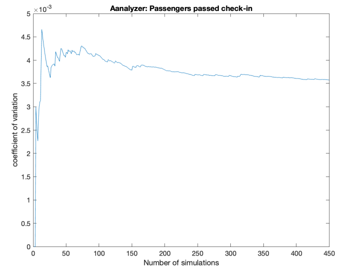

Figure 2.14: Coefficient of Variation for Metric 1 of scenario 2

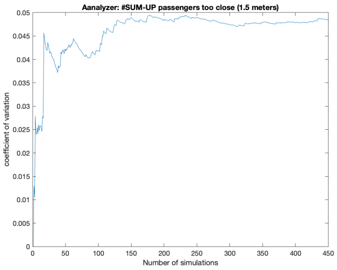

Figure 2.15: Coefficient of Variation for Metric 3 of scenario 3

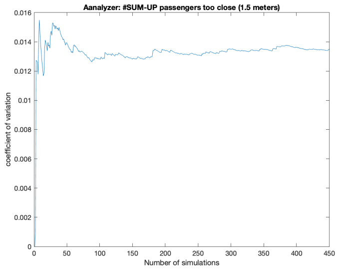

Figure 2.16: Coefficient of Variation for Metric 2 of scenario 3

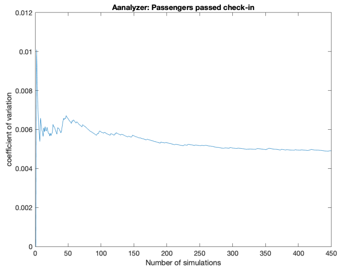

Figure 2.17: Coefficient of Variation for Metric 1 of scenario 3

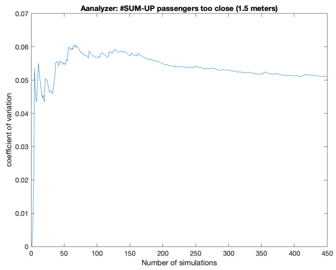

Figure 2.18: Coefficient of Variation for Metric 3 of scenario 4

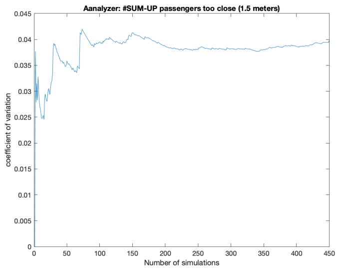

Figure 2.19: Coefficient of Variation for Metric 2 of scenario 4

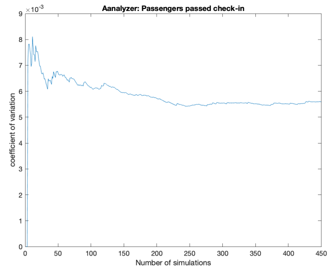

Figure 2.20: Coefficient of Variation for Metric 1 of scenario 4

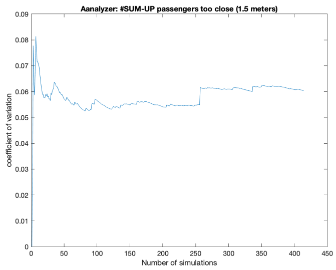

Figure 2.21: Coefficient of Variation for Metric 3 of scenario 5

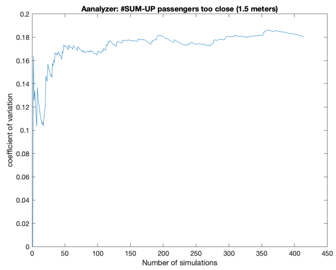

Figure 2.22: Coefficient of Variation for Metric 2 of scenario 5

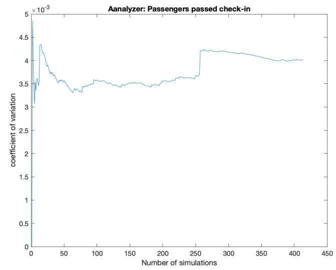

Figure 2.23: Coefficient of Variation for Metric 1 of scenario 5

2.2.2. Security case study

In this section the coefficient of variation plots of the security case study are presented.

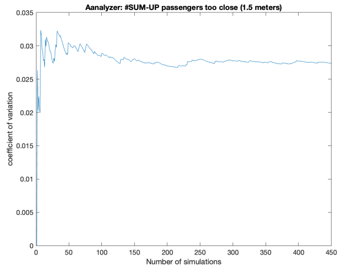

Figure 2.24: Coefficient of Variation for Metric 3 of scenario 1

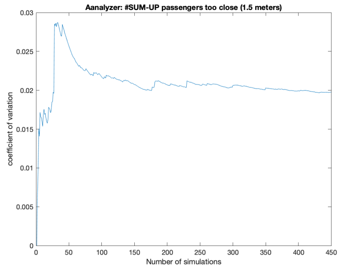

Figure 2.25: Coefficient of Variation for Metric 2 of scenario 1

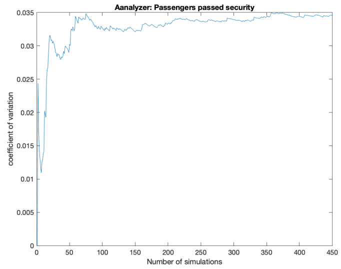

Figure 2.26: Coefficient of Variation for Metric 1 of scenario 1

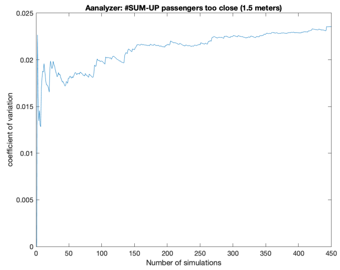

Figure 2.27: Coefficient of Variation for Metric 3 of scenario 2

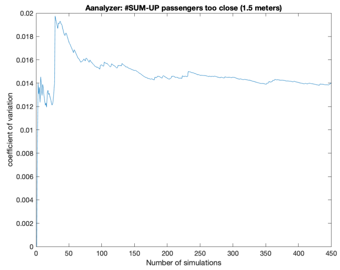

Figure 2.28: Coefficient of Variation for Metric 2 of scenario 2

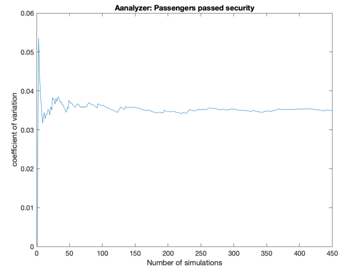

Figure 2.29: Coefficient of Variation for Metric 1 of scenario 2

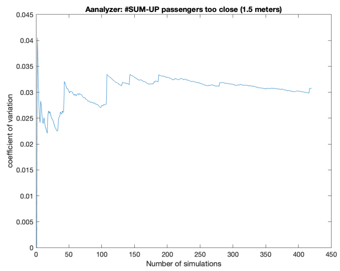

Figure 2.30: Coefficient of Variation for Metric 3 of scenario 3

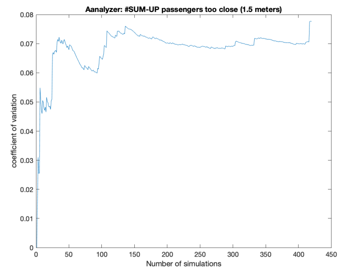

Figure 2.31: Coefficient of Variation for Metric 2 of scenario 3

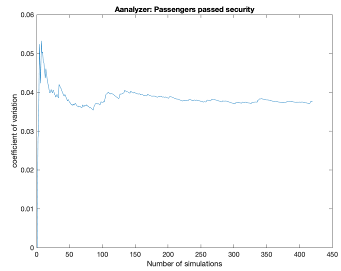

Figure 2.32: Coefficient of Variation for Metric 1 of scenario 3

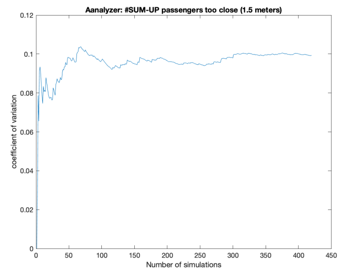

Figure 2.33: Coefficient of Variation for Metric 3 of scenario 4

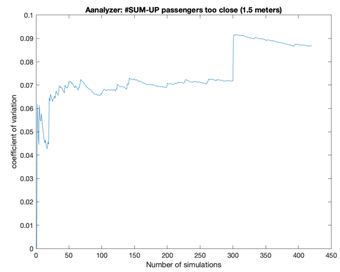

Figure 2.34: Coefficient of Variation for Metric 2 of scenario 4

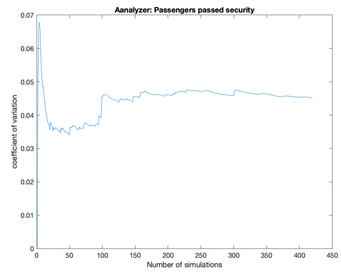

Figure 2.35: Coefficient of Variation for Metric 1 of scenario 4

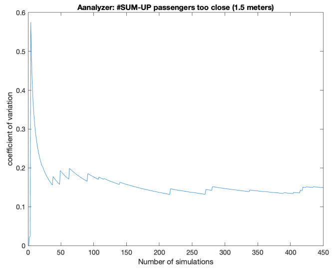

Figure 2.36: Coefficient of Variation for Metric 3 of scenario 5

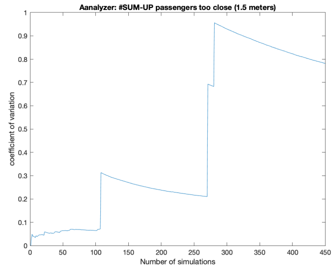

Figure 2.37: Coefficient of Variation for Metric 2 of scenario 5

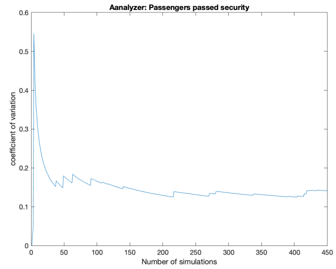

Figure 2.38: Coefficient of Variation for Metric 1 of scenario 5

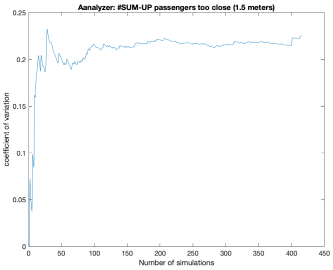

Figure 2.39: Coefficient of Variation for Metric 3 of scenario 6

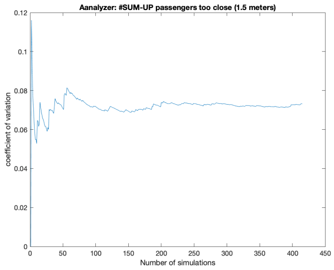

Figure 2.40: Coefficient of Variation for Metric 2 of scenario 6

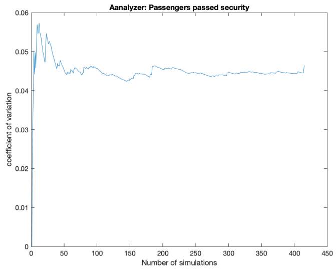

Figure 2.41: Coefficient of Variation for Metric 1 of scenario 6

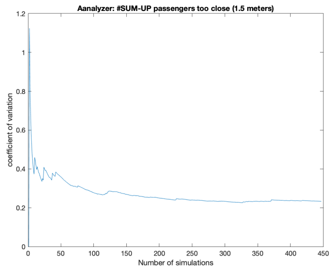

Figure 2.42: Coefficient of Variation for Metric 3 of scenario 7

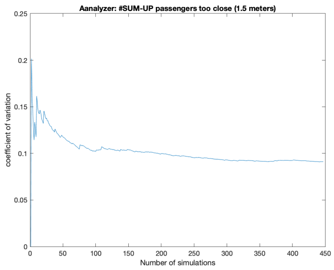

Figure 2.43: Coefficient of Variation for Metric 2 of scenario 7

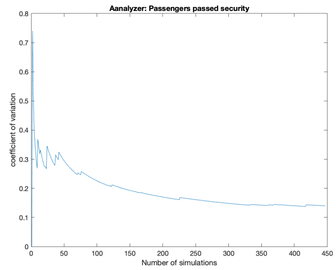

Figure 2.44: Coefficient of Variation for Metric 1 of scenario 7

2.2.3. Boarding case study

In this section the coefficient of variation plots of the boarding case study are presented.

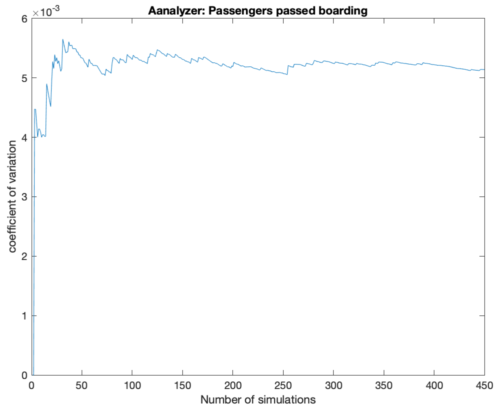

Figure 2.45: Coefficient of Variation for Metric 1 of scenario 1

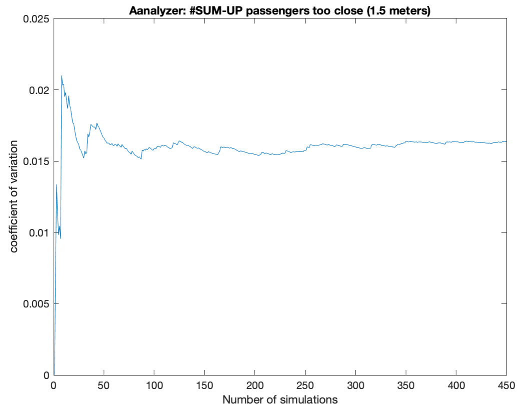

Figure 2.46: Coefficient of Variation for Metric 2 of scenario 1

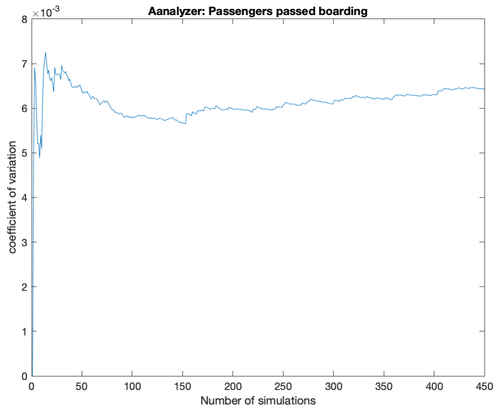

Figure 2.47: Coefficient of Variation for Metric 1 of scenario 2

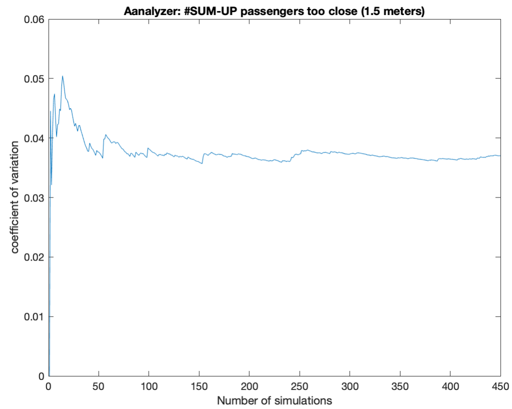

Figure 2.48: Coefficient of Variation for Metric 2 of scenario 2

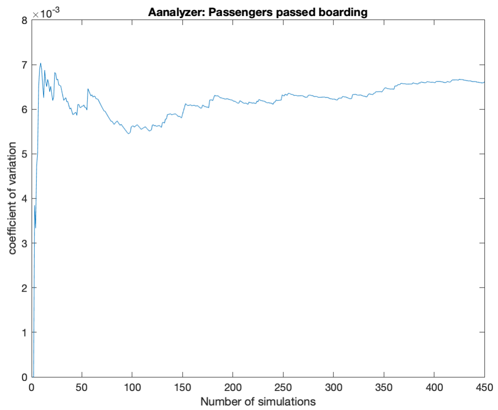

Figure 2.49: Coefficient of Variation for Metric 1 of scenario 3

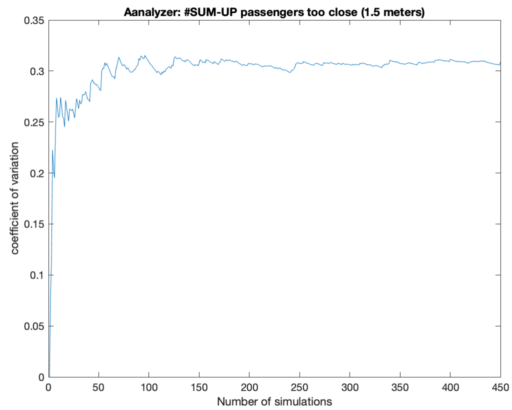

Figure 2.50: Coefficient of Variation for Metric 2 of scenario 3

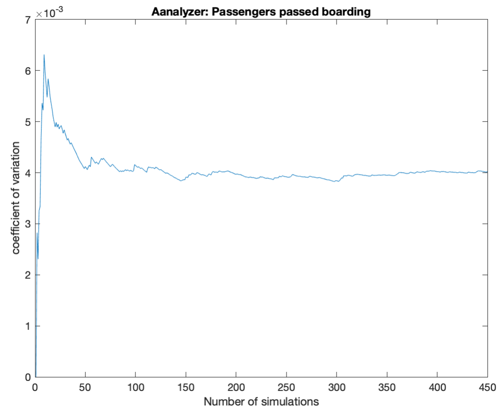

Figure 2.51: Coefficient of Variation for Metric 1 of scenario 4

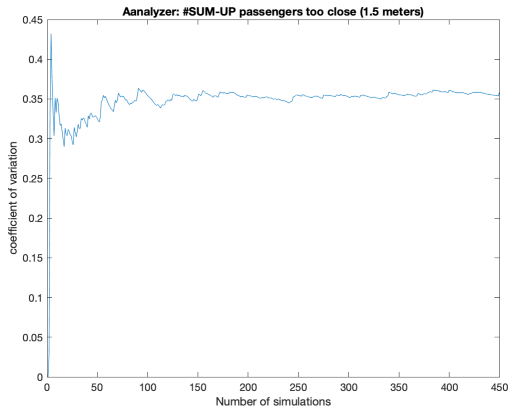

Figure 2.52: Coefficient of Variation for Metric 2 of scenario 4

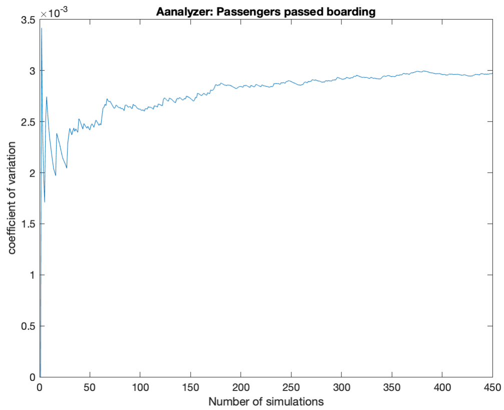

Figure 2.53: Coefficient of Variation for Metric 1 of scenario 5

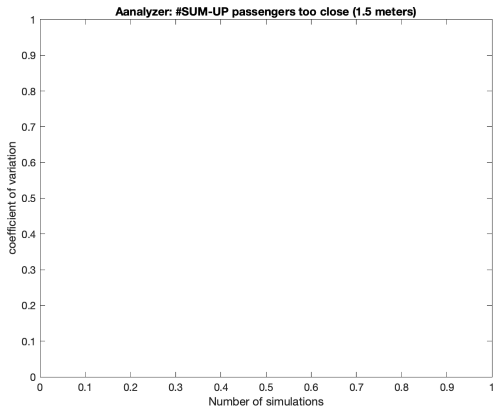

Figure 2.54: Coefficient of Variation for Metric 2 of scenario 5

2.3. Vargha and Delaney A-Test

This section discusses the results of the Vargha and Delaney A_{12} Test [73] [5]. The A_{12}-Test is a non-parametric test and it serves to see how similar two models are. It gives the probability (represented by a value between 0 and 1) that a random output of model 1 is higher then a random output of model 2. A value of $A_{12} = 0.7$ means that in we would obtain higher results 70 percent of the time with model 1. If the two models are equivalent, then A_{12} is equal to 0.5. The A_{12} is computed with Equation 2.2.

$$A_{12} = (R_1/m - (m+1)/2)/n \tag{2.2}$$

where R_1 is the ranksum of the first data group. The ranksum is equivalent to a Mann-Whitney U-test and returns the p-value of a two-sided Wilcoxon rank sum test. m is the data size of model 1 and n is the data size of model 2.

These values of A_{12} can be interpreted as follows:

- Values of 0.5 indicate that the medians are the same.
- Values of 1 and 0 mean that there is no similarity at all.
- Values up to 0.56 indicate a small difference
- Values up to 0.64 indicate a medium difference
- Values over 0.71 indicate large differences
- The same intervals apply below 0.5

The A_{12}-Test is performed for every metric of all three case studies. Each scenario can be considered as a Model.

2.3.1. Check-in case study

In this section the results of the A_{12}-Tests for the check-in case study are presented.

Table 2.1 shows the results for the Throughput metric. Scenario 1 gave in 62 percent of the times a lower throughput than scenario 2. Scenario 3,4 and 5 always returned a higher throughput than scenario 1 and 2. Scenario 3 and 4 are quite similar because their value is close to 0.5. Scenario 5 always returned a higher throughput than scenario 3 and 4.

Table 2.1: Vargha and Delaney A_{12} Check-in Throughput T_C

	Scenario 1	Scenario 2	Scenario 3	Scenario 4	Scenario 5
Scenario 1	0.5	0.62	1	1	1
Scenario 2	0.38	0.5	1	1	1
Scenario 3	0	0	0.5	0.6	0
Scenario 4	0	0	0.4	0.5	0
Scenario 5	0	0	1	1	0.5

Table 2.2 shows the results for the average time a passenger was in contact at check-in. It can be seen that the average contact time per passenger at the check-in for scenario 5 was always lower than for scenario 1.

Table 2.2: Vargha and Delaney A_{12} Check-in Average Contact Time Per Passenger at check-in $C_{pax_{CD}}$

	Scenario 1	Scenario 2	Scenario 3	Scenario 4	Scenario 5
Scenario 1	0.5	0.79	0.52	0.76	1
Scenario 2	0.21	0.5	0.22	0.45	1
Scenario 3	0.48	0.78	0.5	0.75	1
Scenario 4	0.24	0.55	0.25	0.5	1
Scenario 5	0	0	0	0	0.5

Table 2.3 shows the results for the average time a passenger was in contact at queue ($C_{pax_{SQ}}$). These values are in line whit the results which are presented in Section 2.1.

Table 2.3: Vargha and Delaney A_{12} Check-in Average Contact Time Per Passenger in queue $C_{pax_{CQ}}$

	Scenario 1	Scenario 2	Scenario 3	Scenario 4	Scenario 5
Scenario 1	0.5	1	0	1	1
Scenario 2	0	0.5	0	0	1
Scenario 3	1	1	0.5	1	1
Scenario 4	0	1	0	0.5	1
Scenario 5	0	0	0	0	0.5

2.3.2. Security case study

In this section the results of the A_{12}-Tests for the security case study are presented.

Table 2.4 shows the results for the throughput metric. All values in the lower triangle of this table are equal or close to 0. This means that the throughput decreases with each scenario. However, scenario 2 and scenario 3 have the same throughput because here A_{12} equals 0.5.

Table 2.4: Vargha and Delaney A_{12} Security Throughput T_S

	Scenario 1	Scenario 2	Scenario 3	Scenario 4	Scenario 5	Scenario 6	Scenario 7
Scenario 1	0.5	0.99	0.99	1	1	1	1
Scenario 2	0.01	0.5	0.5	1	1	1	1
Scenario 3	0.01	0.5	0.5	1	1	1	1
Scenario 4	0	0	0	0.5	0.7	0.99	1
Scenario 5	0	0	0	0.3	0.5	0.94	0.98
Scenario 6	0	0	0	0.01	0.06	0.5	1
Scenario 7	0	0	0	0	0.02	0	0.5

Table 2.5 shows the results for the average time a passenger was in contact at the security lane ($C_{pax_{SL}}$). Here again almost all values in the lower triangle of this table are equal or close to 0. This means that the $C_{pax_{SL}}$ decreases with each scenario. However the $C_{pax_{SL}}$ for scenario 2 and 3 are higher than for scenario 1. Scenario 2 and 3 are quite similar terms of $C_{pax_{SL}}$ because they have A_{12} value close to 0.5. Lastly, scenario 5 had for 99 percent a higher $C_{pax_{SL}}$ than scenario 4.

Table 2.5: Vargha and Delaney A_{12} Security Average Contact Time at Security Lane $C_{pax_{SL}}$

	Scenario 1	Scenario 2	Scenario 3	Scenario 4	Scenario 5	Scenario 6	Scenario 7
Scenario 1	0.5	0.04	0.05	1	0.88	1	1
Scenario 2	0.96	0.5	0.54	1	0.99	1	1
Scenario 3	0.95	0.46	0.5	1	0.99	1	1
Scenario 4	0	0	0	0.5	0.01	1	1
Scenario 5	0.11	0	0.01	0.99	0.5	0.99	0.99
Scenario 6	0	0	0	0	0	0.5	1
Scenario 7	0	0	0	0	0	0	0.5

Table 2.6 shows the results for the average time a passenger was in contact in the queue ($C_{pax_{SQ}}$). The values all make sense and they are in line with the results presented in Section 2.1.

Table 2.6: Vargha and Delaney A_{12} Security Average Contact Time in Queue $C_{pax_{SQ}}$

	Scenario 1	Scenario 2	Scenario 3	Scenario 4	Scenario 5	Scenario 6	Scenario 7
Scenario 1	0.5	0.01	1	0.94	0.82	0.22	0
Scenario 2	0.99	0.5	1	0.99	0.94	0.78	0
Scenario 3	0	0	0.5	0.01	0	0	0
Scenario 4	0.06	0.01	0.99	0.5	0.31	0.03	0
Scenario 5	0.18	0.06	1	0.69	0.5	0.12	0.02
Scenario 6	0.78	0.22	1	0.97	0.88	0.5	0
Scenario 7	1	1	1	1	0.98	1	0.5

2.3.3. Boarding case study

In this section the results of the A_{12}-Tests for the boarding case study are presented. Table 2.7 shows the results for the time to board 50 passengers. All values in the lower triangle of this table are equal to 1. This means that the time to board 50 passengers increases with each scenario. The same phenomena can be observed for the contact time in Table 2.8. Almost all values in the lower triangle of this table are equal to 0. This means that the contact time decreases with each scenario. Only if we compare scenario 3 to scenario 4 it can be observed that for 81 percent we would have a higher contact time in scenario 4.

Table 2.7: Vargha and Delaney A_{12}-Test for Time To Board 50 passengers T_B

	Scenario 1	Scenario 2	Scenario 3	Scenario 4	Scenario 5
Scenario 1	0.5	0	0	0	0
Scenario 2	1	0.5	0	0	0
Scenario 3	1	1	0.5	0	0
Scenario 4	1	1	1	0.5	0
Scenario 5	1	1	1	1	0.5

Table 2.8: Vargha and Delaney A_{12} Boarding Average Contact Time C_{pax}

	Scenario 1	Scenario 2	Scenario 3	Scenario 4	Scenario 5
Scenario 1	0.5	1	1	1	1
Scenario 2	0	0.5	1	1	1
Scenario 3	0	0	0.5	0.19	1
Scenario 4	0	0	0.81	0.5	1
Scenario 5	0	0	0	0	0.5

2.4. Coefficient of Correlation and P-Values

This section discusses the results for the correlation coefficient and P-value tables.

The correlation coefficient is a measure of the strength and the direction of the linear relationship between the two variables A and B. The correlation coefficient is calculated using Equation 2.3, from [46].

$$\rho_{A,B} = \frac{COV(A,B)}{\sigma_A \sigma_B} \tag{2.3}$$

In Equation 2.3, $COV(X,Y)$ is the covariance between the parameter A and parameter B. σ_A is the standard deviation of parameter A and σ_B is the standard deviation parameter B. When $\rho_{A,B} = 1.0$ then there is a perfect positive relationship between parameter A and parameter B. A value of -1.0 means there is a perfect negative relationship. If the correlation is 0, then the two parameters are not related.

Since each case study had different input parameters and output metrics, a matrix of correlation coefficients for each pairwise parameter combination is used. Below a general representation of a correlation coefficient matrix with N different parameter combinations is shown.

$$R = \begin{pmatrix} \rho_{A,B} & \rho_{A,C} & \cdots & \rho_{A,N} \\ \rho_{B,A} & \rho_{B,C} & \cdots & \rho_{B,N} \\ \vdots & \vdots & \ddots & \vdots \\ \rho_{N,A} & \rho_{N,B} & \cdots & \rho_{N,N} \end{pmatrix}$$

In Section 2.4.1, 2.4.2 and 2.4.3 the results of the correlation coefficients for each case study are given. Also for each correlation coefficient the associated p-value is given. The general rule of thumb is that the hypothesis of "two variables not being correlated" can be rejected if the absolute value of ρ is greater than 0.4 and p-value is below 0.05.

2.4.1. Check-in case study

Table 2.9 presents the correlation coefficients between the parameters of the check-in case study. For this case study the inputs to the model were physical distancing PD, time to check-in (t_{ci}) and queue type QT. The outputs were throughput T_C [pax/h], average contact time per passenger at check-in $C_{pax_{CD}}$ [min:sec] and in the queue $C_{pax_{CQ}}$ [min:sec]. The correlation between inputs are not relevant and therefore they are represented with a "-".

From Table 2.9 it can be observed that physical distancing PD has the strongest negative relationship on the $C_{pax_{CD}}$ with a coefficient of variation of -0.9. Physical distancing PD does have a weak correlation with the throughput T_C of only -0.11. The time to check-in t_{ci} has a very strong negative relationship with the throughput T_C with a correlation coefficient of -0.99. The correlation between t_{ci} and $C_{pax_{CQ}}$ is weaker than the correlation between t_{ci} and $C_{pax_{CD}}$. The queue type QT has a strong positive correlation with the $C_{pax_{CD}}$

and $C_{pax_{CQ}}$ and a weaker positive correlation with the throughput T_C. This confirms the fact that a single queues make the passenger flow more efficient resulting in higher throughput and less contacts between passengers.

From Table 2.10 it can be seen that he associated p-values for all correlation coefficients are all smaller than 0.05. This means that the results are deemed statistically significant.

Table 2.9: Correlation Coefficient for Check-in Case Study

	PD	t_{ci}	QT	T_C	$C_{pax_{CD}}$	$C_{pax_{CQ}}$
PD	-	-	-	-0.11	-0.47	-0.9
t_{ci}	-	-	-	-0.99	0.72	0.25
QT	-	-	-	0.24	-0.86	-0.74
T_C	-0.11	-0.99	0.24	-	-	-
$C_{pax_{CD}}$	-0.47	0.72	-0.86	-	-	-
$C_{pax_{CQ}}$	-0.9	0.25	-0.74	-	-	-

Table 2.10: P-values for Check-in Case Study

	PD	t_c	QT	T_C	$C_{pax_{CD}}$	$C_{pax_{CQ}}$
PD	-	-	-	0	0	0
t_c	-	-	-	0	0	0
QT	-	-	-	0	0	0
T_C	0	0	0	-	-	-
$C_{pax_{CD}}$	0	0	0	-	-	-
$C_{pax_{CQ}}$	0	0	0	-	-	-

2.4.2. Security case study

Table 2.11 presents the correlation coefficients between the parameters of the security case study. For this case study the inputs to the model were physical distancing (PD), number of divest (n_d) positions, number of collect positions (n_c), drop time (t_d) and collect time (t_c). The outputs were throughput [pax/h], average contact time per passenger at security lane ($C_{pax_{SL}}$) [min:sec] and in the queue ($C_{pax_{SQ}}$) [min:sec]. The correlation between inputs are not relevant and therefore they are represented with a "-".

From Table 2.11 it can be observed that physical distancing PD has a negative correlation with the $C_{pax_{SL}}$ and the $C_{pax_{SQ}}$. This confirms that physical distancing PD reduces the $C_{pax_{SL}}$ and the $C_{pax_{SQ}}$. The number of divest positions n_d and the number of collect positions n_c have both a strong positive correlation with throughput T_S and $C_{pax_{SL}}$. The divest t_d and collect t_c time have both a negative correlation on the throughput T_S while they have a positive correlation with the $C_{pax_{SL}}$ and $C_{pax_{SQ}}$.

From Table 2.12 it can be seen that he associated p-values for all correlation coefficients are all smaller than 0.05. This means that the results are deemed statistically significant.

Table 2.11: Correlation Coefficient for Security Case Study

	PD	n_d	n_c	t_d	t_c	T_S	$C_{pax_{SL}}$	$C_{pax_{SQ}}$
PD	-	-	-	-	-	-0.18	-0.66	-0.64
n_d	-	-	-	-	-	0.87	0.9	0.18
n_c	-	-	-	-	-	0.91	0.76	0.22
t_d	-	-	-	-	-	-0.51	0.42	0.39
t_c	-	-	-	-	-	-0.51	0.42	0.39
T_S	-0.18	0.87	0.91	-0.51	-0.51	-	-	-
$C_{pax_{SL}}$	-0.66	0.9	0.76	0.42	0.42	-	-	-
$C_{pax_{SQ}}$	-0.64	0.18	0.22	0.39	0.39	-	-	-

Table 2.12: P-values for Security Case Study

	PD	n_d	n_c	t_d	t_c	T_S	$Cpax_{SL}$	$Cpax_{SQ}$
PD	-	-	-	-	-	0	0	0
n_d	-	-	-	-	-	0	0	0
n_c	-	-	-	-	-	0	0	0
t_d	-	-	-	-	-	0	0	0
t_c	-	-	-	-	-	0	0	0
T_S	0	0	0	0	0	-	-	-
$Cpax_{SL}$	0	0	0	0	0	-	-	-
$Cpax_{SQ}$	0	0	0	0	0	-	-	-

2.4.3. Boarding case study

Table 2.13 presents the correlation coefficients between the parameters of the boarding case study. For this case study the inputs to the model were physical distancing (PD), boarding group size (GS) and the boarding pass check time (t_{bc}). The outputs were time to board 50 passengers (T_B) and average contact time per passenger (C_{pax}). The correlation between inputs are not relevant and therefore they are represented with a "-".

From Table 2.13 it can be seen that physical distancing PD has a positive correlation with the boarding time T_B. Physical distancing (PD) means that the passengers take more time to organise which results in a higher total boarding time (T_B). Physical distancing (PD) has a strong negative correlation with the C_{pax}. The group size (GS) has a strong negative correlation with the T_B while it has a strong positive correlation with the C_{pax}. Lastly the t_{bc} has a strong positive correlation with the T_B and the C_{pax}.

From Table 2.14 it can be seen that he associated p-values for all correlation coefficients are all smaller than 0.05. This means that the results are deemed statistically significant.

Table 2.13: Correlation Coefficient for Boarding Case Study

	PD	GS	t_{bc}	T_B	C_{pax}
PD	-	-	-	0.61	-0.87
GS	-	-	-	-0.8	0.9
t_{bc}	-	-	-	0.87	0.6
T_B	0.61	-0.8	0.87	-	-
C_{pax}	-0.87	0.9	0.6	-	-

Table 2.14: P-values for Boarding Case Study

	PD	GS	t_{bc}	T_B	C_{pax}
PD	-	-	-	0	0
GS	-	-	-	0	0
t_{bc}	-	-	-	0	0
T_B	0	0	0	-	-
C_{pax}	0	0	0	-	-

2.5. Heatmaps

This section presents the heatmaps of the passenger contacts for every scenario and every case study. In this section, a passenger contact is referred to as a passenger agent that is located closer than 1.5 meter to one or more passenger agent(s). The heatmaps do not take into account the type of contact, thus they do not take into account the passenger orientation into account. Section 2.5.1 presents the heatmaps of the check-in case study. Section 2.5.2 presents the heatmaps of the security study. Section 2.5.3 presents the heatmaps of the boarding case study.

2.5.1. Check-in case study

In this section the heatmaps of the check-in case study are presented.

The heatmaps of scenario 1 and scenario 3 are shown in Figure 2.55 and in Figure 2.57. In these two scenarios physical distancing was not implemented. The heatmaps of both scenarios look similar. The blue dots are located relatively close to each other. These blue dots represent the locations where most contacts happen. In scenario 2 and 4, physical distancing was implemented. The heatmaps of scenario 2 and 4 presented in Figure 2.56 and in Figure 2.58. One can see that still most of the contacts are happening in the queue. But not they are located at the corners of the queue. In scneario 5, a different queue type was implemented. One can see the heatmap of this scenario in Figure 2.59. Also here one can see that most of the contacts are still happening in the queue.

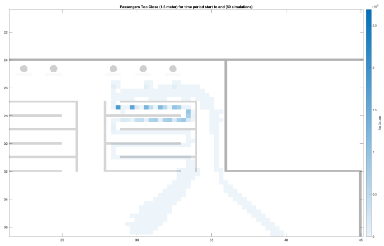

Figure 2.55: Heatmap scenario 1

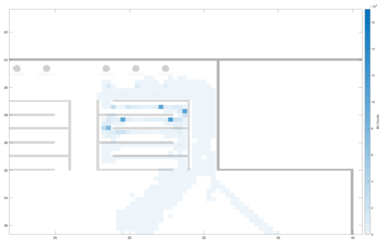

Figure 2.56: Heatmap scenario 2

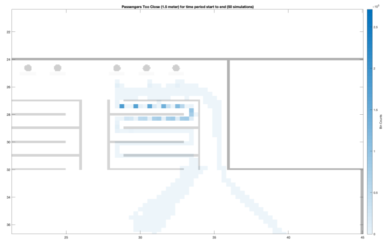

Figure 2.57: Heatmap scenario 3

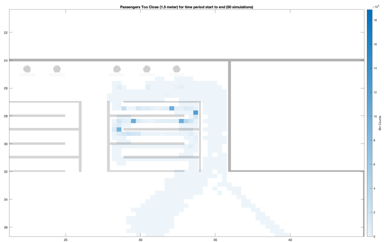

Figure 2.58: Heatmap scenario 4

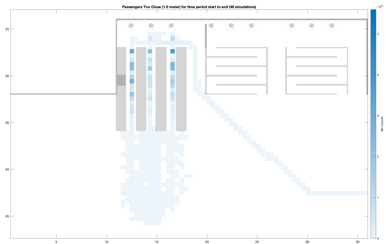

Figure 2.59: Heatmap scenario 5

2.5.2. Security case study

In this section the heatmaps of the security case study are presented.

Figure 2.60 and Figure 2.61 show the heatmaps of scenario 1 and scneario 2. In both scenarios no physical distancing was implemented. The only difference was the time to collect and the time to divest. No difference between these two heatmaps can be observed. Most of the contacts happen in the queue and at the divest and collect positions. The contacts in the queue are evenly and closely spaced from each other. Figure 2.62 shows the heatmap of scenario 3. In scenario 3, physical distancing was implemented. One can observe here that most contacts happen in the luggage divest and luggage collect area of the security. Figure 2.63 shows the heatmap for scenario 4. In this scenario only 2 luggage divest position instead of 3 per lane were simulated. One can see that there are no contacts happening anymore in this area. In scenario 5, the same was done for the luggage collect area. From Figure 2.64 one can see that again there are no contacts happening anymore in the luggage collect area. Lastly, Figure 2.65 shows the heatmap for scenario 7. In this scenario, only one luggage divest and one luggage collect position per lane was implemented. One can observe that no there are no contacts happening anymore at the security lanes. However, there are still contacts happening in the queue.

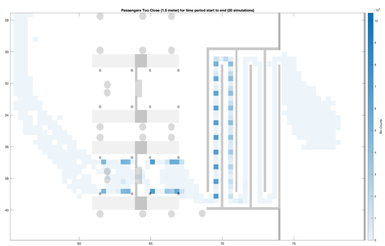

Figure 2.60: Heatmap scenario 1

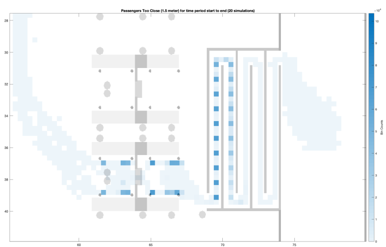

Figure 2.61: Heatmap scenario 2

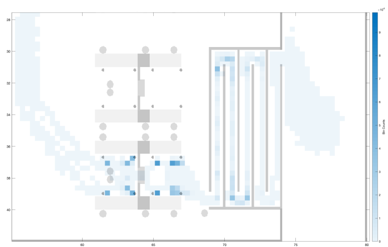

Figure 2.62: Heatmap scenario 3

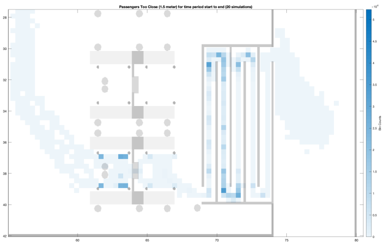

Figure 2.63: Heatmap scenario 4

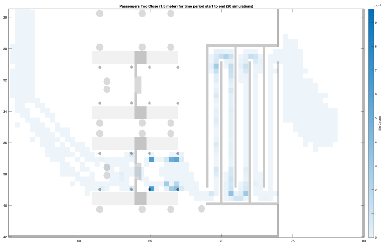

Figure 2.64: Heatmap scenario 5

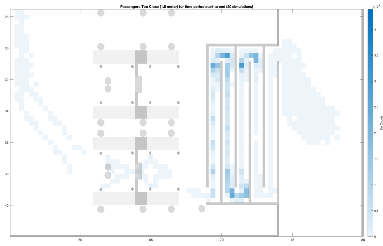

Figure 2.65: Heatmap scenario 7

2.5.3. Boarding case study

In this section the heatmaps of the boarding case study are presented. Figure 2.66 shows the heatmap for scenario 1. In this scenario, no physical distancing was implemented and passengers were boarding in groups of 10. Figure 2.67 shows the heatmap for scenario 2. In this scenario no physical distancing was implemented but passengers were boarding in groups of 5. If we compare both heatmaps, then one can observe in Figure 2.66 that the locations of the contacts are spread over the whole queue. In Figure 2.67 contacts are happening at the end of the queue. The reason is because in scenario 2, the boarding group size is smaller than in scenario 1. Figure 2.68 and Figure 2.69 shows the heatmaps of scenario 3 and scenario 4. In these two scenarios physical distancing was implemented but in scenario 4 a higher BTCT was implemented. However, one can not observe a difference in the heatmaps. Both look the same. If we compare this heatmap with the one from scenario 1, one can observe that for scenario 3 and 4 more contacts happen at the beginning of the queue. This is probably because the passenger agents need to organise themselves before entering the queue. For scenario 5, no heatmap was made because in this scenario no contacts happened.

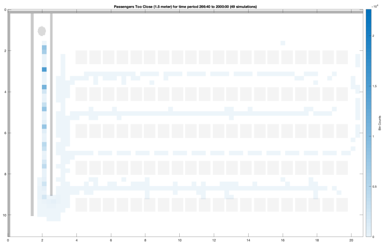

Figure 2.66: Heatmap scenario 1

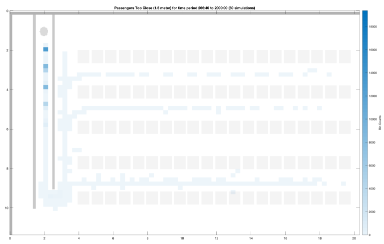

Figure 2.67: Heatmap scenario 2

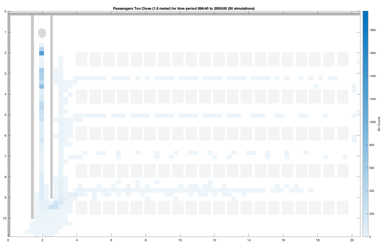

Figure 2.68: Heatmap scenario 3

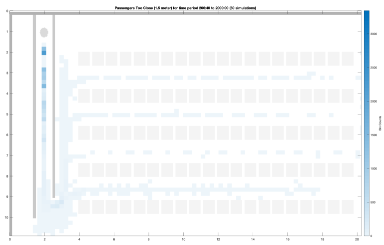

Figure 2.69: Heatmap scenario 4

Bibliography

[1] ACI. Aviation Operations During COVID-19 Business Restart and Recovery. Technical Report 1, Airports Council International, Montreal, Quebec, Canada, May 2020. URL www.aci.aero/publications. Accessed on 2021/03/03.

[2] ACI. Security screening best practices during COVID-19. Technical Report 1, Airports Council International, Montreal, Quebec, Canada, March 2020. URL https://aci.aero/wp-content/. Accessed on 2021/03/03.

[3] ACI. ACI launches accreditation programme to assess airport health measures, 2020. URL https://aci.aero/news/2020/07/24/. Accessed on 2021/03/03.

[4] Rotterdam The Hague Airport. Overzicht verkeer en vervoer, 2020. URL https://www.rotterdamthehagueairport.nl/content/uploads/2020/01/Totaal-per-jaar-januari-2020.pdf. Accessed on 2021/03/03.

[5] Andrea Arcuri and Lionel Briand. A practical guide for using statistical tests to assess randomized algorithms in software engineering. In *2011 33rd International Conference on Software Engineering (ICSE)*, pages 1–10, Waikiki, Honolulu, HI, USA, 2011. Association for Computing Machinery. ISBN 1558-1225 VO -. doi: 10.1145/1985793.1985795. URL https://doi.org/10.1145/1985793.1985795.

[6] Behzad Behdani, Koen Van Dam, and Zofia Lukszo. Agent-based modeling for disruption management in industrial networks and supply chains. In *2011 International Conference on Networking, Sensing and Control, ICNSC 2011*, pages 157–162, 04 2011. doi: 10.1109/ICNSC.2011.5874947.

[7] Ottar N Bjørnstad, Bärbel F Finkenstädt, and Bryan T Grenfell. Dynamics of measles epidemics: estimating scaling of transmission rates using a time series SIR model. *Ecological monographs*, 72(2):169–184, 2002. ISSN 1557-7015.

[8] Pavel Blagov. Adaptive and Dark Personality Traits in the Covid-19 Pandemic: Predicting Health-behavior Endorsement and the Appeal of Public-health Messages. *Social Psychological and Personality Science*, page 1948550620936439, 2020.

[9] Anne-Nynke Blok, Alexei Sharpans'kykh, and Richard Curran. Towards Formalization and Operationalization of Resilience - A study on anticipation in the context of airport security operations. Master's thesis, University of Technology Delft, Mar 2018. URL http://resolver.tudelft.nl/uuid:d052c0a4-e2da-4224-940c-5f2dc661b3b0.

[10] Anne-Nynke Blok, Alexei Sharpanskykh, and Matthieu Vert. Formal and computational modeling of anticipation mechanisms of resilience in the complex sociotechnical air transport system. *Complex Adaptive Systems Modeling*, 6(1):7, 2018. doi: 10.1186/s40294-018-0058-2. URL https://doi.org/10.1186/s40294-018-0058-2.

[11] Irene Bravo. Re-opening airports with covid-19 measures requires re-thinking of terminal processes, 2020. URL https://think.aero/views/. Accessed on 2021/03/03.

[12] Brussels-Airport. Smooth check-in | Brussels Airport, 2020. URL https://www.brusselsairport.be/en/passengers/your-travel-planner/smooth-check-in. Accessed on 2021/03/03.

[13] Martin Butz, Olivier Sigaud, and Pierre Gérard. *Anticipatory Behavior in Adaptive Learning Systems, Foundations, Theories, and Systems*, volume 2684. Springer-Verlag Berlin Heidelberg, 1 2003. doi: 10.1007/b11711.

[14] Martin Butz, Olivier Sigaud, Giovanni Pezzulo, and Gianluca Baldassarre. *Anticipatory Behavior in Adaptive Learning Systems: From Brains to Individual and Social Behavior*. Lecture Notes in Computer Science. Springer Berlin Heidelberg, 2007. ISBN 9783540742616. URL https://books.google.com.jm/books?id=BA8kvh7jgFEC.

[15] Cristiano Castelfranchi, Rino Falcone, and Michele Piunti. Agents with Anticipatory Behaviors: To Be Cautious in a Risky Environment. In *European Conference on Artificial Intelligence, ECAI06*, volume 141, pages 693–694, 1 2006.

[16] Alexis Champion, René Mandiau, Stéphane Espié, and Christophe Kolski. Multi-Agent Road Traffic Simulation: Towards Coordination by Game Theory Based Mechanism. In *Proceedings of the Agents in Traffic and Transportation, workshop in conjunction with the ITS World Congress 2001*, page 12, 10 2001.

[17] Crowdvision. Speed up or spread out? crowdvision blog, 2020. URL https://crowdvision.blog/2020/06/10/speed-up-or-spread-out/. Accessed on 2021/03/03.

[18] Crowdvision. What is Safe Enough to get us Flying Again? CrowdVision Blog, 2020. URL https://crowdvision.blog/2020/04/28/what-is-safe-enough-to-get-us-flying-again/. Accessed on 2021/03/03.

[19] Winnie Daamen. SimPed: a pedestrian simulation tool for large pedestrian areas. In *Conference Proceedings EuroSIW*, page 11. Simulation Interoperability Standards Organization Orlando, Fla., 2002. URL http://citg.tudelft.nl/fileadmin/Faculteit/CiTG/Over_de_faculteit/Afdelingen/Afdeling_Transport_en_Planning/Traffic_management_and_traffic_flow_theory/Dynamisch_Verkeers_Management/Special_Projects/Pedestrians/Publications/doc/EuroSIW02.pdf.

[20] A Doniec, R Mandiau, S Piechowiak, and S Espié. Anticipation based on constraint processing in a multi-agent context. *Autonomous Agents and Multi-Agent Systems*, 17(2):339–361, 2008. ISSN 1573-7454. doi: 10.1007/s10458-008-9048-7. URL https://doi.org/10.1007/s10458-008-9048-7.

[21] Dorine Duives, Winnie Daamen, and Serge Hoogendoorn. State-of-the-art crowd motion simulation models. *Transportation Research Part C: Emerging Technologies TA - TT -*, 37:193–209, 2014. ISSN 0968-090X. doi: 10.1016/j.trc.2013.02.005LK-https://tudelft.on.worldcat.org/oclc/5738127190.

[22] EASA. COVID-19 Aviation Health Safety Protocol | EASA. Technical report, European Union Aviation Safety Agency, Cologne, Germany, June 2020. URL https://www.easa.europa.eu/document-library/general-publications/covid-19-aviation-health-safety-protocol. Accessed on 2021/03/03.

[23] EMA. Treatments and vaccines for COVID-19. Technical report, European Medicine Agency, Amsterdam, The Netherlands, 2020. URL https://www.ema.europa.eu/en/human-regulatory/overview/public-health-threats/. Accessed on 2021/03/03.

[24] Bromage Erin. The Risks - Know Them - Avoid Them, 2020. URL https://www.erinbromage.com/post/the-risks-know-them-avoid-them. Accessed on 2021/03/03.

[25] Milton Friedman and L J Savage. The Utility Analysis of Choices Involving Risk. *Journal of Political Economy*, 56(4):279–304, 1948. ISSN 00223808, 1537534X. URL http://www.jstor.org/stable/1826045.

[26] Linda Geddes. Puzzle over viral load. *New Scientist*, 245(3276):8, 2020. ISSN 0262-4079. doi: https://doi.org/10.1016/S0262-4079(20)30658-8. URL http://www.sciencedirect.com/science/article/pii/S0262407920306588.

[27] P G Gipps and B Marksjö. A micro-simulation model for pedestrian flows. *Mathematics and Computers in Simulation*, 27(2):95–105, 1985. ISSN 0378-4754. doi: https://doi.org/10.1016/0378-4754(85)90027-8. URL http://www.sciencedirect.com/science/article/pii/0378475485900278.

[28] Daniel Harabor and Alban Grastien. Online Graph Pruning for Pathfinding on Grid Maps. In *Proceedings of the Twenty-Fifth AAAI Conference on Artificial Intelligence*, AAAI'11, page 11141119. AAAI Press, 2011.

[29] Dirk Helbing and Stefano Balietti. How to Do Agent-Based Simulations in the Future: From Modeling Social Mechanisms to Emergent Phenomena and Interactive Systems Design. *Technical Report 11-06-024*, 7 2015.

[30] Dirk Helbing, Illés Farkas, and Tamás Vicsek. Simulating dynamical features of escape panic. *Nature*, 407(6803):487–490, 2000. doi: 10.1038/35035023. URL https://www.ncbi.nlm.nih.gov/pubmed/11028994.

[31] Germund Hesslow. Conscious thought as simulation of behaviour and perception. *Trends in Cognitive Sciences*, 6(6):242–247, 2002. ISSN 1364-6613. doi: https://doi.org/10.1016/S1364-6613(02)01913-7. URL http://www.sciencedirect.com/science/article/pii/S1364661302019137.

[32] HLN. Veiligheidspersoneel luchthaven dreigt met staking bij start herfstvakantie, 2019. URL https://www.hln.be/de-krant/veiligheidspersoneel-luchthaven-dreigt-met-staking-bij-start-herfstvakantie~a3 Accessed on 2021/03/03.

[33] Mark Hoogendoorn, Robbert-Jan Merk, and Jan Treur. A decision making model based on Damasios somatic marker hypothesis. In *9th International Conference on Cognitive Modeling, ICCM*, volume 9, page 2009. Citeseer, 2009.

[34] IATA. Safely Restarting Aviation ACI and IATA Joint Approach, 2020. URL https://store.aci.aero/product-category/facilitation/. Accessed on 2021/03/03.

[35] IATA. IATA - EASA/ECDC Guidelines Welcomed, 5 2020. URL https://www.iata.org/en/pressroom/pr/2020-05-21-01/. Accessed on 2021/03/03.

[36] IATA. IATA - After April Passenger Demand Trough, First Signals of Uptick, 2020. URL https://www.iata.org/en/pressroom/pr/2020-06-03-01/. Accessed on 2021/03/03.

[37] Ira, Gershkoff. Shaping the future of Airline Disruption Management (IROPS). Technical Report 1, Amadeus IT Group SA, Madrid, Spain, Jan 2016. URL https://amadeus.com/documents/en/airlines/white-paper/. Accessed on 2021/03/03.

[38] Stef Janssen, Alexei Sharpanskykh, and Richard Curran. Agent-based modelling and analysis of security and efficiency in airport terminals. *Transportation Research Part C: Emerging Technologies*, 100:142–160, 2019. doi: https://doi.org/10.1016/j.trc.2019.01.012. URL http://www.sciencedirect.com/science/article/pii/S0968090X1830809X.

[39] Stef Janssen, Alexei Sharpanskykh, Richard Curran, and Koen Langendoen. Aatom: An agentŋbased airport terminal operations model simulator. Technical report, Delft University of Technology, 2019.

[40] Francisco Jesus Jimenez Serrano and Antonin Kazda. Airline disruption management: yesterday, today and tomorrow. *Transportation Research Procedia*, 28:3–10, 2017. ISSN 2352-1465. doi: https://doi.org/10.1016/j.trpro.2017.12.162. URL http://www.sciencedirect.com/science/article/pii/S2352146517310827.

[41] Arthur Knol. Modelling and analysis of dynamic relations and trade-offs between security and efficiency in airport security operations. Master's thesis, University of Technology Delft, Delft, The Netherlands, Feb 2018.

[42] Taras Lakoba, David Kaup, and Neal Finkelstein. Modifications of the Helbing-Molnár-Farkas-Vicsek Social Force Model for Pedestrian Evolution LK - https://tudelft.on.worldcat.org/oclc/439192621. *Simulation TA - TT -*, 81(5):339–352, 2005. ISSN 0037-5497.

[43] Michael Y Li and James S Muldowney. Global stability for the SEIR model in epidemiology. *Mathematical biosciences*, 125(2):155–164, 1995. ISSN 0025-5564.

[44] Iris Lorscheid, Bernd-Oliver Heine, and Matthias Meyer. Opening the black box of simulations: increased transparency and effective communication through the systematic design of experiments. *Computational and Mathematical Organization Theory*, 18:22–62, 2012.

[45] Gunnar G Løvås. Modeling and simulation of pedestrian traffic flow. *Transportation Research Part B: Methodological*, 28(6):429–443, 1994. ISSN 0191-2615. doi: https://doi.org/10.1016/0191-2615(94)90013-2. URL https://www.sciencedirect.com/science/article/pii/0191261594900132.

[46] Pat Lovie. Coefficient of Variation. *Encyclopedia of Statistics in Behavioral Science*, apr 2005. doi: https://doi.org/10.1002/0470013192.bsa107. URL https://doi.org/10.1002/0470013192.bsa107.

[47] Wenbo Ma. *Agent-based model of passenger flows in airport terminals*. PhD thesis, Queensland University of Technology, Brisbane, Australia, June 2013.

[48] Hader Manfred. How COVID-19 is impacting the Aerospace sector. Technical report, Roland Berger, 2020.

[49] Shigeyuki Okazaki. Study of Pedestrian Movement in Architectural Space Part 2: Concentrated Pedestrian Movement. *Trans. of A.I.J.*, 284:101–110, 10 1979. doi: 10.3130/aijsaxx.284.0{_}101.

[50] Shigeyuki Okazaki and Satoshi Matsushita. A Study of Simulation Model for Pedestrian Movement with Evacuation and Queuing. *Engineering for Crowd Safety*, 432, 1 1993. doi: 10.3130/aijax.432.0{_}79.

[51] Andrew Ortony, Gerald Clore, and Allan Collins. *The Cognitive Structure of Emotion*. Cambridge University Press, 1988. doi: 10.1017/CBO9780511571299.

[52] Andrew Ortony, Gerald L Clore, and Allan Collins. *The cognitive structure of emotions*. Cambridge university press, 1990. ISBN 0521386640.

[53] Katherine OConnell, Kathryn Berluti, Shawn A Rhoads, and Abigail A Marsh. Reduced social distancing early in the COVID-19 pandemic is associated with antisocial behaviors in an online United States sample. *PloS one*, 16(1):e0244974, 2021.

[54] Billy Quilty, Samuel Clifford, Stefan Flasche, and Rosalind Eggo. Effectiveness of airport screening at detecting travellers infected with novel coronavirus (2019-nCoV). *Eurosurveillance*, 25, 2 2020. doi: 10.2807/1560-7917.ES.2020.25.5.2000080.

[55] E. Rea, J. Laflèche, S. Stalker, B. K. Guarda, H. Shapiro, I. Johnson, S. J. Bondy, R. Upshur, M. L. Russell, and M. Eliasziw. Duration and distance of exposure are important predictors of transmission among community contacts of Ontario SARS cases. *Epidemiology and Infection*, 135(6):914–921, 8 2007. ISSN 09502688. doi: 10.1017/S0950268806007771. URL /pmc/articles/PMC2870656/?report=abstracthttps://www.ncbi.nlm.nih.gov/pmc/articles/PMC2870656/.

[56] Enrico Ronchi and Ruggiero Lovreglio. EXPOSED: An occupant exposure model for confined spaces to retrofit crowd models during a pandemic. *Safety Science*, 130:104834 – 104834, 2020.

[57] Robert Rosen, Judith. Rosen, John J Kineman, and Mihai. T A T T Nadin. Anticipatory systems : philosophical, mathematical, and methodological foundations, 2012.

[58] Rotterdam The Hague Airport. Overzicht verkeer en vervoer 2019 per maand, 2019. URL https://www.rotterdamthehagueairport.nl/content/uploads/2020/01/Totaal-per-maand-2019-januari-2020.pdf. Accessed on 2021/03/03.

[59] Rotterdam The Hague Airport. Overzicht verkeer en vervoer 2020 per maand, 2020. URL https://www.rotterdamthehagueairport.nl/content/uploads/2020/07/Totaal-per-maand-2020.pdf.

[60] Ricardo Santos, Goreti Marreiros, Carlos Ramos, José Neves, and José Bulas-Cruz. Multi-agent Approach for Ubiquitous Group Decision Support Involving Emotions BT . In Jianhua Ma, Hai Jin, Laurence T Yang, and Jeffrey J.-P. Tsai, editors, *Ubiquitous Intelligence and Computing*, pages 1174–1185, Berlin, Heidelberg, 2006. Springer Berlin Heidelberg. ISBN 978-3-540-38092-4.

[61] Michael Schultz, S Lehmann, and Hartmut Fricke. A discrete microscopic model for pedestrian dynamics to manage emergency situations in airport terminals BT. In Nathalie Waldau, Peter Gattermann, Hermann Knoflacher, and Michael Schreckenberg, editors, *Pedestrian and Evacuation Dynamics 2005*, pages 369–375, Berlin, Heidelberg, 2007. Springer Berlin Heidelberg. ISBN 978-3-540-47064-9.

[62] Michael Schultz, Bernd Oreschko, Christian Schulz, and Hartmut Fricke. Tracking passengers at airports for user driven terminal design. In *7th EUROCONTROL Innovative Research Workshop*, page 8, Bretigny, 12 2008.

[63] Alexei Sharpanskykh and Jan Treur. *Adaptive Modelling of Social Decision Making by Agents Integrating Simulated Behaviour and Perception Chains BT - Computational Collective Intelligence. Technologies and Applications*. Springer Berlin Heidelberg, Berlin, Heidelberg, 2010. ISBN 978-3-642-16693-8.

[64] Nirajan Shiwakoti and Takashi Nakatsuji. Pedestrian simulations using microscopic and macroscopic model. *Infrastructure Planning*, pages 1–4, 1 2005. URL https://www.jsce.or.jp/library/open/proc/maglist2/00039/200511_no32/pdf/17.pdf.

[65] Jeroen Spans. An integrated approach for efficient and resilient airport management. Master's thesis, Delft University of Technology, 2018.

[66] Anne-Nynke Blok Stef Janssen Arthur Knol. AATOM - An Agent-based Airport Terminal Operations Model. Technical report, University of Technology delft, 2018.

[67] Bas Steunebrink, Mehdi Dastani, John-Jules Ch, and John-jules Meyer. The OCC model revisited. In *Proc. of the 4th Workshop on Emotion and Computing*, 1 2009.

[68] Bas R. Steunebrink, Mehdi Dastani, and John-Jules Ch. Meyer. A Logic of Emotions for Intelligent Agents. In *Proceedings of the 22nd National Conference on Artificial Intelligence - Volume 1*, AAAI'07, page 142147. AAAI Press, 2007. ISBN 9781577353232.

[69] Fiona Strens. CrowdVision - Online Webinar, 2020. URL https://vimeo.com/410129425. Accessed on 2021/03/03.

[70] Kardi Teknomo, Yasushi Takeyama, and Hajime Inamura. Review on Microscopic Pedestrian Simulation Model. *arXiv e-prints*, art. arXiv:1609.01808, September 2016.

[71] Stephen J Turnovsky. Essays in the Theory of Risk-Bearing. Kenneth J. Arrow . *Journal of Political Economy*, 80(6):1328–1329, 11 1972. ISSN 0022-3808. doi: 10.1086/259978. URL https://doi.org/10.1086/259978.

[72] Koen H Van Dam, Igor Nikolic, and Zofia Lukszo. *Agent-based modelling of socio-technical systems*, volume 9. Springer Science & Business Media, 2012. ISBN 9400749333.

[73] András Vargha and Harold D Delaney. A Critique and Improvement of the "CL" Common Language Effect Size Statistics of McGraw and Wong. *Journal of Educational and Behavioral Statistics*, 25(2):101–132, mar 2000. ISSN 10769986, 19351054. doi: 10.2307/1165329. URL http://www.jstor.org.tudelft.idm.oclc.org/stable/1165329.

[74] John von Neumann, Oskar Morgenstern, and Ariel Rubinstein. *Theory of Games and Economic Behavior (60th Anniversary Commemorative Edition)*. Princeton University Press, 8 1944. ISBN 9780691130613. doi: 10.2307/j.ctt1r2gkx. URL http://www.jstor.org/stable/j.ctt1r2gkx.

[75] World Health Organization. Clinical Management of COVID-19 - Interim Guidance, 2020. URL https://www.who.int/publications/i/item/clinical-management-of-covid-19. Accessed on 2021/03/03.

[76] I T S Yu, Yuguo Li, Tze Wai Wong, Wilson Tam, Andy Chan, Joseph Lee, Dennis Leung, and Tommy Ho. Evidence of Airborne Transmission of the Severe Acute Respiratory Syndrome Virus. *The New England journal of medicine*, 350:1731–1739, 5 2004. doi: 10.1056/NEJMoa032867.